

EPIDEMIOLOGY, BIOLOGY, MOLECULAR DETECTION, AND POPULATION
STRUCTURE OF THE OAK WILT FUNGUS, *BRETZIELLA FAGACEARUM*

By

Karandeep Singh Chahal

A DISSERTATION

Submitted to
Michigan State University
in partial fulfillment of the requirements
for the degree of

Plant Pathology- Doctor of Philosophy

ABSTRACT

Oak wilt, caused by the ascomycete fungus *Bretziella fagacearum*, is a lethal vascular disease affecting Fagaceae hosts, primarily oaks (*Quercus* spp.), in both forest and urban settings in the United States. *B. fagacearum* is vectored by sap beetles (Coleoptera: Nitidulidae) when spore-laden insects visit fresh wounds on healthy trees. The pathogen also spreads through functional root grafts. Oak wilt has been confirmed in 24 states in the U.S., with widespread occurrence in the Midwest and Texas. This dissertation investigates various aspects of oak wilt, including epidemiology, biology, diagnosis, complete genome analysis, and population genetics of *B. fagacearum*. The epidemiology of oak wilt was studied by inoculating mature northern red oaks (*Q. rubra*) at three field sites in northwest Michigan with a conidial suspension (2×10^6 conidia/ml) at 4-week intervals from March to November. Inoculated trees were evaluated to assess disease progression at 15-day intervals. Trees inoculated from March to September were succumbed to infection, with rapid disease progression in June and July. Inoculations in October and November did not result in infection. The progression of oak wilt was correlated with predicted sap flow rates, indicating that seasonal sap flow variations, influenced by sapwood development, affect disease incidence and progression. These findings provide valuable information on key risk periods for infection, which can be used to refine management guidelines to prevent tree injury. The biology of *B. fagacearum* was studied by monitoring sporulation on infected northern red oaks at 12 field sites in northwest Michigan, from March to November 2018-2020. Mycelial mats (sporulating structures) were categorized into eight developmental and morphological stages, with significant variation in colony-forming units among the stages. This visual rating system helps distinguish between infectious and non-infectious mats and assess the risk of above-ground infection, providing critical information for

arborists and forestry professionals. The study identified two peaks of mycelial mat production, one in early summer (May and June) and another in early fall (August and September). *B. fagacearum* detection from diseased samples was enhanced through the optimization and validation of a TaqMan real-time PCR assay, offering greater specificity and sensitivity than traditional methods. A non-destructive sampling method for detecting *B. fagacearum* in red oaks and chestnuts was also developed and validated. Best practices for traditional, and non-destructive sampling were streamlined for culture-based detection method. The complete genome of *B. fagacearum* was sequenced and annotated, revealing a total length of 27,072,536 bp and 7,554 predicted proteins. This genome resource providing a crucial reference for population studies and insights into the molecular epidemiology and biology of the pathogen. Population genetic analyses using whole genome resequencing of 93 isolates from 15 states identified significant stratification, revealing four distinct genetic clusters corresponding to specific geographical regions: Upper Midwest, Mid-Atlantic and Southeast, Michigan, and Texas. The Upper Midwest served as a center of genetic diversity with potential gene flow among populations, while Texas isolates formed a highly distinct cluster, suggesting potentially limited gene flow and local adaptation. The first report of *B. fagacearum* infecting orchard-grown chestnut trees in Michigan underscores the need for constant vigilance and monitoring in chestnut orchards to promptly detect and manage potential infections. This dissertation also includes detailed methods for diagnosing oak wilt, *B. fagacearum* identification, storage and assays for pathogenicity trials in non-lignified seedlings and mature trees.

Copyright by
KARANDEEP SINGH CHAHAL
2024

I dedicate this dissertation to the Chahals and Sharmas in my life: Jang Singh, Surjeet Kaur, Jasdev Singh, Sukhwinder Kaur, Amarjit Kaur, Jaspreet Singh, Kuljit Kaur, Nancy Sharma, Rattanjit Kumar, Meenakshi, and Mohit Sharma for their unwavering love and rock-solid support.

ACKNOWLEDGEMENTS

First and foremost, I would like to express my deepest gratitude to my advisor, Dr. Timothy D. Miles, for his guidance, encouragement, and direction to complete this milestone. I am so thankful for his mentorship, which extended beyond the scope of my Ph.D., helping me achieve my career aspirations. I am grateful to my former advisor and committee member, Dr. Monique L. Sakalidis, for providing this great research opportunity. I sincerely appreciate the invaluable feedback and support from my committee members, Dr. Deborah G. McCullough and Dr. Bert Creg, throughout this journey. Special thanks to Dr. Carmen Medina-Mora and Laura A. Miles for their invaluable assistance and guidance. I am also grateful to my lab colleagues and research aides: Nancy Sharma, Tina Guo, Emily Ruda, Crystal Nelson, Muhammad Zunair Latif, Muddassar Hussain, Becky Harkness, Adam Grove, Ethan Wachendorf, Giorgia Bastianelli, Ava Stallmann, as well as Scott Lint and Phillip Kureja for their field assistance. I extend my heartfelt thanks to my friends Jagdeep Singh Sidhu, Sukhdeep Singh, Lovepreet Singh Chahal and Mohit Mahey for their emotional support and science talks. Lastly, I extend my heartfelt thanks to my wife, Nancy Sharma, who has been my best friend, amazing colleague, and my occasional therapist (lol, but seriously, she's great at it- and has the patience of a saint!) and my parents (Jasdev Singh, Sukhwinder Kaur and Rattanjit Kumar, Meenakshi) and brothers (Jaspreet Singh, Mohit Sharma) for their emotional support and encouragement, which played a crucial role in the completion of my Ph.D.

TABLE OF CONTENTS

CHAPTER 1: A DIAGNOSTIC GUIDE FOR OAK WILT DISEASE IN OAK AND CHESTNUT.....	1
LITERATURE CITED:.....	28
CHAPTER 2: EPIDEMIOLOGY OF OAK WILT CAUSED BY BRETZIELLA FAGACEARUM ON QUERCUS RUBRA IN MICHIGAN.....	35
LITERATURE CITED:.....	60
CHAPTER 3: NOVEL NON-DESTRUCTIVE DETECTION METHODS FOR BRETZIELLA FAGACEARUM IN NORTHERN RED OAK AND CHESTNUT.....	63
LITERATURE CITED:.....	94
CHAPTER 4: COMPLETE GENOME RESOURCE OF BRETZIELLA FAGACEARUM, THE CAUSAL FUNGUS OF OAK WILT.....	99
LITERATURE CITED:.....	110
CHAPTER 5: POPULATION STRUCTURE OF OAK WILT FUNGUS, BRETZIELLA FAGACEARUM IN THE UNITED STATES.....	113
LITERATURE CITED:.....	141
CONCLUSION AND FUTURE DIRECTIONS.....	144
APPENDIX A: FIRST REPORT OF BRETZIELLA FAGACEARUM INFECTING CHESTNUT IN MICHIGAN.....	146
APPENDIX B: CLASSIFICATION AND SPORE LOADS ON OAK WILT FUNGUS, BRETZIELLA FAGACEARUM MYCELIAL MATS.....	147
APPENDIX C: SUPPLEMENTAL TABLES.....	158
APPENDIX D: SUPPLEMENTAL SAMPLING PROTOCOL.....	161

CHAPTER 1: A DIAGNOSTIC GUIDE FOR OAK WILT DISEASE IN OAK AND CHESTNUT

Abstract

Oak wilt caused by the ascomycete fungus *Bretziella fagacearum*, is a deadly vascular disease affecting numerous hosts in the Fagaceae family, including important forest species and orchard trees. The fungal pathogen is spread by nitidulid (Nitidulidae) vectors and through root grafts. Symptoms include leaf wilting, foliar desiccation, defoliation, limb dieback and/or mortality depending on the host species. This guide describes methods used to diagnose oak wilt in oak and chestnut. *B. fagacearum* is isolated from infected sapwood or nitidulid beetles using the acidified potato dextrose agar. Molecular identification of axenic cultures is based on the amplification and sequencing of LSU, 60S, MCM7, ITS and TEF1 α regions. Mix cultures can be confirmed with amplifications of the species-specific primers by conventional or real-time PCR. Current detection methods use DNA extracted directly from infected material and include the amplification of specific DNA regions through nested PCR, real-time PCR, or LAMP. Besides detailed protocols on how to diagnose the disease and confirm the presence of the causal agent, we include protocols on pathogen preservation and inoculation. Although this guide focuses on oaks and chestnut, the techniques included here can be implemented to diagnose oak wilt in other susceptible species.

Host

B. fagacearum can infect several hosts within the Fagaceae family, including oaks (*Quercus* spp.), chestnuts (*Castanea* spp.), chinkapins (*Castanopsis* spp.) and tanoak (*Lithocarpus* spp.), chinquapin (*Chrysolepis* spp.) (Bretz 1955, 1957; Bretz and Long 1950; Chahal et al. 2024). Additionally, artificial inoculation on mature apple plants (*Malus domestica*)

over 30 years old resulted in disease symptoms with successful re-isolation of the pathogen (Bart 1957, 1960). Over 50 Fagaceae species are recognized as host of *B. fagacearum* as determined by artificial inoculation studies or through natural infection (Table 1.1) (Appel 1944, 1986; Bretz 1951a, 1952a, 1953, 1955, 1957; Farr et al. 1989; Fergus and William 1953; Hoffman 1953; Jones 1958; Liese and Ruetze 1987; MacDonald et al. 2001; Parmeter et al. 1956). Except for *C. mollissima*, and hybrid *C. sativa* × *C. crenata*, all reports for non-*Quercus* spp. result from artificial inoculation experiments. Notably, American chestnut (*C. dentata*) appears to be susceptible only in indoor inoculation experiments (Ernst and Bretz 1953), not in the field inoculations (Merrill 1975). Oak species have different levels of susceptibility to *B. fagacearum*. Red oak species in the section *Lobatae* (i.e., *Q. rubra*, *Q. nigra*) are highly susceptible and can die within months of infection (Appel 1995; Chahal et al. 2022b). White oak species in the section *Quercus* (i.e., *Q. macrocarpa*, *Q. alba*) are moderate to low in susceptibility based on disease severity. In white oaks, *B. fagacearum* infection typically leads to branch dieback, and tree mortality is rare, sometimes taking decades to occur (Juzwik et al. 2011). Texas live oak (*Quercus fusiformis*, section *Virentes*) shows intermediate susceptibility compared to red and white oaks (Appel 1995). However, clonal propagation of Texas live oak through sprouts originating from a shared root system facilitates spread of *B. fagacearum*, leading to expanding pockets of mortality (Appel 1995). While there is variation in the rate of disease progression among oak species, none of the *Quercus* species are immune to the disease.

Pathogen

B. fagacearum, (Bretz) Z.W. de Beer, Marinc., T.A. Duong & M.J. Wingf. is a vascular wilt pathogen infecting mainly *Quercus* spp. and other Fagaceae. *B. fagacearum* is vectored by sap beetles (Nitidulidae) when spore-laden insects visit fresh wounds on healthy trees (De Beer

et al. 2017). The pathogen can be transmitted from an infected oak to healthy oaks via underground root grafts, leading to expanding disease centers, especially in stands where oaks are dominant or relatively abundant (Juzwik et al. 2011). Oak wilt was first described as a disease of oaks in 1942 in Wisconsin (Henry et al. 1944) and causal fungal pathogen was identified as *Chalara quercina* (Henry 1944). Bretz (1951b) and Hepting (1951, 1952) found that the fungus was heterothallic, and its sexual state could be induced by crossing opposite mating type isolates. Bretz (1952b) described the sexual state as *Endoconidiophora fagacearum*. Bakshi (1951) synonymized *Endoconidiophora* (Münch 1907) with *Ceratocystis*, a classification that quickly gained widespread acceptance (Hunt 1956). And oak wilt fungus was treated as *C. fagacearum* for six decades following Hunt (1956). Paulin-Mahady et al. (2002) proposed that the asexual state of *C. fagacearum* be classified as *Thielaviopsis quercina*, according to the dual nomenclature system. A phylogenetic study by De Beer et al. (2017) showed *C. fagacearum* belongs to a lineage distinct from the genera *Ceratocystis*, *Endoconidiophora*, *Thielaviopsis*, and *Chalara*. De Beer et al. (2017) concluded that this lineage represents an undescribed, monotypic genus in the Ceratocystidaceae, named *Bretziella*, Z.W. de Beer, Marinc., T.A. Duong & M.J. Wingf., gen. Nov.

Fungus

Kingdom Fungi, subkingdom Dikarya, phylum Ascomycota, subphylum Pezizomycotina, class Sordariomycetes, subclass Hypocreomycetidae, order Microascales, family Ceratocystidaceae, genus *Bretziella*, species *B. fagacearum* (De Beer et al. (2017). Phylogenetic analyses by De Beer et al. (2017) established the monophyletic genus *Bretziella* within Ceratocystidaceae to accommodate the oak wilt fungus due to its distinct differences from other genera. The formation of sporulating mats as mirror image structures on the outer sapwood and

inner phloem, with pressure cushions to open the bark, is unique to this species, further supporting the taxonomic revision. The current taxonomic description can be found at MycoBank

(<https://www.mycobank.org/page/Name%20details%20page/field/Mycobank%20%23/455495>)

or EPPO Global Database (<https://gd.eppo.int/taxon/CERAFA>). The ex-epitype specimen of *B. fagacearum*, isolated from *Q. rubra* in 1991 in West Des Moines, IA, is deposited at the Westerdijk Fungal Biodiversity Institute (Formerly Centraal Bureau voor Schimmelcultuur CBS, Fungal Biodiversity Center, Utrecht, Netherlands), specimen CBS 138363. And epitype (CMW 2656) of the same strain is deposited in Culture collection of the Forestry and Agricultural Biotechnology Institute, University of Pretoria, Pretoria, South Africa. DNA sequences obtained for the LSU, 60S, MCM7, ITS and TEF1 α regions of this strain have been deposited in the RefSeq Targeted Loci (RTL) database in NCBI GenBank (Schoch et al. 2014).

Vectors

Native sap or nitidulid beetles, belonging to the kingdom Animalia, phylum Arthropoda, class Insecta, order Coleoptera, superfamily Cucujoidea, family Nitidulidae, subfamilies, Carpophilinae, Cryptarchinae, and Nitidulinae are the primary vectors of *B. fagacearum*. Research studies conducted in oak wilt epidemic centers in the Midwestern states and Texas have been reported reported several *Colopterus* spp. and *Carpophilus sayi* serve as key vectors of *B. fagacearum* (Appel 1995; Ambourn et al. 2005, Cease and Juzwik, 2001, Jagemann et al. 2018, Juzwik et al. 2004, Juzwik et al. 2011). Oak bark beetles belonging to the kingdom Animalia, phylum Arthropoda, class Insecta, order Coleoptera, superfamily Curculionoidea, family Curculionidae, subfamily Scolytinae, genus *Pseudopityophthorus*, species *P. minutissimus*, *P. pruinosus* have been implicated as vectors of *B. fagacearum* in controlled

environment experiments (Rexrode and Jones 1970). However, it is unlikely that bark beetles satisfy the criteria (Leach 1940) to serve as vectors of *B. fagacearum* in nature. Although, bark beetles may acquire *B. fagacearum* during feeding and colonization on oak wilt infected trees (Ambourn et al. 2006; Buchanan 1956; Stambaugh et al. 1955), however they commonly feed on stressed/diseased trees (Chahal et al. 2019a), which reduces the likelihood of initiating an infection on healthy oaks.

Symptoms and signs

Foliar symptoms are most notable in red oaks, appear within 2 to 4 weeks of infection, leading to rapid crown wilting (Chahal et al. 2022b; Juzwik et al. 2011). Wilt usually starts at the top or outer areas of the crown and progresses downward, varying with pathogen entry. For instance, the side of the crown nearest to a diseased tree may wilt first, indicating fungal invasion through connected roots (Juzwik et al. 2011, K. Chahal, *unpublished data*). Initial symptoms include terminal leaf wilting (green wilting), progressing to leaf desiccation or bronzing, sometimes with a water-soaked appearance (Fig. 1.1) (Chahal et al. 2019b; Juzwik et al. 2011). Leaves later turn yellow and/or brown, curl around the midrib and are shed at branch tips. Leaf abscission of completely green and symptomatic leaves is a distinctive feature of the disease. Oak wilt-infected trees are often discovered by the symptomatic leaves littering the ground during peak growing season. On individual leaves, characteristic tanning, not restricted by leaf veins, start from outer edges and progressed towards the midrib and base of leaves. Short-lived water sprouts or epicormic shoots may grow on trunks and large limbs but soon become symptomatic. Desiccated leaves may remain attached to branches for a few months (Fig 2). Crown symptoms in the white oak group are variable (Juzwik et al. 2011; Parmeter 1956). While white oaks can show quick mortality like red oaks, they typically decline slowly over several

years, with only a few branches dying each year and leaves often remaining attached with marginal discoloration. Sometimes, white oaks may even recover from infection (Juzwik et al. 2011). In Texas, live oaks develop symptoms more slowly than red oaks but usually die within 3 to 8 months (Appel 1986). Distinctive symptoms in live oaks include veinal chlorosis and necrosis, along with typical leaf abscission (Appel 1995).

Internal symptoms include vascular staining in the xylem (sapwood) of branches and main stem of diseased trees (Fig. 1.2). In white oak species, this discoloration appears as dark brown to black streaks in the outer xylem when the bark is removed from an infected branch. A ring of discolored xylem tissue may also be visible in cross-sections of such branches. In red oak species, bluish gray to dark brown vascular discoloration occurs but is often more difficult to detect.

The diagnostic sign and sporulation structures of *B. fagacearum*, known mycelial mats (Fig. 1.2), predominantly occur on red oaks, rarely on white oaks and have never reported on Texas live oak (Appel 1986; Juzwik et al. 2011). Mycelial mats typically form on recently killed trees, but their concealed nature and the deeply furrowed bark of large diameter oaks make them challenging to detect (Appel 1995). These mats can cause vertical cracks in the tree bark, serving as symptoms of oak wilt (Chahal et al. 2021). Another diagnostic feature is expanding infection centers (Fig. 1.3), indicating root-graft transmission of the pathogen (Blaedow and Juzwik 2010) which accounts for 95% of tree mortalities compared to the 5% caused by insect vectors.

Oak wilt look-alikes

Oak wilt symptoms can be confused with other biotic and abiotic stressors commonly observed in oaks. These symptoms can be confused with bacterial leaf scorch (*Xylella fastidiosa*), Armillaria root rot (*Armillaria* spp.), Anthracnose (*Apiognomonina quercinia*), bur

oak blight (*Tubakia iowensis*), Tubakia leaf spot (*Tubakia* spp.), and oak decline (Abrams 2003; Gould and Lashomb 2007; Harrington et al. 2012; Lee et al. 2016; Pearce and Williams-Woodward 2009). Abiotic stress and insect infestations such as environmental scorch, two-lined chestnut borer (*Agrilus bilineatus*), cynipid gall wasp (*Cynipis* spp.) can result in crown flagging resembling oak wilt symptoms (Haack and Acciavatti 1992; Rauschendorfer et al. 2022). Annual repeated spongy moth (i.e. *Lymantria dispar*) infestation may cause dieback of twigs and branches in the upper crown, sprouting of epicormic shoots, and eventually leading to tree death (Haack and Acciavatti 1992). Leaf galls, such as cynipid wasp gall, may lead to leaf shedding later in the summer and fall, coinciding with the period when leaf fall due to oak wilt is commonly observed (Stone et al. 2002; Scott Lint, *personal communication*). Under heat or drought stress, particularly where drought conditions prevail, leaf shedding tends to occur when temperatures exceed 29-32°C (85-90°F) in summer (Scott Lint, *personal communication*). An entire tree affected by environmental leaf scorch may exhibit a reddish-brown crown (Rauschendorfer et al. 2022), which can be misidentified as/misjudged to be oak wilt. In the past decade, concerns have escalated regarding herbicide injury in red oaks, varying from minor damage to severe outcomes such as tree death (Samtani et al. 2010). This issue is exacerbated by the high sensitivity of red oaks to Imazapyr, further complicating *B. fagacearum* detection (Scott Lint, *personal communication*). Variability in symptoms development in white oaks poses an additional challenge for diagnosing based on crown symptoms (Juzwik et al. 2011). Due to these oak wilt look-alike issues a precise and timely laboratory diagnosis is crucial when implementing management options (Chahal et al. 2019b).

Geographical distribution

The origin of *B. fagacearum* is unknown, it seems likely that the fungus was introduced into the U.S. from Mexico, Central or South America (Hipp et al. 2018; Juzwik et al. 2008). Oak wilt was first described as a disease of oaks in 1942 in Wisconsin (Henry et al. 1944). However, historical accounts indicate oak wilt likely killing oaks as early as the 1890s in the upper Mississippi River valley (Gibbs and French 1980). In the two decades following its initial discovery, oak wilt was reported from midwestern, north-central, mid-Atlantic states and Texas, where it affects live oaks (Rexrode and Lincoln 1965). Though first officially documented in Texas in 1961, records of widespread live oak mortality exhibiting features similar to oak wilt from the 1930s suggest that the disease may have been present for a longer period (Appel 1995). Currently, oak wilt has been confirmed in 24 states (Arkansas, Illinois, Indiana, Iowa, Kansas, Kentucky, Maryland, Michigan, Minnesota, Mississippi, Missouri, Nebraska, New York, North Carolina, Ohio, Oklahoma, Pennsylvania, South Carolina, South Dakota, Tennessee, Texas, Virginia, West Virginia, Wisconsin.) in the U.S with widespread epidemics are reported in the midwestern states and Texas (Fig. 1.4) (Chahal et al. 2019b, 2021; Juzwik et al. 2011). Geographic range of oak wilt is limited, considering suitable hosts and climates in parts of the western U.S., like California (Appel 1994), and nonaffected areas in the northeast and southeast. However, oak wilt continues to spread and is expanding into new geographical locations where it was not previously reported (Gauthier et al. 2023; McLaughlin et al. 2022). Detection of oak wilt in Ontario, Canada, in June 2023 marked the first time this pathogen had been identified outside the U.S. (Canadian Food Inspection Agency 2023).

Pathogen isolation and insect-vectors monitoring

B. fagacearum can be isolated from asymptomatic sapwood, however symptomatic xylem is preferred due to consistent recovery from discolored sapwood (Pokorny 1999; K. Chahal, unpublished data). Pokorny (1999) provides a detailed protocol for sampling and isolating *B. fagacearum* from branch and stem samples. From each tree, select at least three recently wilted branches (15-20 cm long, 2.5-5 cm diameter) with green cambium and discolored sapwood. Keep samples in a sealed plastic bag and cold until delivered to a diagnostic clinic. In the lab, wipe samples with 70% ethanol and expose the sapwood using a sterile razorblade or drawknife. Briefly, flame-sterilize the samples after spraying with 95% ethanol (Fig. 1.5). Excise sapwood chips (~1.5 x 0.5 cm) from the outer 1-2 sapwood rings. Culture 5 chips per Petri dish (4 plates/tree) containing acidified potato dextrose broth (aPDA) and incubate at room temperature and ambient light. *B. fagacearum* colonies can be observed after 5-7 days. Gray to olive-green colonies of *B. fagacearum* can be confirmed from a fruity odor, and presence of endoconidia (De Beer et al. 2017). Following a non-destructive sampling approach, *B. fagacearum* can be isolated from petioles of fallen leaves (K. Chahal, unpublished data).

B. fagacearum can also be isolated from nitidulid insect-vectors. Beetles can be collected and monitored using funnel, modified pitfall and wind-oriented traps designed for nitidulid beetles (DiGirolomo et al. 2020; Dowd et al. 1992). Traps can be baited with fermenting whole wheat bread dough (Morris 2020), fermenting liquid (DiGirolomo et al. 2020) and male-produced aggregation pheromone lures available for *Ca. sayi*, and *Co. truncatus* (Great Lakes IPM, Vestaburg, MI) (Bartelt et al. 2004, Cosse and Bartelt 2000, Kyhl et al. 2002). Nitidulid beetles are attracted to fresh wounds on healthy oaks (Dorsey et al. 1953, Juzwik et al. 2004; Norris 1956) and mycelial mats produced under the bark on trunks and large branches of red

oaks recently killed by oak wilt (Cease and Juzwik 2001; Juzwik and French 1983). Beetles can be directly collected from fresh wounds and mycelial mats (Cease and Juzwik 2001; Hayslett et al 2008; Juzwik et al. 1998). Once captured, individual beetles are transferred to sterile 1.7-ml microcentrifuge tubes and macerated in 500 μ l of sterile deionized water using a tip sonicator for 3-5 s. The beetle suspension is serially diluted to make two additional 10-fold dilutions. Then 500-900 μ l aliquots of each dilution and 100 μ l of undiluted rinsate are spread onto duplicate aPDA plates, totaling five Petri dishes per beetle (Morris 2020). Alternatively, dilutions can be plated onto Barnett's agar medium (Barnett 1953a) and mating type of fungal propagules can be determined using a spermitization assay as detailed in Appel et al. (1990). Cultures are incubated at 25°C in the dark and inspected periodically for 14 days. Number of *B. fagacearum* colonies on each plate is counted and colony forming units per beetle are calculated (Morris 2020; Hayslett et al. 2008).

Pathogen identification

A detailed morphological description of *B. fagacearum* can be found in Barnett (1953b) and De Beer et al. (2017). Two-week or older colonies growing on PDA present a fluffy mycelial mat, 1-3 mm high, gray to olive-green with occasional patches of tan, and a characteristic fruity odor. Conidiophores are cylindrical tapering towards the apex, single, upright, straight or slightly curved, occasionally branched, 3-9 septate, up to 140 μ m long including conidiogenous cells, 3–5 μ m wide at the base (De Beer et al. 2017). Conidiogenous cells are cylindrical, tapering towards the apex, 20–32 μ m long, 2.5–3.5 μ m wide at the base, 2–3 μ m wide near the apex. Conidia are endogenous, hyaline, one-celled, rectangular shaped, 4–8.5 \times 2–3 μ m, produced in chains. The presence of typical conidiophores and endoconidia is usually considered as positive identification of *B. fagacearum* (Barnett 1953b; Pokorny 1999). But caution should be used since

endoconidia producing other fungi have been isolated from infected oaks and nitidulid beetles (K. Chahal, unpublished data). Phenotypic plasticity across *B. fagacearum* isolates collected from different host and geographical locations has been observed (Fig 6). Molecular identification must be considered if morphological identification of axenic cultures is doubtful. Amplification and sequencing of the ITS, TEF1 α and phylogenetically important genes for *B. fagacearum* such as LSU, 60S, MCM7 regions of reference isolates are frequently used to confirm the species (Schoch et al. 2014). But this method relies on using axenic cultures and requires additional time and resources for Sanger sequencing. Using species-specific primers targeting the ITS rDNA region Kurdyla and Appel (2011), Bourgault et al. (2022) and EF1 Lamarche et al. (2015) able to identify *B. fagacearum* either through conventional or real-time PCR. A rapid identification of *B. fagacearum* colonies from axenic and mixed cultures can be performed using a DNA extraction as detailed in Chahal et al. (2022a).

A critical aspect in oak wilt diagnosis is the ability to detect the pathogen directly from infected plant tissue or from the nitidulid insect vector. Molecular assays for detection of *B. fagacearum* in sapwood include three real-time PCR assays (Bourgault et al. 2022; Kurdyla and Appel 2011; Lamarche et al. 2015), a nested PCR (Wu et al. 2011), a nanoaggregation-enhanced chemiluminescence assay (Singh et al. 2017) and an in-field detection assays include DNA endonuclease-targeted CRISPR trans reporter (DETECTR) (Bourgault et al. 2022). Sapwood samples can be obtained from sawdust obtained with a 2.8-mm-diameter drill bit or wood shavings removed with a scalpel or knife (Fig. 1.5) (Chahal et al. 2022a). The DNA extractions from sapwood samples are performed using QIAamp Fast DNA Stool Mini Kit (Qiagen, Germantown, MD) following the manufacturer's suggested protocol. The tissue lysis step of incubation at 95°C for 5 min is opted. Sapwood and petiole pieces are transferred into Lysing

Matrix A (MP Biomedicals, SKU:116910050-CF) 2-ml tubes with two ceramic beads. After adding 1000 μ l of InhibitEX buffer, samples are macerated using a Bead Mill 24 homogenizer (Fisher Scientific) or FastPrep-FP120 (Thermo Fisher Scientific, Waltham, MA), with two 45-second cycles at 6.5 m/s speed and a 5-minute rest in between. Samples were visually inspected to confirm complete maceration. If necessary, a third maceration cycle was performed. Primer and probe sequences of the molecular assays are presented in Table 1.2. The in-field detection assay (DETECTR) (Bourgault et al. 2022) and the commercially available LAMP assay (AgroLAMP, PureBioX, Saint Paul, MN), lack in detection accuracy. Therefore, there is still a need to develop or optimize field-deployable technologies to detect molecules secreted by the pathogen or by the host in host colonization.

Pathogen storage

Single-spore or hyphal-tip isolates of *B. fagacearum* can be sub-cultured on fresh media (PDA, acidified PDA) for short-term storage without any reported loss of virulence. For Medium-term storage of up to 2 years, samples are kept at 4 to -20°C . Agar plugs exhibiting sporulation from 12- to 14-day-old cultures are cut out using a sterile scalpel or cork-borer and placed into 1.5 or 2-ml sterile centrifuge tubes or cryovials. To facilitate further growth of mycelium around cut plugs, tubes are kept at room temperature for 48 to 72 hours before storing at 4 or -20°C freezers. Another method involves growing mycelium in potato dextrose broth for 7-10 days, harvesting, drying with sterile paper towels, wrapping it in aluminum foil, and storing it at -20°C . For long-term storage beyond 3 years, harvested mycelium (scraped from Petri dishes or grown in broth) can be lyophilized in cryovials and immediately stored at -80°C . Alternatively, harvested mycelium is frozen in 15 % glycerol. Sporulating mycelium is scraped off and transferred to 2-ml sterile cryovials, sterile 15% glycerol is added until the mycelium is

submerged. If mycelial plugs taken with media chunks, glycerol concentration of 40% can be used. The cryovials are kept at 4°C overnight before moving to -80°C. To revive the isolate, an agar piece is removed with sterile forceps and placed in a microcentrifuge tube with 1 ml of phosphate buffer saline (Li and Hulcr 2020). The tube is inverted to wash off excess glycerol, and the agar plug is then transferred to an agar plate. The Microbank system (ProLab Diagnostics, PL.170C) is efficient, effective for long-term storage of *B. fagacearum* at -80°C. It includes cryogenic vials with 25 porous glass beads in a cryopreservative solution. A piece of sporulating agar (~1 × 0.5 cm) is excised with a sterile scalpel and transferred to the vial. The vial is vortexed at low speed for 20 seconds and incubated at room temperature for at least 1 hour to allow conidia to bind to the beads. After incubation, 380-400 µl of cryo-preservative is removed, the vial is sealed tightly, and stored in -80°C. To revive an isolate, remove a Microbank vial from -80°C using a freezer block. Extract a single bead with a sterile loop or forceps and streak or embed it onto solid media (PDA or aPDA). Return the Microbank vials to -80°C as soon as possible to maintain the viability of isolates. Only remove vials needed for revival without thawing the entire Microbank.

Pathogenicity tests

Conidial suspensions for inoculations can be prepared by growing *B. fagacearum* on full-strength Potato Dextrose Agar (PDA) or acidified PDA (80% lactic acid, JT Baker, Phillipsburg, NJ) for two weeks at room temperature (~24°C) under ambient lighting. To make acidified PDA, 1 ml of 80% lactic acid was added into autoclaved 1 L of full-strength PDA. To dislodge the endoconidia plates are flooded with sterile deionized water (3 ml) and colony surfaces are gently scraped with a microbiological loop (Navia-Urrutia et al. 2022). Harvested conidial suspensions are filtered twice using a double layer of Miracloth (Miracloth, EMD Millipore, Billerica, MA)

to remove potential mycelium and hyphae. A high concentration of inoculum, 1×10^7 conidia per ml required for seedlings with non-lignified stems comparative to 1×10^6 conidia per ml for mature field trees because only a small amount of inoculum suspension can be introduced into the stem holes on seedlings (Chahal et al. 2019b, 2022b, 2024). Therefore, multiple plates with sporulating colonies might be required. The stock solution might need to be diluted (e.g., 1:10 dilution) to count the propagules accurately using a hemocytometer. To confirm the concentration of the suspension, serial dilutions (10^{-1} to 10^{-6}) are prepared, and 100 μ l of the 10^{-5} and 10^{-6} dilutions are spread over agar plates (PDA or acidified PDA) with a glass rod, in triplicate. Additionally, plates are prepared from the remaining inoculum suspension after the inoculation process to check if propagule viability was affected by temperature changes or light exposure. The spore germination is assessed after 24 hours using a compound microscope. A spore is considered germinated when the germ tube is equal to or greater than the size of the spore itself. Seedling inoculations is performed using a conical drill bit, two 0.4 mm diameter holes are drilled, one is 5 cm above the soil line at a 45° angle and the other is on the opposite side of the stem at least 10 cm above the soil line (Fig. 1.7). In each hole, 50 μ l conidial suspension (100 μ l total, 10^6 conidia per plant) is applied and the holes are sealed with Parafilm (Chahal et al. 2024). Inoculated plants are maintained under greenhouse conditions (12-hour photoperiod, $27 \pm 2^\circ\text{C}$), with initial symptoms typically appearing 14 days post-inoculation. Before the green or brown leaf wilting, Leaf epinasty with bent petioles is commonly observed (Fig. 1.6). Inoculation on mature field trees is done using an increment borer (Forestry Suppliers, Jackson, Mississippi, USA, stock number: 63383), two 12 mm diameter, 3 - 4 cm deep holes perpendicular at DBH to the north and south direction of each tree are made (Chahal et al. 2019b, 2022b). A one ml conidial suspension containing 1×10^6 conidia is poured dropwise into

each hole on a tree using a syringe (BD 1 ml syringe, BD Franklin Lakes, NJ) without needle. The inoculation hole entrances are plugged using a silicone sealant (GE silicones, manufacturer no. 2812566) and then the tree trunk was wrapped with a bench paper (Cole-Parmer, manufacturer no. F246750000) to avoid entry of sap beetles. Deionized sterile water is used for mock inoculations. Two weeks after inoculation, disease severity is assessed on a scale of 1 to 10 or 1 to 5, based on the percentage of leaves exhibiting symptoms (Navia-Urrutia et al. 2022; Pegg et al. 2011). *B. fagacearum* is reisolated from symptomatic seedlings by surface sterilizing various disease samples such as branch sapwood chips or petioles with 75% ethanol (30 s), followed by 10% (v/v) bleach (1 min), and two rinses with sterile deionized water (>1 min) (Chahal et al. 2024). Diseased samples are plated on Petri dishes containing aPDA and incubated at room temperature and ambient light for 10-14 days. Recovered colonies of *B. fagacearum* can be observed and confirmed using the procedures described before.

Acknowledgments

We appreciate Scott Lint's feedback on the various look-alikes of oak wilt, which pose challenges in its diagnosis and currently lack detailed descriptions in the literature.

Figures

Figure 1.1. Foliar symptoms of oak wilt. Initially, leaves exhibit wilting, resembling physiological wilt or drought stress (**A**). Subsequently, leaves transition to a dull green to bronze hue, displaying a water-soaked appearance with heightened wilting (**B**). Ultimately, the leaves adopt a yellow to brown coloration and exhibit curling around the midrib (**C**). Notably, a distinctive progression of well-defined bronzing and tanning is often observed on fallen leaves, originating from the leaf blade, and progressing towards the midrib and base of the leaves; species of red oaks (**D, E**) and white oak (**F**). In live oaks, leaves exhibit interveinal chlorosis (**G**), and marginal scorch or tip burn (**H**). Epicormic shoots frequently emerge on red oaks (**I**), but eventually succumb to the infection (**J**). Photo credits: All pictures by Karandeep Chahal, except **G** and **H** by Demian Gomez, Texas A&M Forest Service.

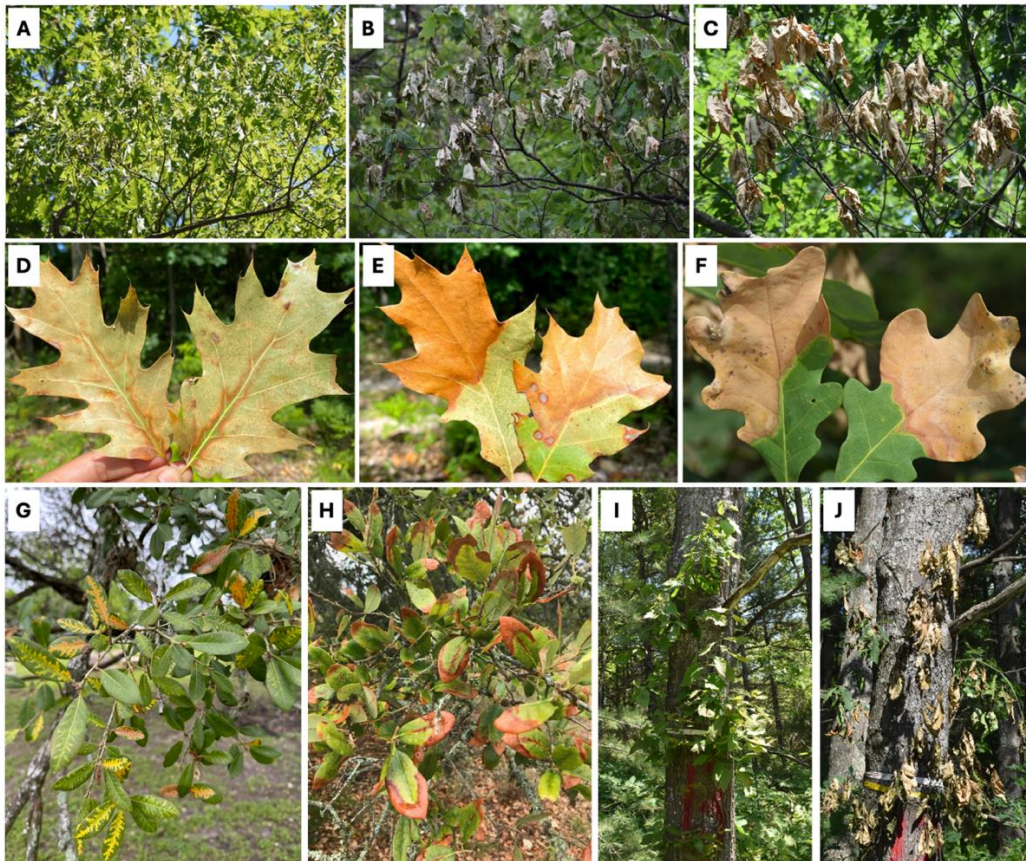


Figure 1.2. Oak wilt progression on northern red oak, *Quercus rubra* and internal symptoms, signs, and key vectors of *B. fagacearum*. Early (**A**), advanced (**B**) and symptoms at complete mortality (**C**). Internal symptoms include sapwood discoloration, on branch (**D**, infected branch on left, healthy branch without discoloration on right), in the outermost xylem rings (**E**), and on main stem (**F**). Bark cracks (**G**), indicate the formation of mycelial mats (**H**), a sign of *B. fagacearum*. The key insect vectors of *B. fagacearum*, *Carpophilus sayi* (**I**), and *Colopterus truncatus* (**J**). Photo credits: All pictures by Karandeep Chahal, except **I** and **J** by Joe A. MacGown, Mississippi Entomological Museum, Mississippi State University.

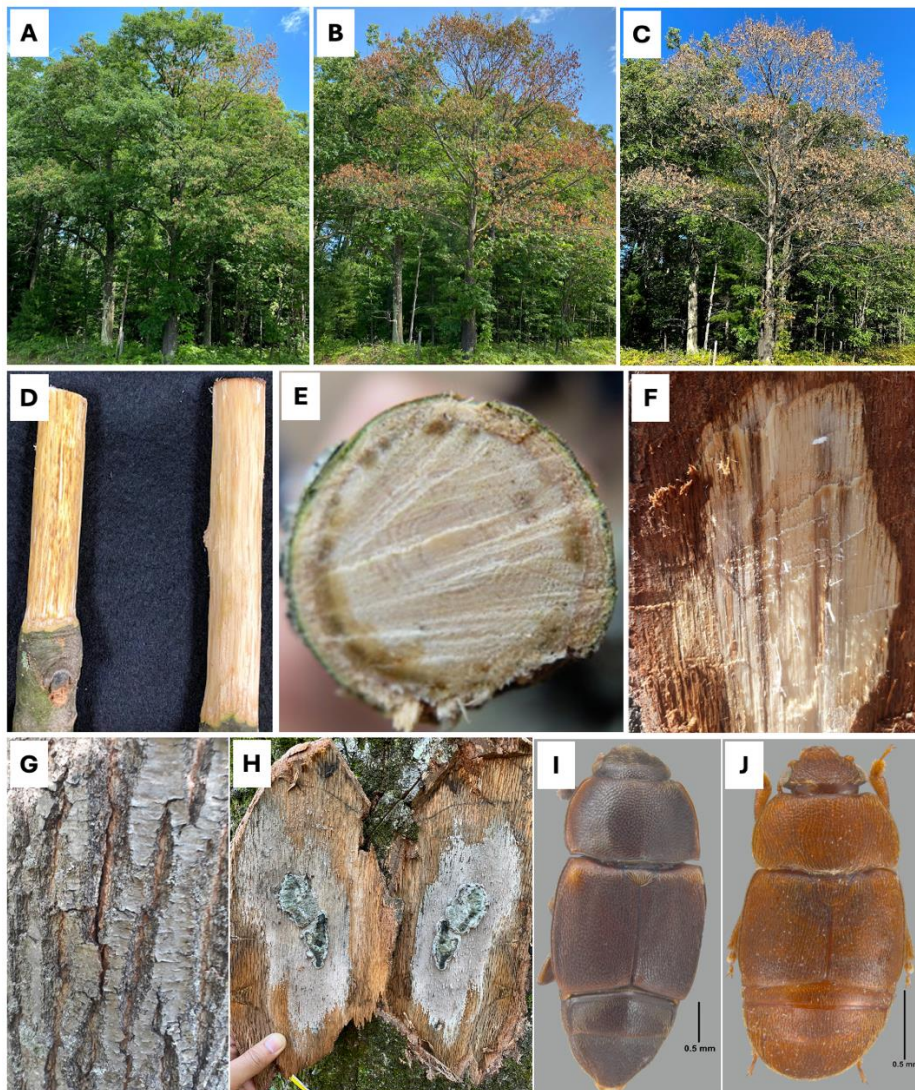


Figure 1.3. Oak wilt infection centers. Expanding *B. fagacearum* infection centers indicate root-graft transmission of the pathogen in northern red oak (A), Texas live oak (B), and chestnut (C).

Photo credit: All pictures by Karandeep Chahal, except B by Demian Gomez, Texas A&M Forest Service.

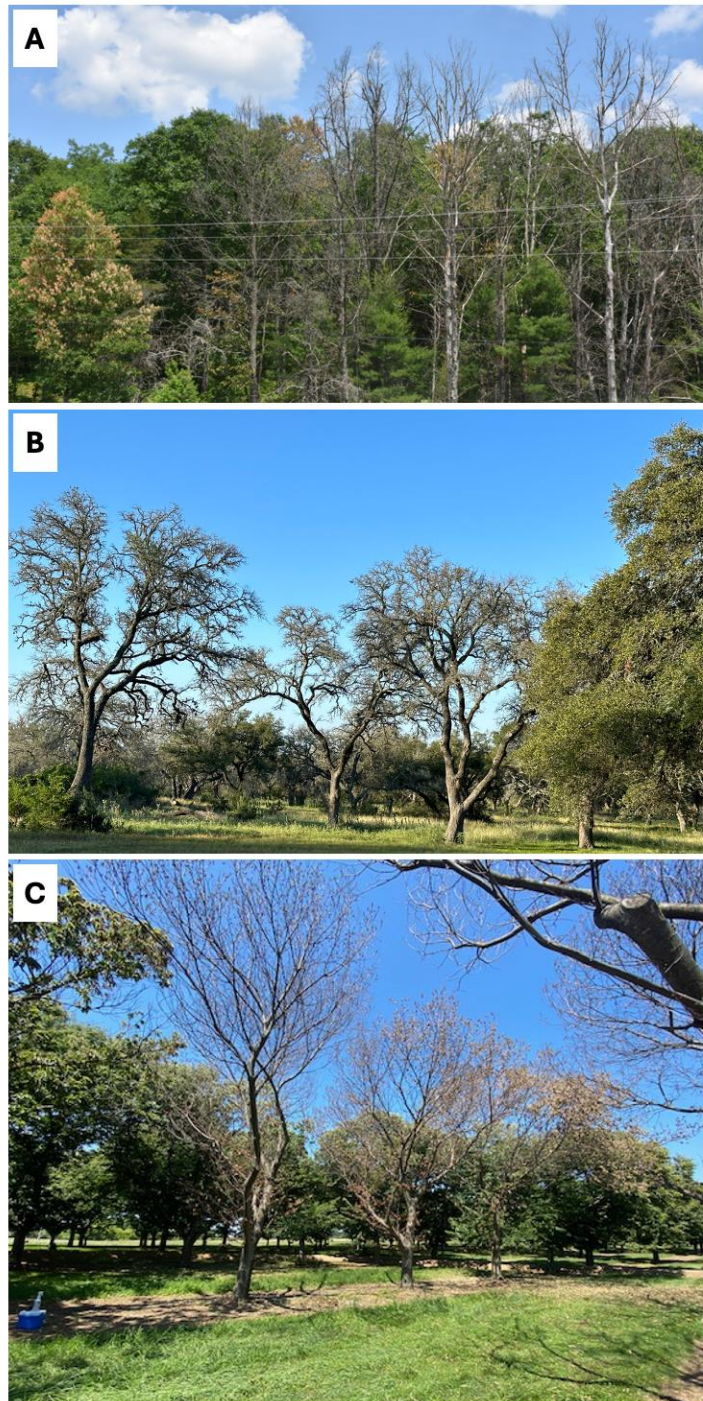


Figure 1.4. Oak wilt distribution in the United States and Canada. Labelled counties in the light green color indicate the confirmed report(s) from respective counties not the magnitude of disease incidence. Source: EDDMapS. 2024. Early Detection & Distribution Mapping System. The University of Georgia - Center for Invasive Species and Ecosystem Health. Available online at <http://www.eddmaps.org/>. Last accessed June 13, 2024.

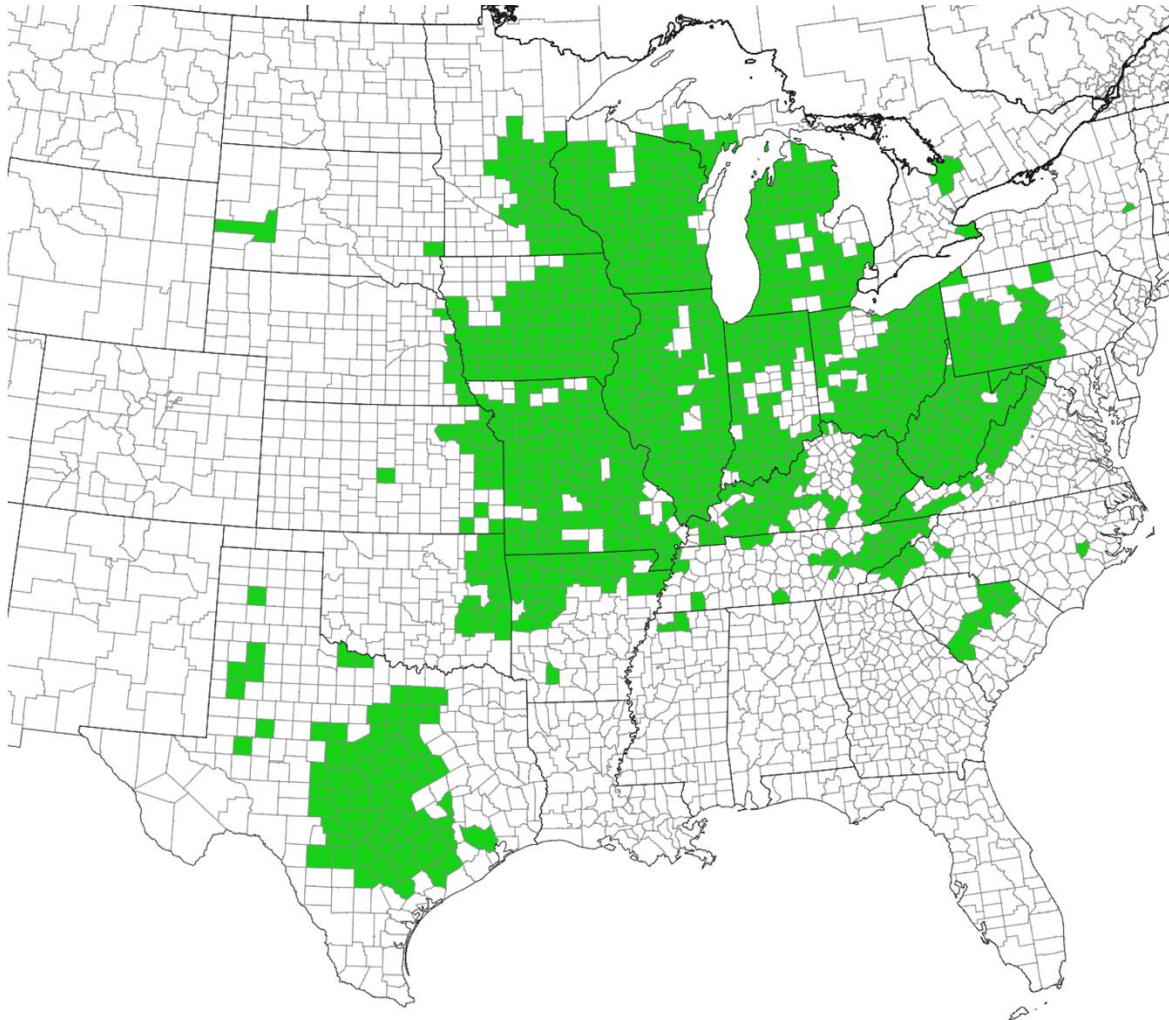


Figure 1.5. Sample collection, isolation, and molecular detection of *Bretziella fagacearum*.

Select branch samples with sapwood discoloration, *Quercus rubra* (A), streaking on *Q. alba* (B), absent (C). Flame sterilize samples after spraying with 95% ethanol (D). Only the outer 1-2 layers of sapwood are excised (E) and cut into ~1.5 X 0.5 cm chips for plating (F). A microfunnel (G) (bottomless microcentrifuge tube) is used to collect drill shavings (H), while drilling directly on the symptomatic tissue (I). Excised sapwood slivers chopped into ~0.3 X 0.2 cm pieces for DNA extraction (J). For *B. fagacearum* isolation wood chips are plated onto acidified potato dextrose agar: brownish to olive-green mycelium growing from infected tissue can be observed 10 days after incubation on upper and underside of the plate, respectively (K, L). Individual *B. fagacearum* colonies from beetle rinsates can be detected on Petri dishes when observed against light (M).

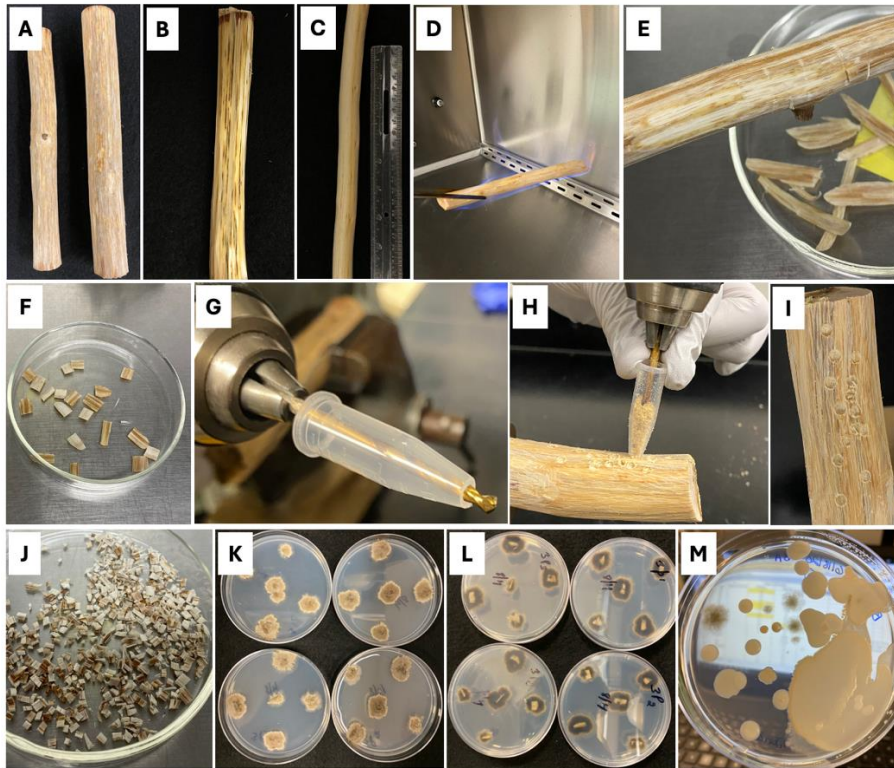


Figure 1.6. Variations in the colony morphologies of *Bretziella fagacearum*.

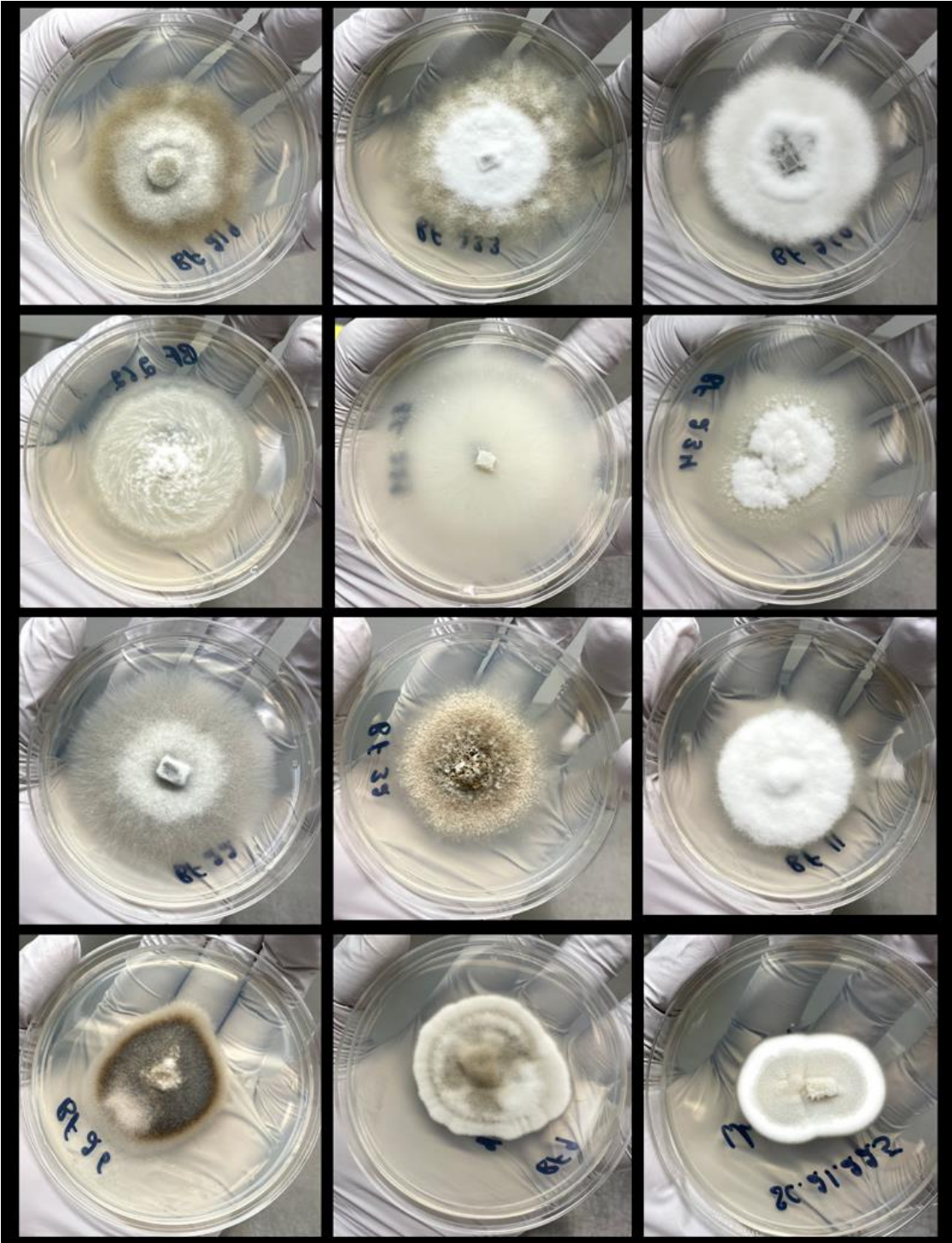
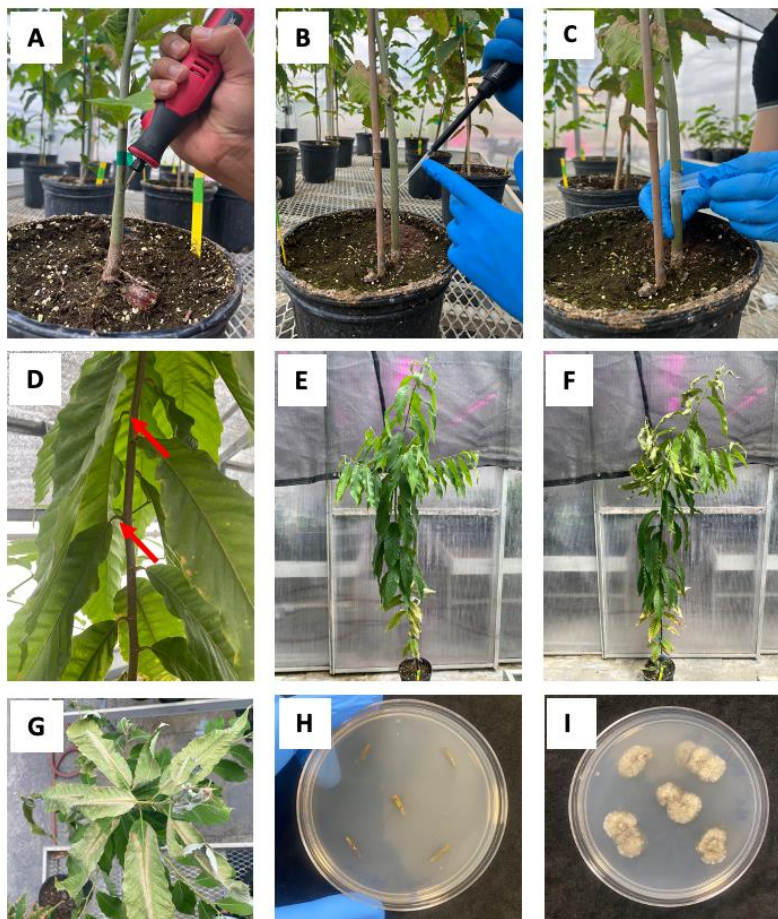


Figure 1.7. Pathogenicity trial of *Bretziella fagacearum* on chestnut cv. ‘Colossal’ seedlings.

Inoculations were performed after making two drill holes using a conical drill bit at a 45° angle (A), 50 µl of the inoculum was placed into each hole using a micropipette (B), and holes were wrapped with Parafilm to avoid inoculum evaporation (C). External symptoms starting with the bending of the petiole were visible after 14 days (D), and subsequently “physiological” (E) and “necrotic” (F) leaf wilting was observed. A “classic” foliar symptom of oak wilt, well-defined tanning of the leaf tips and outer edges that move towards the midrib and base of leaves was observed (G). *Bretziella fagacearum* was reisolated from symptomatic plants: surface sterilized petioles were placed onto acidified potato dextrose agar (H). Mycelium growing from infected tissue can be observed 7 days after incubation (I).



Tables

Table 1.1. Hosts in the Fagaceae family known to be susceptible to the oak wilt fungus, *Bretziella fagacearum*.

Scientific name	Common name	Place of origin
<i>Castanea dentata</i>	American Chestnut	North America
<i>Castanea mollissima</i>	Chinese Chestnut	China
<i>Castanea pumila</i>	Allegheny Chinkapin	United States
<i>Castanea sativa</i>	Sweet Chestnut	Southern Europe, Asia Minor
<i>Castanea sativa</i> × <i>C. crenata</i>	Hybrid Chestnut	Cultivated Hybrid
<i>Castanopsis kawakamii</i>	Kawakamii Oak	China, Taiwan
<i>Chrysolepis sempervirens</i>	Bush Chinquapin	Western United States
<i>Lithocarpus densiflorus</i>	Tanoak	Western North America
<i>Notholithocarpus densiflorus</i>	Tanoak	Western North America
<i>Quercus acuta</i>	Japanese Evergreen Oak	Japan, Korea, Taiwan, China
<i>Quercus acutissima</i>	Sawtooth Oak	East Asia
<i>Quercus agrifolia</i>	Coast Live Oak	California, USA
<i>Quercus alba</i>	White Oak	Eastern North America
<i>Quercus aliena</i> var. <i>acutesserrata</i>	Oriental White Oak	East Asia
<i>Quercus brutia</i>	Calabrian Oak	Eastern Mediterranean
<i>Quercus castaneaefolia</i>	Chestnut-leaved Oak	Western Asia
<i>Quercus cerris</i>	Turkey Oak	Southern Europe, Asia Minor
<i>Quercus chrysolepis</i>	Canyon Live Oak	Western United States
<i>Quercus coccinea</i>	Scarlet Oak	Eastern and Central United States
<i>Quercus dentata</i>	Japanese Emperor Oak	East Asia
<i>Quercus dumosa</i>	California Scrub Oak	California, USA
<i>Quercus durata</i>	Leather Oak	California, USA
<i>Quercus ellipsoidalis</i>	Northern Pin Oak	Midwestern United States
<i>Quercus engelmannii</i>	Engelmann Oak	California, USA
<i>Quercus falcata</i>	Southern Red Oak	Southeastern United States
<i>Quercus fusiformis</i>	Texas Live Oak	Texas, USA
<i>Quercus garryana</i>	Oregon White Oak	Pacific Northwest, USA
<i>Quercus glandulifera</i>	Oriental White Oak	East Asia

Table 1.1. (cont'd)

<i>Quercus glauca</i>	Ring-cupped Oak	East Asia
<i>Quercus haas</i>	Herder Oak	Caucasus, Northern Iran
<i>Quercus ilex</i>	Holm Oak	Mediterranean region
<i>Quercus ilicifolia</i>	Bear Oak	Eastern United States
<i>Quercus imbricaria</i>	Shingle Oak	Eastern and Central United States
<i>Quercus kelloggii</i>	California Black Oak	Western United States
<i>Quercus laevis</i>	Turkey Oak	Southeastern United States
<i>Quercus laurifolia</i>	Laurel Oak	Southeastern United States
<i>Quercus lobata</i>	Valley Oak	California, USA
<i>Quercus longinux</i>	Gansu Oak	China
<i>Quercus macrocarpa</i>	Bur Oak	North America
<i>Quercus macrolepis</i>	Valonia Oak	Mediterranean region
<i>Quercus marilandica</i>	Blackjack Oak	Central and Eastern United States
<i>Quercus muehlenbergii</i>	Chinkapin Oak	Central and Eastern United States
<i>Quercus myrsinifolia</i>	Bamboo-leaf Oak	East Asia
<i>Quercus nigra</i>	Water Oak	Southeastern United States
<i>Quercus palustris</i>	Pin Oak	Central and Eastern United States
<i>Quercus petraea</i>	Sessile Oak	Europe
<i>Quercus phellos</i>	Willow Oak	Southeastern United States
<i>Quercus prinus</i>	Chestnut Oak	Eastern United States
<i>Quercus pubescens</i>	Downy Oak	Southern Europe, Western Asia
<i>Quercus robur</i>	English Oak	Europe
<i>Quercus rubra</i>	Northern Red Oak	Eastern North America
<i>Quercus shumardii</i>	Shumard Oak	Central and Eastern United States
<i>Quercus stellata</i>	Post Oak	Central and Eastern United States
<i>Quercus suber</i>	Cork Oak	Western Mediterranean
<i>Quercus texana</i>	Nuttall Oak	South-central United States
<i>Quercus thomasii</i>	Swamp Chestnut Oak	Southeastern United States
<i>Quercus tomentella</i>	Island Oak	California Channel Islands, USA
<i>Quercus variabilis</i>	Chinese Cork Oak	East Asia
<i>Quercus velutina</i>	Black Oak	Eastern North America

Table 1.1. (cont'd)

Quercus virginiana
Quercus wislizenii

Southern Live Oak
Interior Live Oak

Southeastern United States
California, USA

Table 1.2. Primers used for identification and detection of *Bretziella fagacearum*.

Primer or probe	Sequence (5'-3')	Methodology	Reference	Target gene	Amplicon length (bp)
ITS1F	CTTGGTCATTTAGAGGAAGTAA	Nested PCR	Gardes and Bruns 1993	ITS	600
ITS4R	TCCTCCGCTTATTGATATC		White et al. 1990		
CF01	GGCAGGGACTTCTTTCTT		Wu et al. 2011		280
CF02	AAGGCTTGAGTGGTGAAG		Wu et al. 2011		
Cfp2-01	TGGCAGGGACTTCTTTCTTCA	Real-time PCR	Kurdyla and Appel (2011)	ITS	
Cfp2-02	TGGTTAAATGCAACTCAGCAATGA				
Cfp2	56-FAM/ATGTTTCTGCCAGTA GTATT/3BHQ_1				
Cfag_F315	GTCTGTAGAAGGGGG	Real-time PCR	Lamarche et al. 2015	EF1	92
Cfag_R406	CTCCATTCCTTACTACAAC				
Cfag_T357	6-Fam/AGAAGTAAC/ZEN/ TGGACAACCGTCT/3IABkQ				
Probe DNA 1	ACTCAGCAATGA-thio	nanoaggregation-enhanced chemiluminescence assay	Singh et al. 2017	ITS	
Probe DNA 2	thio-TGGTTAAATGCA				
Cfag ITS F 75-97	TAAAACCATTTGTGAACATACCA	Real-time PCR	Bourgault et al. (2022)	ITS	168
Cfag ITS R2 215-43	TGAAAGTTTTAACTATTTTGTTAAA TGCA				
Cfag ITS T RC 126-50	AACATCCCCTGAAGAAAGAAGTCC				

Table 1.2. (cont'd)

Cfag ITS crRNA-2	TGCCAGTAGTATTTACAAACTCTT	DNA endonuclease-targeted CRISPR trans reporter (DETECTR)	Bourgault et al. 2022)	ITS	
FQ-reporter	56-FAM/ttatt/3IABkFQ		Zhang et al. 2020		

LITERATURE CITED

- Abrams, M. D. 2003. Where has all the white oak gone? *BioScience* 53:927-939.
- Ambourn, A., Juzwik, J., and Eggers, J. E. 2006. Flight periodicities, phoresy rates, and levels of *Pseudopityophthorus minutissimus* branch colonization in oak wilt centers. *For. Sci.* 52:243-250.
- Ambourn, A. K., Juzwik, J., and Moon, R. D. 2005. Seasonal dispersal of the oak wilt fungus by *Colopterus truncatus* and *Carpophilus sayi* in Minnesota. *Plant Dis.* 89:1067-1076.
- Appel, D. N. 1986. Recognition of oak wilt in live oak. *J. Arboric.* 12:213-218.
- Appel, D. N. 1994. The potential for a California oak wilt epidemic. *J. Arboric.* 20:79-86.
- Appel, D. N. 1995. The oak wilt enigma: perspectives from the Texas epidemic. *Annu. Rev. Phytopathol.* 33:103-118.
- Appel, D. N., Kurdyla, T., and Lewis Jr., R. 1990. Nitidulids as vectors of the oak wilt fungus and other *Ceratocystis* spp. in Texas. *Eur. J. For. Pathol.* 20:412-417.
- Bakshi, B. K. 1951. Studies on four species of *Ceratocystis*, with a discussion on fungi causing sap-stain in Britain. *Mycol. Pap.* 35:1-16.
- Barnett, H. L. 1953a. A unisexual male culture of *Chalara quercina*. *Mycologia* 45:450-457.
- Barnett, H. L. 1953b. Isolation and identification of the oak wilt fungus. *W. Va. Univ. Agric. Exp. Stn. Bull.* 359T.
- Bart, G. 1957. Susceptibility of non-oak species to *Endoconidiophora fagacearum*. *Phytopathology* 47:3.
- Bart, G. 1960. Susceptibility of various apple varieties to the oak wilt fungus. *Phytopathology* 50:177-178.
- Bartelt, R. J., Kyhl, J. F., Ambourn, A. K., Juzwik, J., and Seybold, S. J. 2004. Male-produced aggregation pheromone of *Carpophilus sayi*, a nitidulid vector of oak wilt disease, and pheromonal comparison with *Carpophilus lugubris*. *Agric. For. Entomol.* 6:39-46.
- Blaedow, R. A., and Juzwik, J. 2010. Spatial and temporal distribution of *Ceratocystis fagacearum* in roots and root grafts of oak wilt affected red oaks. *J. Arboric.* 36:28-34.
- Bourgault, É., Gauthier, M. K., Potvin, A., Stewart, D., Chahal, K., Sakalidis, M. L., and Tanguay, P. 2022. Benchmarking a fast and simple on-site detection assay for the oak wilt pathogen *Bretziella fagacearum*. *Front. For. Glob. Change.* 5:1068135.
<https://doi.org/10.3389/ffgc.2022.1068135>

- Bretz, T. W. 1951a. Oak wilt fungus pathogenic to Chinese chestnut. *Plant Dis. Rep.* 35:28.
- Bretz, T. W. 1951b. A preliminary report on the perithecial stage of *Chalara quercina* Henry. *Plant Dis. Rep.* 35:298-299.
- Bretz, T. W. 1952a. New hosts for the oak wilt fungus, *Chalara quercina* Henry. *Phytopathology* 42:3.
- Bretz, T. W. 1952b. The ascigerous stage of the oak wilt fungus. *Phytopathology* 42:435-437.
- Bretz, T. W. 1953. Oak wilt, a new threat. *Plant Dis. U. S. Dept. Agric., Yearbook of Agriculture.* 1953:851-855.
- Bretz, T. W. 1955. Some additional native and exotic species of Fagaceae susceptible to oak wilt. *Plant Dis. Rep.* 39:495-497.
- Bretz, T. W. 1957. The Allegheny chinkapin and two exotic oaks susceptible to oak wilt. *Plant Dis. Rep.* 41:368.
- Bretz, T., and Long, W. 1950. Oak wilt fungus isolated from Chinese chestnut. *Plant Dis. Rep.* 34:291.
- Buchanan, W. D. 1956. Preliminary tests indicate that the small oak bark beetle may be a vector of oak wilt fungus. *Plant Dis. Rep.* 40:654.
- Cease, K. R., and Juzwik, J. 2001. Predominant nitidulid species (Coleoptera: Nitidulidae) associated with spring oak wilt mats in Minnesota. *Can. J. For. Res.* 31:635-643.
- Chahal, K., Gazis, R., Klingeman, W., Hadziabdic, D., Lambdin, P., Grant, J., and Windham, M. 2019a. Assessment of alternative candidate subcortical insect vectors from walnut crowns in habitats quarantined for thousand cankers disease. *Environ. Entomol.* 48:882-893.
- Chahal, K., Gazis, R., Klingeman, W., Lambdin, P., Grant, J., Windham, M., and Hadziabdic, D. 2022a. Differential virulence among *Geosmithia morbida* isolates collected across the United States occurrence range of thousand cankers disease. *Front. For. Glob. Change* 5:726388. <https://doi.org/10.3389/ffgc.2022.726388>
- Chahal, K., Morris, O., McCullough, D. G., and Sakalidis, M. L. 2019b. Biology, epidemiology and detection of oak wilt in Michigan. (Abstr). *Phytopathology* 109:33. <https://doi.org/10.1094/PHYTO-109-10-S2.1>
- Chahal, K., Morris, O., McCullough, D. G., Cregg, B., and Sakalidis, M. L. 2021. Sporulation timing of the invasive oak wilt fungus, *Bretziella fagacearum* in Michigan. (Abstr.). *Phytopathology* 111:51. <https://doi.org/10.1094/PHYTO-111-10-S2.1>

Chahal, K. S., Wachendorf, E. J., Miles, L. A., Stallmann, A., Lizotte, E. L., Mandujano, M., Byrne, J., Miles, T. D., and Sakalidis, M. L. 2024. First report of *Bretziella fagacearum* infecting chestnut in Michigan. Plant Dis. <https://doi.org/10.1094/PDIS-10-23-2267-PDN>

Chahal, K., Morris, O. R., McCullough, D. G., Cregg, B., and Sakalidis, M. L. 2022b. Seasonal variation of northern red oak, *Quercus rubra*, infection by *Bretziella fagacearum* (oak wilt) in Michigan. (Abstr.). Phytopathology 112:37. <https://doi.org/10.1094/PHYTO-112-11-S3.1>

Cosse, A. A., and Bartelt, R. J. 2000. Male-produced aggregation pheromone of *Colopterus truncatus*: structure, electrophysiological, and behavioral activity. J. Chem. Ecol. 26:1735-1748.

De Beer, Z. W., Marincowitz, S., Duong, T. A., and Wingfield, M. J. 2017. *Bretziella*, a new genus to accommodate the oak wilt fungus, *Ceratocystis fagacearum* (Microascales, Ascomycota). MycoKeys 27:1-19.

DiGirolomo, M. F., Munck, I. A., Dodds, K. J., and Cancelliere, J. 2020. Sap beetles (Coleoptera: Nitidulidae) in oak forests of two Northeastern states: a comparison of trapping methods and monitoring for phoretic fungi. J. Econ. Entomol. 113:2758-2771.

Dorsey, C. K., Jewell, F. F., Leach, J. G., and True, R. P. 1953. Experimental transmission of oak wilt by four species of Nitidulidae. Plant Dis. Rep. 37:419-420.

Dowd, P. F., Bartelt, R. J., and Wicklow, D. T. 1992. Novel insect trap useful in capturing sap beetles (Coleoptera: Nitidulidae) and other flying insects. J. Econ. Entomol. 85:772-778.

Ernst, R. A., and Bretz, T. W. 1953. American chestnut susceptible to oak wilt fungus. Plant Dis. Rep. 37:163.

Farr, D. F., Bills, G. F., Chamuris, G. P., and Rossman, A. Y. 1989. Fungi on plants and plant products in the United States. APS Press, St. Paul, MN, USA. 1252 pp.

Fergus, C. L., and William, L. Y. 1953. Scrub oak susceptible to oak wilt. Plant Dis. Rep. 37:567.

Gauthier, M. K., Bourgault, É., Potvin, A., Bilodeau, G. J., Gustavsson, S., Reed, S., Therrien, P., Barrette, É., and Tanguay, P. 2023. Biosurveillance of oak wilt disease in Canadian areas at risk. Can. J. Plant Pathol. 46:27-38. <https://doi.org/10.1080/07060661.2023.2261890>

Gould, A. B., and Lashomb, J. H. 2007. Bacterial leaf scorch (BLS) of shade trees. Plant Health Instr. <https://doi.org/10.1094/PHI-I-2007-0403-07>

Gibbs, J. N., and French, D. W. 1980. The transmission of oak wilt. USDA Forest Service Research Paper NC-185. Central Forest Experiment Station, St. Paul, MN.

- Haack, R. A., and Acciavatti, R. E. 1992. Twolined chestnut borer. USDA Forest Service Forest Insect and Disease Leaflet 168. USDA Forest Service, North Central Forest Experiment Station, East Lansing, MI.
- Harrington, T. C., McNew, D., and Yun, H. Y. 2012. Bur oak blight, a new disease on *Quercus macrocarpa* caused by *Tubakia iowensis* sp. nov. *Mycologia* 104:79-92.
- Hayslett, M., Juzwik, J., and Moltzan, B. 2008. Three *Colopterus* beetle species carry the oak wilt fungus to fresh wounds on red oak in Missouri. *Plant Dis.* 92:270-275.
- Henry, B. W. 1944. *Chalara quercina* n. sp., the cause of oak wilt. *Phytopathology* 34:631-635.
- Henry, B. W., Moses, C. S., Richards, C. A., and Riker, A. J. 1944. Oak wilt, its significance, symptoms, and cause. *Phytopathology* 34:636-647.
- Hepting, G. H., Toole, E. R., and Boyce, J. S. 1951. Perithecia produced in an unpaired isolate *Chalara quercina* and its possible significance in oak wilt control. *Plant Dis. Rep.* 35:555.
- Hepting, G. H., Toole, E. R., and Boyce, J. S. 1952. Sex and compatibility in the oak wilt fungus. *Plant Dis. Rep.* 36:64.
- Hipp, A. L., Manos, P. S., González-Rodríguez, A., Hahn, M., Kaproth, M., McVay, J. D., Avalos, S. V., and Cavender-Bares, J. 2018. Sympatric parallel diversification of major oak clades in the Americas and the origins of Mexican species diversity. *New Phytol.* 217:439-452.
- Hunt, J. 1956. Taxonomy of the genus *Ceratocystis*. *Lloydia.* 19:1-58.
- Hoffman, P. F. 1953. Oak wilt fungus pathogenic on *Quercus chrysolepis* and *Quercus agrifolia*. *Plant Dis. Rep.* 10:527.
- Jagemann, S. M., Juzwik, J., Tobin, P. C., and Raffa, K. F. 2018. Seasonal and regional distributions, degree-day models, and phorsey rates of the major sap beetle (Coleoptera: Nitidulidae) vectors of the oak wilt fungus, *Bretziella fagacearum*, in Wisconsin. *Environ. Entomol.* 47:1152-1164.
- Jones, T. W. 1958. Mortality in wilt infected oaks. *Plant Dis. Rep.* 42:552-553.
- Juzwik, J., Appel, D. N., MacDonald, W. L., and Burks, S. 2011. Challenges and successes in managing oak wilt in the United States. *Plant Dis.* 95:888-900.
- Juzwik, J., Harrington, T. C., MacDonald, W. L., and Appel, D. N. 2008. The origin of *Ceratocystis fagacearum*, the oak wilt fungus. *Annu. Rev. Phytopathol.* 46:13-26.
- Juzwik, J., Cease, K. R., and Meyer, J. M. 1998. Acquisition of *Ophiostoma quercus* and *Ceratocystis fagacearum* by nitidulids from *O. quercus*-colonized oak wilt mats. *Plant Dis.* 82:239-243.

Juzwik, J., and French, D. W. 1983. *Ceratocystis fagacearum* and *C. piceae* on the surfaces of free-flying and fungus-mat-inhabiting nitidulids. *Phytopathology* 73:1164-1168.

Juzwik, J., Skalbeck, T. C., and Neuman, M. F. 2004. Sap beetle species (Coleoptera: Nitidulidae) visiting fresh wounds on healthy oaks during spring in Minnesota. *For. Sci.* 50:757-764.

Kurdyla, T., and Appel, D. 2011. The detection of *Ceratocystis fagacearum* in Texas live oak using real-time polymerase chain reaction. (Abstr.). *Phytopathology* 101. S95.

Kyhl, K. F., Bartelt, R. J., Cosse, A., Juzwik, J., and Seybold, S. J. 2002. Semiochemical-mediated flight responses of sap beetle vectors of oak wilt, *Ceratocystis fagacearum*. *J. Chem. Ecol.* 28:1527-1547.

Lamarche, J., Potvin, A., Pelletier, G., Stewart, D., Feau, N., Alayon, D. I. O., Dale, A. L., Coelho, A., Uzunovic, A., Bilodeau, G. J., Briere, S. C., Hamelin, R. C., and Tanguay, P. 2015. Molecular detection of 10 of the most unwanted alien forest pathogens in Canada using real-time PCR. *PLoS One* 10. e0134265. <https://doi.org/10.1371/journal.pone.0134265>

Leach, J. G. 1940. *Insect Transmission of Plant Diseases*. McGraw-Hill Book Co., New York, USA.

Lee, C. A., Dey, D. C., and Muzika, R. M. 2016. Oak stump-sprout vigor and *Armillar* infection after clearcutting in southeastern Missouri, USA. *For. Ecol. Manag.* 374:211-219.

Li, Y., and Hulcr, J. 2020. Fungi Permanent Storage. [protocols.io](https://doi.org/10.17504/protocols.io.bnu5mey6)
<https://doi.org/10.17504/protocols.io.bnu5mey6>

Liese, W., and Ruetze, M. 1987. On the risk of introducing oak wilt on white oak logs from North America. *Arboric. J.* 11:237-244.

MacDonald, W. L., Pinon, J., Tainter, F. H., and Double, M. L. 2001. European oaks – Susceptible to oak wilt? *Proc. Shade Tree Wilt Diseases. Proceedings from Wilt Diseases of Shade Trees: a National Conference*, St. Paul, MN, USA.

McLaughlin, K., Snover-Clift, K., Somers, L., Cancelliere, J., and Cole, R. 2022. Early detection of the oak wilt fungus (*Bretziella fagacearum*) using trapped nitidulid beetle vectors. *For. Pathol.* 52. e12767. <https://doi.org/10.1111/efp.12767>

Merrill, W. 1975. American chestnut and chestnut oak not reservoirs of the oak wilt fungus in Pennsylvania. *Plant Dis. Rep.* 59:564-566.

Morris, O. R. 2020. Seasonal Activity and Phoresy Rates of Sap Beetles (Coleoptera: Nitidulidae) in Oak Wilt Infection Centers, Volatile Organic Compounds Related to the Oak Wilt Cycle, and Long-Term Evaluation of Red Oak Provenances. Master's thesis, Michigan State University.

- Münch, E. 1907. Die Blaufäule des Nadelholzes. I-II. Naturwissenschaftliche Zeitschrift für Forst- und Landwirtschaft. 5:531-573.
- Navia-Urrutia, M., Sánchez-Pinzón, L., Parra, P. P., and Gazis, R. 2022. A diagnostic guide for laurel wilt disease in avocado. *Plant Health Prog.* 23:345-354.
- Norris, D. M. Jr. 1956. Association of insects with the oak tree and *Endoconidiophora fagacearum* Bretz. PhD Thesis, Dept. of Zoology and Entomology, Iowa State College.
- Parmeter, J. R., Kuntz, J. E., and Riker, A. J. 1956. Oak wilt development in bur oaks. *Phytopathology* 46:423-436.
- Paulin-Mahady, A. E., Harrington, T. C., and McNew, D. 2002. Phylogenetic and taxonomic evaluation of *Chalara*, *Chalaropsis*, and *Thielaviopsis* anamorphs associated with *Ceratocystis*. *Mycologia* 94:62-72.
- Pearce, M., and Williams-Woodward, J. 2009. Key to diseases of oaks in the landscape. The University of Georgia Cooperative Extension Bulletin 1287, 16 pp.
https://secure.caes.uga.edu/extension/publications/files/pdf/B%201287_3.PDF (last accessed 26 June 2024).
- Pegg, G. S., Nahrung, H., Carnegie, A. J., Wingfield, M. J., and Drenth, A. 2011. Spread and development of quambalaria shoot blight in spotted gum plantations. *Plant Pathol.* 60:1096-1106.
- Pokorny, J. 1999. How to collect field samples and identify the oak wilt fungus in the laboratory. NA-FR-01-99. USDA Forest Service, Northeastern Area State and Private Forestry, St. Paul, MN.
- Rauschendorfer, J., Rooney, R., and Külheim, C. 2022. Strategies to mitigate shifts in red oak (*Quercus sect. Lobatae*) distribution under a changing climate. *Tree Physiol.* 42:2383-2400.
- Rexrode, C. O., and Lincoln, A. C. 1965. Distribution of oak wilt. *Plant Dis. Rep.* 49:1007-1010.
- Rexrode, C. O., and Jones, T. W. 1970. Oak bark beetles—important vectors of oak wilt. *J. For.* 68:294-297.
- Samtani, J. B., Masiunas, J. B., and Appleby, J. E. 2010. White oak and northern red oak leaf injury from exposure to chloroacetanilide herbicides. *HortScience* 45:696-700.
- Schoch, C. L., Robbertse, B., Robert, V., Vu, D., Cardinali, G., Irinyi, L., Meyer, W., Nilsson, R. H., Hughes, K., Miller, A. N., Kirk, P. M., Abarenkov, K., Aime, M. C., Ariyawansa, H. A., Bidartondo, M., Boekhout, T., Buyck, B., Cai, Q., Chen, J., Crespo, A., Crous, P. W., Damm, U., De Beer, Z. W., Dentinger, B. T. M., Divakar, P. K., Dueñas, M., Feau, N., Fliegerova, K., García, M. A., Ge, Z.-W., Griffith, G. W., Groenewald, J. Z., Groenewald, M., Grube, M., Gryzenhout, M., Gueidan, C., Guo, L., Hambleton, S., Hamelin, R., Hansen, K., Hofstetter, V., Hong, S.-B., Houbraken, J., Hyde, K. D., Inderbitzin, P., Johnston, P. R., Karunarathna, S. C.,

Kõljalg, U., Kovács, G. M., Kraichak, E., Krizsan, K., Kurtzman, C. P., Larsson, K.-H., Leavitt, S., Letcher, P. M., Liimatainen, K., Liu, J.-K., Lodge, D. J., Luangsa-ard, J. J., Lumbsch, H. T., Maharachchikumbura, S. S. N., Manamgoda, D., Martín, M. P., Minnis, A. M., Moncalvo, J.-M., Mulè, G., Nakasone, K. K., Niskanen, T., Olariaga, I., Papp, T., Petkovits, T., Pino-Bodas, R., Powell, M. J., Raja, H. A., Redecker, D., Sarmiento-Ramirez, J. M., Seifert, K. A., Shrestha, B., Stenroos, S., Stielow, B., Suh, S.-O., Tanaka, K., Tedersoo, L., Telleria, M. T., Udayanga, D., Untereiner, W. A., Diéguez-Uribeondo, J., Subbarao, K. V., Vágvölgyi, C., Visagie, C., Voigt, K., Walker, D. M., Weir, B. S., Weiß, M., Wijayawardene, N. N., Wingfield, M. J., Xu, J.-P., Yang, Z. L., Zhang, N., Zhuang, W.-Y., and Federhen, S. 2014. Finding needles in haystacks: linking scientific names, reference specimens and molecular data for fungi. Database 2014. <https://doi.org/10.1093/database/bau061>

Singh, R., Feltmeyer, A., Saiapina, O., Juzwik, J., Arenz, B., and Abbas, A. 2017. Rapid and PCR-free DNA detection by nanoaggregation-enhanced chemiluminescence. Sci. Rep. 7:14011. <https://doi.org/10.1038/s41598-017-14580-w>

Stambaugh, W. J., Fergus, C. L., Craighead, F. C., and Thompson, H. E. 1955. Viable spores of *Endoconidiophora fagacearum* from bark and wood-borne beetles. Plant Dis. Rep. 39:867-871.

Stone, G. N., Schönrogge, K., Atkinson, R. J., Bellido, D., and Pujade-Villar, J. 2002. The population biology of oak gall wasps (Hymenoptera: Cynipidae). Annu. Rev. Entomol. 47:633-668.

Wu, C. P., Chen, G. Y., Li, B., Su, H., An, Y. L., Zhen, S. Z., and Ye, J. R. 2011. Rapid and accurate detection of *Ceratocystis fagacearum* from stained wood and soil by nested and real-time PCR. For. Pathol. 41:15-21.

Zhang, Y., Zhang, Y., Zhang, Y., and Xie, K. 2020. Evaluation of CRISPR/Cas12a-based DNA detection for fast pathogen diagnosis and GMO test in rice. Mol. Breed. 40:1-12. <https://doi.org/10.1007/s11032-019-1092-2>

CHAPTER 2: EPIDEMIOLOGY OF OAK WILT CAUSED BY *BRETZIELLA FAGACEARUM* ON *QUERCUS RUBRA* IN MICHIGAN

Abstract

Oak wilt caused by the fungus *Bretziella fagacearum* is established in 24 states in the U.S. to date and continues to spread. Overland spread occurs when sap beetles (Coleoptera: Nitidulidae) introduce *B. fagacearum* conidia while visiting fresh wounds or via root grafts between infected and uninfected oaks (*Quercus* spp). We investigated the seasonal susceptibility of red oaks to *B. fagacearum* infection to determine if infection rates vary between large diameter earlywood xylem cells and thick-walled latewood cells. Mature northern red oaks (*Q. rubra*) in northern MI were inoculated with a *B. fagacearum* conidial suspension (2×10^6 conidia/ml) at 4-week intervals annually from March to November in 2017 to 2020., then visually evaluated to assess disease progression at 15-day intervals. Short increment cores were collected from inoculated trees at approximately 15-day interval in 2018 and 2019 to monitor xylem development. Red oaks inoculated between March and September became infected. The disease progressed most rapidly in trees inoculated in June and July compared with other months. Oaks inoculated in October and November did not become infected. Earlywood vessels were produced from mid-May through mid-June in 2018 and from late-May to mid-July in 2019, corresponding with relatively rapid disease progression. Trees inoculated later in the season, however, also became infected by *B. fagacearum* even when xylem was composed of latewood vessels. Predicted sap flow rates were correlated with oak wilt progression on inoculated trees. Results indicate seasonal fluctuations in predicted sap flow rate in-part influenced by sapwood development influence disease incidence, and progression. Data provide information on key risk

periods for *B. fagacearum* infection and can be used to improve current management guidelines for activities that may lead to tree injury.

Introduction

Oak wilt caused by the fungal pathogen, *Bretziella fagacearum* (Bretz) Z.W. de Beer, Marinc., T.A. Duong & M.J. Wingf., previously known as *Ceratocystis fagacearum* (Bretz) Hunt, is an important vascular wilt disease of oaks (*Quercus* spp.) in the United States (de Beer et al. 2017; Juzwik et al. 2011). While the origin of *B. fagacearum* is unknown, it seems likely that the fungus was introduced into the U.S. from Mexico, Central or South America (Hipp et al. 2018; Juzwik et al. 2008). Oak wilt was first described as a disease of oaks in 1942 in Wisconsin (Henry et al. 1944). However, historical accounts indicate oak wilt likely killing oaks as early as the 1890s in the upper Mississippi River valley (Gibbs and French 1980). In the two decades following its initial discovery, oak wilt was reported from midwestern, north-central, mid-Atlantic states and Texas, where it affects live oaks (Rexrode and Lincoln 1965). Currently, oak wilt has been confirmed in 24 states in the U.S. and is widespread in midwestern states and Texas.

Interspecific variation in susceptibility to *B. fagacearum* has been consistently observed. Red oaks in section *Lobatae* (i.e., *Q. rubra*, *Q. nigra*) are highly vulnerable to oak wilt and can die within three weeks of infection (Juzwik 2007). In contrast, white oaks (i.e., *Q. alba*) in section *Quercus* exhibit moderate to high levels of resistance. *Bretziella fagacearum* infection in white oaks typically results in some canopy dieback but tree mortality is rare (Juzwik 2007). *Quercus* is the most dominant tree genus in North America, both in terms of species number and biomass (Hipp et al. 2018), comprising approximately 38% of the total hardwood volume in the U.S. (Rioux and Blais 2023). Current growing stock of oaks in the U.S. was estimated at 3,913

million m³ in 2017 (Rioux and Blais 2023). Oak is one of the most economically valuable North American hardwoods and is used for making furniture, cabinets, interior architectural woodwork, and flooring (Rioux and Blais 2023). In addition to domestic use of oak timber, the U.S. exports oak logs and processed lumber valued at \$154 million USD, and \$517 million USD, respectively, to over 70 countries (USDA-FAS 2022). Oaks serve as crucial ecological hubs, offering habitat and food for a multitude of wildlife species. Oak wilt continues to spread within oak wilt positive states and is expanding into new geographical locations where it was not previously reported. Detection of oak wilt in Ontario, Canada, in June 2023 marked the first time this pathogen had been identified outside the U.S. (Canadian Food Inspection Agency 2023).

Bretziella fagacearum can spread underground via grafted roots and overland via insect vectors or contaminated wood (Appel 1995). The majority of oak mortality results from expanding patches of dying oaks within an oak wilt epicenter. Over 90% of trees that die from oak wilt likely become infected when *B. fagacearum* is transmitted through root grafts (Cook 2001; Wilson 2005). Overland transmission, which refers to long-distance spread and initiation of new disease epicenters (Juzwik et al. 2011), results from insect vectors introducing the fungus into fresh wounds on oaks. Many species of sap beetles (Coleoptera: Nitidulidae) are attracted to sporulating mycelial mats typically produced by *B. fagacearum* 6-12 months after a tree dies from oak wilt (Appel 1995; Cobb et al. 1965, Juzwik et al. 2011, Morris 2020). As a mat grows, it produces a dense cushion-like structure called a “pressure pad” which pushes against the outer bark leading to a crack in the bark, which allows insects to access the mat. Sap beetles feed on the mats and fungal propagules adhere to their exoskeleton. Sap beetles are attractive to volatile compounds emitted by freshly cut logs, stumps, or wounds, which remain susceptible for up to three days (Gibbs and French 1980). Spore-laden beetles can transmit the pathogen to xylem-

penetrating wounds on otherwise healthy trees. Oak wilt is also thought to be spread when beetles visit mycelial mats on logs and firewood produced from recently killed trees. Movement of contaminated firewood is thought to have led to the introduction of *B. fagacearum* and oak wilt disease in New York (Snover-Clift and Rosenthal 2016).

Oaks, like other ring-porous species, produce large diameter vessels in the earlywood, often exceeding 300 μm , while the diameter of latewood vessels is frequently no more than 50 μm (Rioux and Blais 2023). Earlywood vessels transport a high volume of sap from roots to the canopy early in the growing season (Kitin and Funada 2016) while thick-walled latewood vessels, produced after leaves are fully expanded, offers protection against embolisms caused by drought (Kitin and Funada 2016). Earlywood vessels are ideal for the movement of fungal pathogens through sap flow (Keykhasaber et al. 2018; Tchernoff 1965). The propagules of numerous vascular wilt pathogens in trees move rapidly through the sap or transpiration stream. This movement results in rapid disease progression (Banfield WM 1941; Ploetz et al. 2015). The velocity of sap flow is closely related to the overall rate of transpiration of the crown. Under non-limiting soil moisture, daily sap flow is correlated with reference evapotranspiration, which encompasses multiple factors including solar radiation, vapor pressure deficit, wind speed, air temperature, and soil moisture etc. (Allen et al. 1998). Patterns of daily sap flow can be predicted from evapotranspiration and strong positive correlations have been observed between evapotranspiration and sap flow in trees when soil moisture is non-limiting (Er-Raki et al. 2009; Forster, 2021; Nicolas et al., 2005; Pereira et al., 2006). Understanding the relationship among xylem development, patterns of sap flow, environmental factors and disease progression can provide valuable insights into the dynamics of oak wilt disease and development of effective management strategies.

The most effective means to manage oak wilt is to prevent establishment of new infection centers and limit expansion of existing infection centers. Periodic root flare injections with propiconazole (FRAC 3 fungicide) are sometimes used prophylactically to protect high value trees from oak wilt. Injections are costly and rarely practical for large infection centers and will not cure already infected trees (FRAC 2022; Juzwik et al. 2011). Lateral expansion of an infection center can be limited by disrupting root grafts between diseased and healthy trees (Juzwik et al. 2011). However vibratory plowing is often not a feasible option due to cost, inaccessible field sites, and underground utility lines. Overland disease spread can be reduced by avoiding wounding oaks during high-risk of infection periods when peak insect-vector activity overlaps with *B. fagacearum* sporulation and host susceptibility. In the Great Lake states, the high-risk period for oak wilt spread is usually mid-April to mid-July (Ambourn et al. 2005; Morris 2020). However, the studies suggest possibility of contaminated nitidulid beetles spreading the pathogen as late in August-October.

This research was conducted to examine the seasonal susceptibility of *Q. rubra* to *B. fagacearum* infection to (1) determine the peak periods and temporal range of vulnerability, (2) assess if trees are susceptible to infection after initiating latewood formation, (3) predict patterns of mycelial mat production on succumbed trees.

Materials and methods

Study sites and tree selection:

Three locations that contained large numbers of *Q. rubra* and active oak wilt pockets (determined by the presence of sporulating mats) were chosen to evaluate tree susceptibility to artificial infection; Bunker Hill (44.7366944, -85.44555556), Coyote Rd (44.51058333, -84.83761111), and Nessen Rd (44.55819444, -85.80116667) in the northwest of the lower

peninsula of Michigan. These sites were selected due to existing natural oak wilt infection, preventing the introduction of the disease to new areas. The infected trees, or disease epicenters, were at least 800 m away from the trees selected for artificial inoculations. Co-dominant *Q. rubra* trees were selected and tagged. Basal area of the *Q. rubra* trees at the locations and inoculated trees were at three locations. *Q. rubra* trees with trunk diameters at breast height (DBH) ranging from 6 to 61 cm were randomly selected for the pathogenicity trial.

Pathogenicity trial:

Conidial suspensions for inoculations were prepared by growing *B. fagacearum* isolate (MIFCC2152- collected from an oak wilt epicenter in Grand Traverse County, Michigan, USA in July 2017) on acidified (80% lactic acid, JT Baker, Phillipsburg, NJ, USA) full strength potato dextrose agar (PDA; Difco™, Sparks, MD) for two weeks at ambient room temperature. To make acidified PDA, 1 ml of 80% lactic acid was added into autoclaved 1 L of full-strength PDA. Five days before inoculation, conidia were harvested by flooding pure cultures of MIFCC2152 isolate, then filtering twice using a double layer of Miracloth (Miracloth, EMD Millipore, Billerica, MA). The conidial concentration was measured using a hemocytometer and adjusted to 1×10^6 conidia per ml using sterile water and 40% glycerol. Each conidial suspension contained 50% volume of 40% glycerol to ensure viability during transportation. Conidial suspensions were stored at -20 °C until the day of inoculation and then transported to inoculation sites in ice coolers packed with reusable ice. Viability and colony forming units (CFUs) of conidia were determined before and after every field trip by plating conidia suspensions on full strength PDA and examining colonies for *B. fagacearum* microscopic characteristics (de Beer et al. 2017).

To inoculate trees, two 12 mm diameter holes perpendicular at DBH to the north and south direction of each tree were made 3 – 4 cm deep using an increment borer (Forestry Suppliers, Jackson, Mississippi, USA, stock number: 63383) or a DeWalt DCD780 hand-held drill (Dewalt Industrial Tool Co., Hampstead, Maryland, USA). A one ml conidial suspension containing 1×10^6 conidia or control inoculations containing 1 ml suspensions of sterile water and 40 % glycerol was poured dropwise into each hole on a tree using a syringe (BD 1 ml syringe, BD Franklin Lakes, NJ) without needle. The inoculation hole entrances were plugged using a silicone sealant (GE silicones, manufacturer no. 2812566) and then the tree trunk was wrapped with a bench paper (Cole-Parmer, manufacturer no. F246750000). Monthly inoculation of two trees (one with *B. fagacearum* and one with water) were completed at each of the three field sites. In 2017, monthly inoculations were conducted from August to October. In 2018, and 2019 monthly inoculations were conducted throughout April to November, and March to November, respectively. In 2020, inoculations were conducted only in March (Table 2.1).

Disease severity ratings:

Inoculated trees were rated for disease progression every 15 days from inoculation until complete tree mortality, marked by the entire tree crown showing necrosis or defoliation. The trees were assessed for typical oak wilt symptoms, including wilting, discoloration, browning, and defoliation of leaves (see, results). Severity of symptoms on inoculated trees were rated on a scale of 0–5, where 0 = no symptoms; 1 = 1–25% of the crown symptomatic; 2 = 26–50%; 3 = 51- 75%; 4= 76-99%; and 5 = dead or completely symptomatic. Tree phenology parameters such as leaf phenophases (buds dormant, buds swollen, buds broken, leaves visible, leaves fully expanded) and tightness of bark (bark tight, bark loose) were also recorded at the time of

inoculation, throughout disease progression stages. To observe mycelial mat formation, inoculated trees were inspected for an additional year following complete mortality.

Xylem vessel development:

Short increment cores were collected 1.3 m above ground from two asymptomatic, non-inoculated *Q. rubra* trees per site approximately 15 days from March to early August in 2018 and 2019 as detailed in Morris (2020). Cores were stored in glass vials with 70% ethanol until they could be examined under a stereo microscope to determine if earlywood or latewood cells were present. Cores continued to be collected and evaluated until all sampled trees were producing only latewood in two successive samples (Morris, 2020).

Reference evapotranspiration as proxy for sap flow:

Reference potential evapotranspiration (PETref) data were recorded by the MSU Enviroweather stations closest to field sites. Data from stations at Benzonia, Kalkaska, and Williamsburg, Michigan, were accessed for weather-related variables for field sites Nessen, Coyote, and Bunker, respectively (<https://enviroweather.msu.edu/>). Daily average PETref data were calculated over a 21-day period following each inoculation, across different months, sites, and years. These data were plotted against the number of days until symptom onset and mortality for each *B. fagacearum*-inoculated tree at each site and year.

Mycelial mat production and Koch's postulates:

Pressure from mycelial mats splits and pushes bark away from sapwood. Striking bark above a mat with a hatchet produced a distinct hollow sound, aiding in locating a mat. Tree trunks were tapped with a hatchet to find mats, while binoculars were used locating mats above 3 m, based on visible bark splits. Only mats causing bark ruptures were recorded on trunks above 3 m. Trees were monitored for mycelial mat development at 15-days intervals from 2018 - 2020.

Koch's postulates were satisfied after sampling mycelial mats or symptomatic branches and *B. fagacearum* was detected using a culture-based method or qPCR test (Yang and Juzwik 2017).

Statistical analysis

The effect of month of inoculation on rate of disease symptom development was analyzed using the PHREG procedure in SAS 9.4 (SAS Institute Inc. 2013. SAS®9.4). Dependent variables in the model included number of days between inoculation and (1) the onset of symptoms and (2) complete tree mortality. Month of inoculation was the independent variable and location, year, and tree DBH were considered as covariates. Analyses were based on the Cox proportional hazards model which was used to determine the effect of explanatory variable on dependent variables (Johnson and Shih 2007). The LSMEANS statement in proc phreg was used for the post-hoc comparison among month of inoculation at a significance level of 0.05. Linear relationships between the number of mats produced on wilted oaks each month (the response variable) and metrological variables (temperature, rainfall, humidity) were examined using multiple regression. However, relationship was strongly associated with temperature only and other variables were not included in data analyses. Data were log transformed, and 2nd order negative binomial regression was the best fit model. Number of new mats observed on each observation date was the dependent variable; average temperature recorded for 15 days prior to the observation date served as independent variable. Relationships between PETref rate and disease progression was determined using Pearson's correlation analysis conducted in SAS 9.4 (P =0.05).

Results

Variations in patterns of symptoms production:

Oak wilt symptoms, observed on trees inoculated between March-August, included drooping of leaves starting at the tree crown's top or outer areas, progressing downward (Fig. 2.1, 2.2). Affected leaves transitioned from wilted to desiccated, exhibiting dull green or bronze, sometimes appeared water soaked. Following the onset of leaf wilt, rapid defoliation occurred throughout the crown. On individual leaves, characteristic tanning, not restricted by leaf veins, started from outer edges and progressed towards the midrib and base of leaves (Fig. 2.2). Water sprouts or epicormic shoots emerged on infected tree trunks and large limbs but were short-lived and rapidly became symptomatic (Fig. 2.3). The onset of one or combination of these symptoms on a tree varied depending on the month of inoculation. Trees inoculated in June displayed fastest onset of symptoms after 29 ± 2 days, while those inoculated in March exhibited symptoms within 95 ± 13 days after inoculation.

On trees inoculated in September, no symptoms were observed until the last fortnight of May the following spring at the field sites. On these trees, the timing and appearance of swelling buds and bud break was similar to asymptomatic trees. However, inoculated trees leafed out sparsely and formed a thin or transparent crown relative to control trees (Fig. 2.3). After full expansion in June, leaves were smaller than those on control trees, yet they did not display any typical symptoms of oak wilt such as leaf wilting, bronzing (Fig. 2.3). In early July, foliage turned bronze and tan with defoliation throughout the crown. Symptom onset occurred 246 ± 64 days post-inoculation, with mortality taking 313 ± 17 days, marked by complete crown defoliation or necrosis.

Temporal variations in host susceptibility:

Disease incidence was 100% in trees inoculated in June and July, followed by September (91%), May (85%), April (80%), respectively, but only 50% on trees inoculated in March and August. Control trees remained asymptomatic throughout the experiment. Onset of symptoms, and mortality post inoculations did not significantly differ among field sites, $X^2 = 3.72$, $df = 2$, $P = 0.15$, and $X^2 = 1.69$, $df = 2$, $P = 0.43$, respectively. Similarly, year of inoculation did not significantly affect onset of symptoms, and mortality after monthly inoculations ($X^2 = 6.57$, $df = 3$, $P = 0.09$, and $X^2 = 5.12$, $df = 3$, $P = 0.16$). Therefore, data were combined from different field sites and year for final analysis.

Month of inoculation (treated as an independent variable) significantly affected number of days before symptoms were observed (Wald $X^2 = 43.86$, $df = 8$, $P < 0.001$) and trees died ($X^2 = 4.08$, $df = 8$, $P < 0.001$). Symptoms on trees inoculated in June were apparently faster than on trees inoculated in other months, averaging 29 ± 2 days, post-inoculation, followed by July and May (Fig. 2.4). Trees inoculated in September exhibited the longest time to develop foliar symptoms, followed by March and April, occurring at 246 ± 64 , 95 ± 13 , and 60 ± 5 days post-inoculation, respectively. Trees inoculated in October, and November did not become symptomatic and remained asymptomatic throughout the experiment. Mortality was rapid in trees inoculated in June followed by July and May, occurring at 68 ± 9 , 78 ± 21 , and 93 ± 8 days post-inoculation, respectively. Trees inoculated in September took the longest time to succumb to infection followed by August, and March, occurring 313 ± 17 , 202 ± 103 , and 150 ± 9 days after inoculation, respectively. Trees inoculated between March and July died rapidly during the same calendar year, while trees inoculated in August and September died in the following year after bud break.

Xylem vessel development:

In 2018, red oaks in the field sites produced earlywood from 24 April through 19 June. In 2019, earlywood development was observed in cores extracted on 7 May and continued through 16 July (Olivia R. Morris, 2020). Earlywood production began approximately two weeks before swollen apical buds were observed and continued until leaves throughout the entire canopy were fully expanded. The vulnerability of *Q. rubra* to infection exhibited seasonal variation, corresponding to the transition of xylem from earlywood to latewood, as illustrated by the onset of symptoms and mortality following monthly inoculations (Fig. 2.4). Tree mortality was faster during the period of earlywood production than the period when trees were producing latewood.

Reference evapotranspiration in relation to sap flow:

PET_{ref} was negatively correlated with the first observation of foliar symptoms ($r = -0.71$, $P < 0.001$), and days to mortality ($r = -0.61$, $P < 0.001$) post-inoculation. In other words, disease symptoms and tree mortality occurred more rapidly when PET_{ref}, as an indicator of sap flow, was high.

Mycelial mat production and Koch's postulates:

Mycelial mats were formed on 15 out of 40 inoculated trees that became infected. Mats were more commonly formed on trees inoculated in August or September compared to trees inoculated between March and May. On average, 6.2 mats per tree formed on trees inoculated from March through May, versus an average of 11.6 mats per tree on trees inoculated in August and September. No mats were observed on trees inoculated in June or July.

Overall, data indicate mat formation peaked in late spring and early fall (Fig. 2.5), a pattern that may reflect ambient temperatures experienced by trees during the two-week intervals between mat surveys. Significant relationship ($P < 0.05$) between production of mycelial mats

and average of mean daily temperatures 15 days prior to mat observation was predicted for respective years (Fig. 2.6). In 2018, regression equation for prediction of mats (y) = $0.05 + 8.38*\text{temperature} - 3.96*(\text{temperature})^2$, with $R^2 = 0.52$. For 2019 data, regression equation was, $y = 0.43 + 9.72*\text{temperature} - 8.28*(\text{temperature})^2$, with $R^2 = 0.78$. Similarly for 2020 data, $y = 1.73 + 3.34*\text{temperature} - 2.66*(\text{temperature})^2$, with $R^2 = 0.32$. Mat production began in mid-April once average daily temperatures rose above freezing and continued until average daily temperatures fell below freezing in mid-November. Peak production occurred when average daily temperatures ranged from 12.5°C to 17.0 °C (Fig. 2.6). Production was limited by average daily temperatures above 22°C, particularly in July (Fig. 2.6). Onset of mat formation on trees inoculated in August or September 2017 was observed in end April and August of 2018 and continued until May, June of 2019. Mat formed on trees inoculated before May 31 in the August-September of same year, and started next April-June, and occasionally continued till September. *B. fagacearum* was confirmed from all the symptomatic trees to satisfy Koch's postulates.

Discussion

This is the first study to examine *Q. rubra* seasonal susceptibility to *B. fagacearum* infection in Michigan. Our findings demonstrate that *Q. rubra* trees are vulnerable to infection from March to September, while those inoculated in October and November remain free of infection. All trees subjected to inoculation in June and July exhibited the fastest onset of disease symptoms and mortality. Furthermore, trees inoculated between March and July displayed symptoms and succumbed within the same calendar year. In the case of August inoculations, symptoms manifested within the same calendar year, with mortality occurring in the subsequent spring. Conversely, trees inoculated in September exhibited symptoms and ultimately died in the

following spring. Once trees exhibited symptoms they succumbed to infection. No symptomatic tree recovered from *B. fagacearum* infection.

Quercus rubra trees were most vulnerable to oak wilt infection in spring and early summer. During this period, the xylem was comprised of large-diameter (earlywood) and thin-walled vessels. This vulnerability decreases compared to later in the summer when thick-walled latewood vessels, with relatively small diameters, were produced. To our knowledge, we are reporting severe disease progression in relation to earlywood vessel formation for the first time in oak wilt pathosystem. In ring-porous tree species such as oaks and elms, earlywood vessels serve as the primary conduits for transporting a larger volume of sap during the initial phase of the growing season, following bud burst. Subsequently, the production of latewood vessels initiates once the leaves have reached full expansion, providing a protective mechanism against embolisms induced by drought (Kitin and Funada 2016). Other artificial and natural inoculation studies conducted in various geographical regions in the U.S. have similarly indicated that red oaks are more susceptible early in the growing season (Engelhard 1956; Kuntz and Drake 1957; Norris 1955). We attribute the observed accelerated progression of oak wilt during the early growing season to biological and physiological factors associated with earlywood vessels. Specifically, the thin-walled nature of earlywood vessels, in contrast to latewood vessels, may render them more susceptible to infection and facilitate the spread of *B. fagacearum* within the host. Similar findings in studies on Dutch elm disease (DED), a homologous pathosystem to oak wilt, have demonstrated that the susceptibility of large vessels contributes to the heightened vulnerability of elms early in the growing season (Tchernoff 1965). The long and broad earlywood vessels provide an ideal conduit for the dissemination of fungal propagules within the xylem of both elm and oak trees. In the case of DED, the most severe infections coincided with

the maturation of earlywood vessels in the spring (Tchernoff 1965). We propose that the rapid movement of *B. fagacearum* was facilitated by the rapid sap flow during the production of early sapwood, contributing to the accelerated disease progression. Furthermore, earlywood vessels are prone to cavitation, influenced by infection, wounding, and drought, potentially playing a role in the development of symptoms and tree mortality.

Nevertheless, red oaks demonstrated susceptibility to *B. fagacearum* infection even during periods when the xylem comprised latewood vessels, specifically in March, August, and September. However, the incidence of the disease during these periods was comparatively lower than during the early growing season, indicating that while earlywood vessels play a significant role, they do not solely determine the potential disease incidence. Our hypothesis suggests that the cessation of sap flow later in the season may partly determines disease incidence. It is evident from the absence of infections in trees inoculated in October and November when the sap flow rate drops drastically, as predicted from PETref. We propose that this phenomenon may be attributed to limited movement and distribution of *B. fagacearum* within the host when sap flow has ceased. Cobb et al. (1965) also suggested that the lower disease incidence in branch vs stem inoculations in their study could be due to slow movement of the fungus with branch sap flow. Similar findings were also reported in a study conducted in Iowa. Engelhard (1956) inoculated fresh stem wounds on red oaks at 4- to 5-week intervals throughout the year, and disease incidence was limited to trees inoculated between April 25 and August 28. Similarly, onset of symptoms and tree mortality showed significant correlation to proxy of sap flow. This indicates faster sap flow rates will lead to quicker spread of the pathogen within inoculated host. Consequently, leading to faster development of disease symptoms and eventually tree mortality. In laurel wilt, a similar pathosystem to oak wilt, similar pattern was reported. An avocado

cultivar with highest sap flow rate was more susceptible to infection than inoculated cultivars with lower sap flow rate (Ploetz et al. 2015).

Surprisingly, we observed a lower disease incidence in August, particularly when compared to inoculations carried out in September. This outcome was unexpected, as disease incidence is typically anticipated to be lower in September comparative to August inoculations. This expectation stems from the predicted reduction in sap flow, also evident from observed leaf phenophases, as trees undergo senescence during this period. However, these results could be attributed to a dry spell in August. For instance, the average monthly rainfall was markedly low at 0.47 and 1.33 inches in August 2018 and 2019, respectively. This scarcity in rainfall may have resulted in decreased soil moisture, consequently leading to reduced sap flow and a subsequent decline in disease incidence. Cobb et al. (1965) also documented a parallel unexpected reduction in disease incidence potentially influenced by diminished soil moisture. This underscores the constrained spread of the pathogen in tandem with reduced sap flow. Additionally, significant faster development of symptoms and tree mortality from June and July inoculations coincide with highest predicted sap flow. This observation further emphasizes the pivotal role of sap flow in influencing both the incidence and progression of oak wilt.

Moreover, the variations in symptom development observed between early and late-season inoculations could be attributed to predicted differences in the sap flow during the time of inoculation. These sap flow disparities suggest varying movement of the pathogen in the tree. Notably, differences in the disease progression between August and September inoculations are apparent. Trees inoculated in August displayed disease symptoms within the same calendar year, while those inoculated in September exhibited symptoms following spring. Furthermore, trees inoculated in September experienced a slower rate of mortality compared to those inoculated in

August. It indicates a delayed pathogen spread within trees inoculated in September. Another potential explanation might be that the slower spread of the pathogen with sap flow allows the host tree more time to induce a defense response, potentially leading to observed delayed symptoms and mortality as predicted by sap flow dynamics.

Mycelial mat production is significantly influenced by ambient temperature. Mat production is hindered in July when daily average temperatures exceed 22°C. No mycelial mat production on trees inoculated in June and July is potentially attributed to fastest progression of the disease. The rapid death of trees appears to result in sapwood moisture diminishing below the requirement for mat production. The formation of oak wilt mats is dependent on the moisture content of the sapwood and requires 37 to 55 % moisture to be induced (Tainter and Baker, 1996). Sapwood of trees inoculated in June and July might have dried out rapidly before favorable temperatures could be met in late fall and early next spring. It seems reasonable to observe that trees inoculated in August and September formed considerably more mats than those inoculated in March to May. It is likely that trees inoculated in late fall lose moisture slowly throughout winter, remaining fresh until reaching the sapwood stage associated with mat production in the next spring. Conversely, trees inoculated in March-May might have lost moisture throughout the summer, deviating sapwood moisture from favorable requirement for mat production.

To mitigate the risk of false disease escape due to low conidia concentrations, this study employed double the standard conidia concentration typically used in plant pathology experiments. The number of conidia required for natural infection through nitidulid vectors remains unclear. Although various studies have documented a variable number of *B. fagacearum* conidia carried by insect species in different geographical conditions (Hayslett et al. 2008;

Jagemann et al. 2018; Juzwik et al. 2004). In Michigan, six species of nitidulid beetles found carrying an average of 6,000 conidia per beetle (Morris et al., in prep). Nevertheless, the number of beetles necessary to visit a wound and cause a successful infection remains undetermined. Future inoculation trials that can mimic conidial concentrations required for natural infections are warranted to ascertain temporal host susceptibility especially during the growing season.

In this study, we observed that the predicted sap flow rate was significantly correlated with oak wilt progression, indicating that host susceptibility to *B. fagacearum* was related to its ability to conduct water. The survival of red oaks from *B. fagacearum* infection has been observed in Minnesota; however, this phenomenon has never been reported before (Dr. Jennifer Juzwik, personal communication). We speculate whether the recovery of the red oaks patch is associated with reduced sap flow. Screening the progenies of these oaks for potential host tolerance to *B. fagacearum* may facilitate the selection of red oaks with potential oak wilt tolerance.

Acknowledgements

We are thankful to Scott Lint, and Phillip Kurzeja (Michigan Department of Natural Resources), and Tina Guo, Emily Ruda for their assistance in the field. We appreciate statistical consulting support by Sukhdeep Singh and Guanqi Lu at College of Agriculture and Natural Resources, Michigan State University. This research was funded in part by the Michigan Invasive Species Grant Program and Project GREEN.

Figures

Figure 2.1. Oak wilt early season infection symptoms on *Quercus rubra*: An infected tree is often first noticed when leaves on the top of the upper crown turn yellowish-brown. Flagging of upper and outer canopy branches can occur (picture taken, July 9, 2019) (A), followed by rapid defoliation of leaves and downward progression of wilt symptoms in the tree crown (picture taken, July 23, 2019) (B). Eventually, an infected tree can defoliate the crown; however, some necrotic leaves may stay on branches (picture taken, August 13, 2019) (C). Abundant green, brown, and bronzed leaves with marginal scorch are often seen under the crown of an infected tree (D).

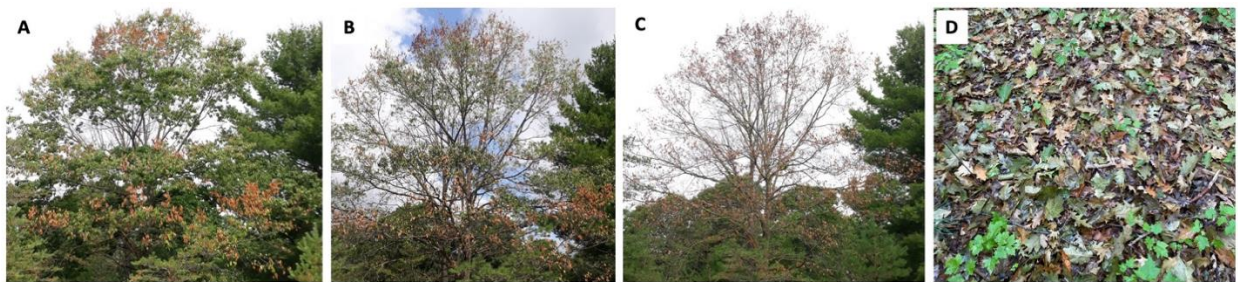


Figure 2.2. Foliar symptoms of oak wilt on *Quercus rubra*. Initially, leaves exhibit wilting, resembling physiological wilt or drought stress (A). Subsequently, leaves transition to a dull green to bronze hue, displaying a water-soaked appearance with heightened wilting (B). Ultimately, the leaves adopt a yellow to brown coloration and exhibit curling around the midrib (C). Notably, a distinctive progression of well-defined bronzing and tanning is often observed on fallen leaves, originating from the leaf blade, and progressing towards the midrib and base of the leaves (D).



Figure 2.3. Oak wilt late-season infection symptoms on *Quercus rubra* (A, B): Trees inoculated in August and September exhibited no disease symptoms until the subsequent spring, and the pattern of symptom development differed from early-season inoculations. Instead of the flagging of the upper tree crown, trees that were inoculated later leafed out resembling healthy trees, albeit with a sparse crown, and fully expanded leaves that were smaller in size (photograph taken on June 2, 2020) (A). Ultimately, the leaves wilted and turned necrotic (photograph taken on July 6, 2020) (B). Epicormic shoots frequently emerged on both early and late-season inoculated trees (C, D): Infected trees developed epicormic shoots as a final survival attempt (photograph taken on June 18, 2020) (C), but these epicormic shoots eventually succumbed to the infection (photograph taken on July 23, 2020) (D).

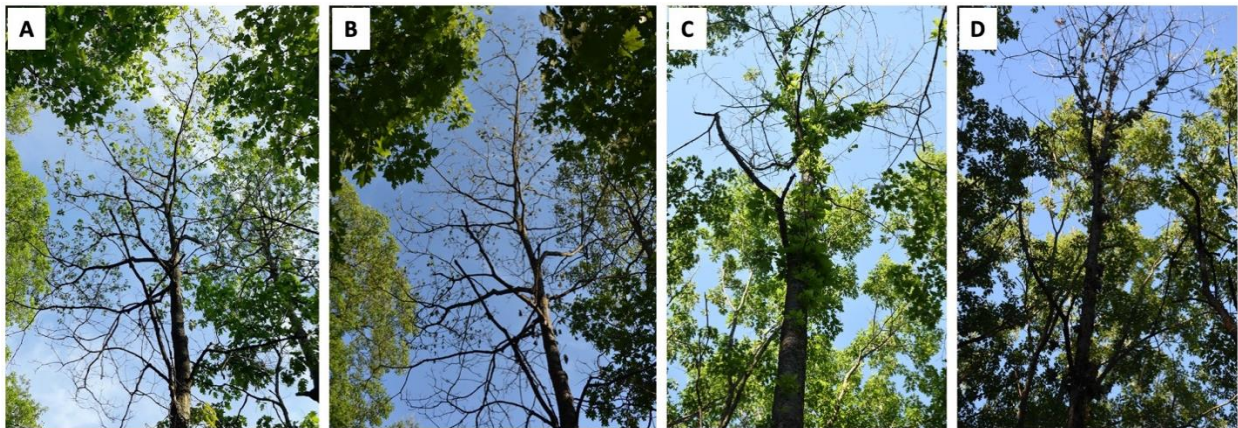


Figure 2.4. Average number of days for symptom development and tree mortality following monthly inoculations from 2017 to 2020. The correlation between the progression of oak wilt (average days to symptom onset and mortality) and predicted sap flow from reference evapotranspiration is depicted. Bars sharing the same letter indicate no significant differences ($P=0.05$).

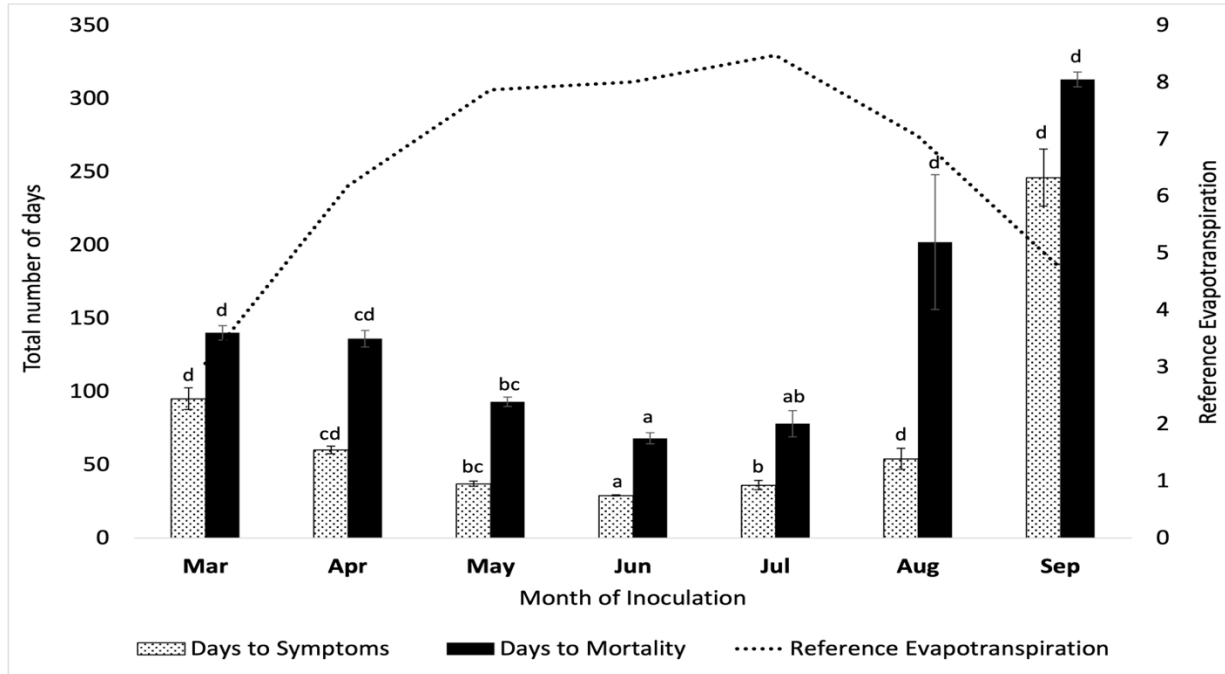


Figure 2.5. The total number of *B. fagacearum* mycelial mats observed on infected *Quercus rubra* trees from 2018 to 2020 was determined. Trees were inspected for mycelial mats at 15-day intervals from March through November 2018-2020.

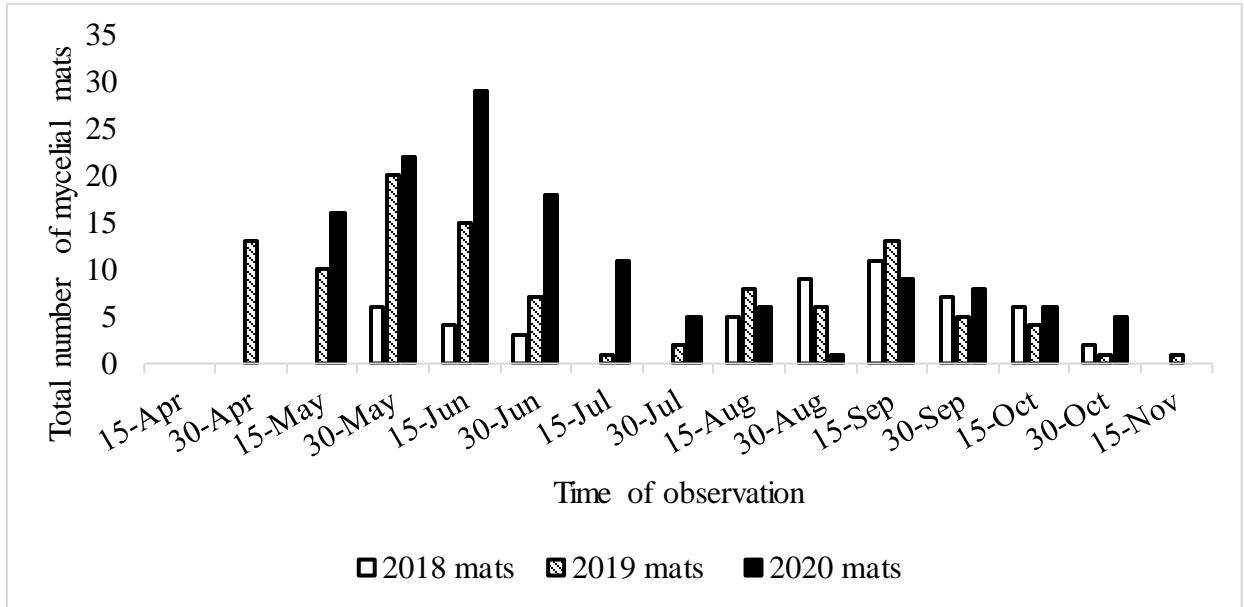
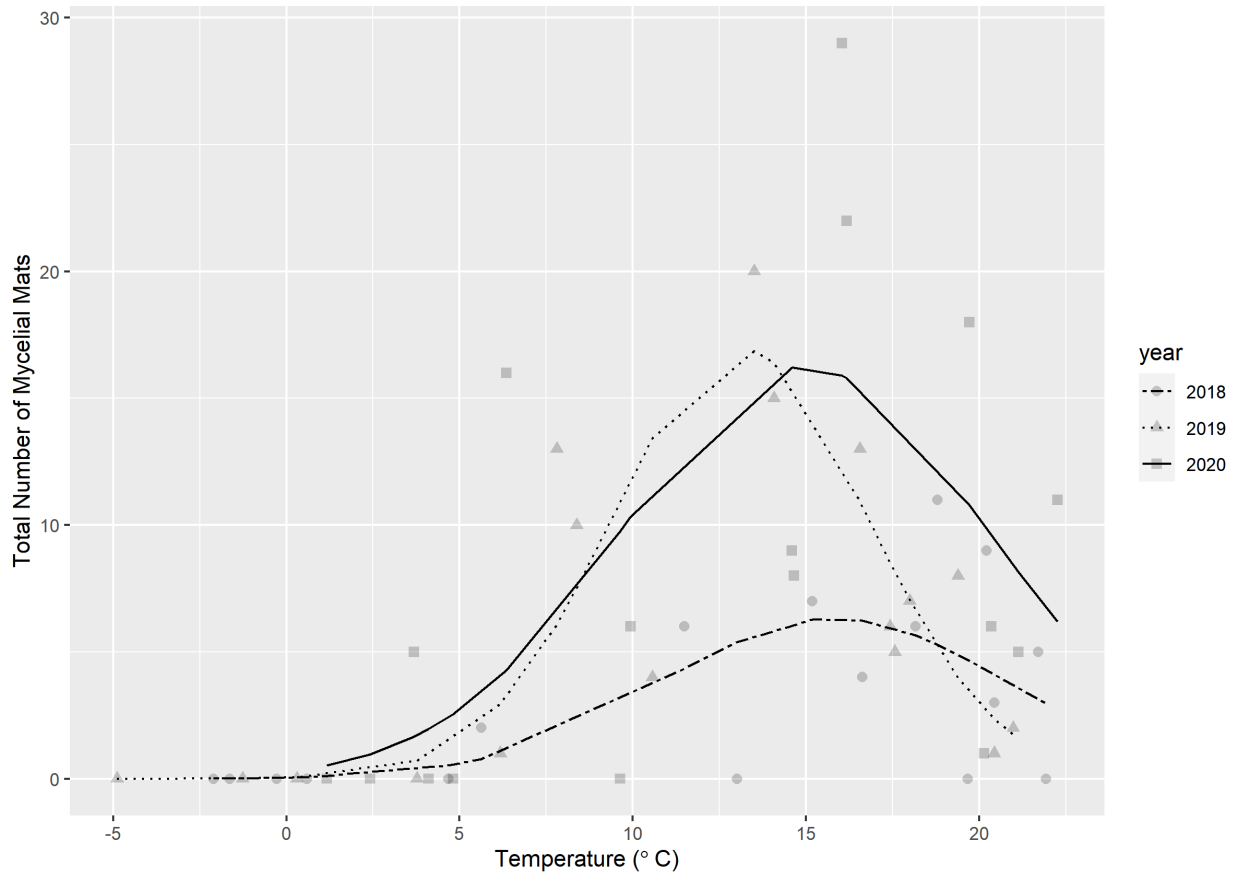


Figure 2.6. The relationship between mycelial mat production on infected trees and the average daily temperatures recorded 15 days prior to the observation date was determined using multiple regression analyses. Mycelial mat production was observed on inoculated trees from 2018 to 2020.



TABLES

Table 2.1. Mortality of northern red oak trees, *Quercus rubra* following oak wilt fungus, *Bretziella fagacearum* inoculations in the years of 2017, 2018, 2019, and 2020.

Year^a	Month^b	Day^c	Mortality^d	Healthy-Replicate^e	Phenophases^f
2017	August	1	Yes	-	Fully expanded
2017	September	6	Yes	-	Fully expanded
2017	September	27	Yes	-	Fully expanded
2017	October	28	No	-	Leaf senescence
2018	April	20	Yes	-	Buds dormant
2018	May	8	Yes	-	Buds swollen
2018	June	8	Yes	-	Fully expanded
2018	July	12	Yes	-	Fully expanded
2018	August	10	Yes*	Bunker, Coyote	Fully expanded
2018	September	12	Yes*	Nessen	Fully expanded
2018	October	17	No	-	Leaf senescence
2018	November	13	No	-	Buds dormant
2019	March	28	Yes*	Nessen, Coyote	Buds dormant
2019	April	18	Yes*	Bunker	Buds dormant
2019	May	14	Yes*	Coyote	Buds swollen
2019	June	11	Yes	-	Fully expanded
2019	July	9	Yes	-	Fully expanded
2019	August	13	Yes*	Nessen, Coyote	Fully expanded
2019	September	13	Yes	-	Fully expanded
2019	October	11	No	-	Leaf senescence
2019	November	8	No	-	Buds dormant
2020	March	17	Yes*	Coyote	Buds dormant

^a Year of inoculation

^b Month of inoculation

^c Specific date of a month on which inoculations were conducted

^d Yes, if one or more inoculated trees showed disease incidence/mortality

* If, not all the inoculated replicates were succumbed to infection

^e At which field sites trees didn't succumb to infection out of total 3 sites

^f Observed phenology of leaves at the time of inoculation

LITERATURE CITED

Allen, R. G., Pereira, L. S., Raes, D., and Smith, M. 1998. Crop evapotranspiration-Guidelines for computing crop water requirements. FAO Irrigation and Drainage Papers 56. Food and Agricultural Organization of the United Nations, Rome.

Ambourn, A. K., Juzwik, J., and Moon, R. D. 2005. Seasonal dispersal of the oak wilt fungus by *Colopterus truncatus* and *Carpophilus sayi* in Minnesota. *Plant Dis.* 89:1067-1076.

Appel, D. N. 1995. The oak wilt enigma: perspectives from the Texas epidemic. *Annu. Rev. Phytopathol.* 33:103-118.

Banfield, W. M. 1941. Distribution by the sap stream of spores of three fungi that induce vascular wilt diseases of elm. *J. Agric. Res.* 62:637-681.

Canadian Food Inspection Agency. 2023. <https://inspection.canada.ca/plant-health/invasive-species/plant-diseases/oak-wilt/eng/1325624048625/1325624535106>. Last accessed December 2023.

Cobb, F. W., Fergus, C. L., and Stambaugh, W. J. 1965. Factors affecting infection of red and chestnut oaks by *Ceratocystis fagacearum*. *Phytopathology* 55:1194-1199.

Cook, S. J. 2001. Current practices and suppression methods for managing oak wilt disease. Pages 93-100 in: *Shade Tree Wilt Diseases*. C. L. Ash, ed. APS Press, St. Paul, MN.

De Beer, Z. W., Marincowitz, S., Duong, T. A., and Wingfield, M. J. 2017. *Bretziella*, a new genus to accommodate the oak wilt fungus, *Ceratocystis fagacearum* (Microascales, Ascomycota). *MycoKeys* 27:1-19.

Engelhard, A. W. 1956. Influence of time of year and type of inoculum on infection of oak trees inoculated with the oak wilt fungus. *Plant Dis. Rep.* 40:1010-1014.

Er-Raki, S., Chehbouni, A., Ezzahar, J., Khabba, S., Boulet, G., Hanich, L., and Williams, D. 2009. Evapotranspiration partitioning from sap flow and eddy covariance techniques for olive orchards in semi-arid region. *Acta Hort.* 846:201-208.

Forster, M. A. 2021. A test of the relationship between sap flow and evapotranspiration, normalized via leaf area, under non-limiting soil moisture. *Forests* 12:875. <https://doi.org/10.3390/f12070875>.

FRAC. 2022. FRAC Code List ©2022: Fungal control agents sorted by cross-resistance pattern and mode of action (including coding for FRAC Groups on product labels). <http://www.frac.info>. Accessed 02 December 2023.

Gibbs, J. N., and French, D. W. 1980. The transmission of oak wilt. USDA Forest Service Research Paper NC-185. Central Forest Experiment Station, St. Paul, MN.

- Hayslett, M., Juzwik, J., and Moltzan, B. 2008. Three *Colopterus* beetle species carry the oak wilt fungus to fresh wounds on red oak in Missouri. *Plant Dis.* 92:270-275.
- Henry, B. W., Moses, C. S., Richards, C. A., and Riker, A. J. 1944. Oak wilt, its significance, symptoms, and cause. *Phytopathology* 34:636-647.
- Hipp, A. L., Manos, P. S., González-Rodríguez, A., Hahn, M., Kaproth, M., McVay, J. D., Avalos, S. V., and Cavender-Bares, J. 2018. Sympatric parallel diversification of major oak clades in the Americas and the origins of Mexican species diversity. *New Phytol.* 217:439-452.
- Jagemann, S. M., Juzwik, J., Tobin, P. C., and Raffa, K. F. 2018. Seasonal and regional distributions, degree-day models, and phorsey rates of the major sap beetle (Coleoptera: Nitidulidae) vectors of the oak wilt fungus, *Bretziella fagacearum*, in Wisconsin. *Environ. Entomol.* 47:1152-1164.
- Johnson, L. L., and Shih, J. H. 2007. An introduction to survival analysis. <https://doi.org/10.1016/B978-012369440-9/50024-4>.
- Juzwik, J. 2007. Epidemiology and occurrence of oak wilt in Midwestern, Middle, and South Atlantic states. Pages 49-60 in: *Proceedings of the National Oak Wilt Symposium*. R. F. Billings and D. N. Appel, eds. Texas Forest Service Publication 166, Austin, TX.
- Juzwik, J., Appel, D. N., MacDonald, W. L., and Burks, S. 2011. Challenges and successes in managing oak wilt in the United States. *Plant Dis.* 95:888-900.
- Juzwik, J., Harrington, T. C., MacDonald, W. L., and Appel, D. N. 2008. The origin of *Ceratocystis fagacearum*, the oak wilt fungus. *Annu. Rev. Phytopathol.* 46:13-26.
- Juzwik, J., Skalbeck, T. C., and Neuman, M. F. 2004. Sap beetle species (Coleoptera: Nitidulidae) visiting fresh wounds on healthy oaks during spring in Minnesota. *For. Sci.* 50:757-764.
- Keykhasaber, M., Thomma, B. P., and Hiemstra, J. A. 2018. Distribution and persistence of *Verticillium dahlia* in the xylem of Norway maple and European ash trees. *Eur. J. Plant Pathol.* 150:323-339.
- Kitin, P., and Funada, R. 2016. Earlywood vessels in ring-porous trees become functional for water transport after bud burst and before the maturation of the current-year leaves. *IAWA J.* 37:315-331.
- Kuntz, J. E., and Drake, C. R. 1957. Tree wounds and long distance spread of oak wilt. *Phytopathology* 47:22.
- Morris, O. R. 2020. Seasonal activity and phorsey rates of sap beetles (Coleoptera: Nitidulidae) in oak wilt infection centers, volatile organic compounds related to the oak wilt cycle, and long-term evaluation of red oak provenances. Master's thesis, Michigan State University.

- Nicolas, E., Torrecillas, A., Ortuno, M. F., Domingo, R., and Alarcón, J. J. 2005. Evaluation of transpiration in adult apricot trees from sap flow measurements. *Agric. Water Manag.* 72:131-145.
- Norris, D. M. Jr. 1955. Natural spread of *Endoconidiophora fagacearum* Bretz to wounded red oaks in Iowa. *Plant Dis. Rep.* 39:249-253.
- Pereira, A. R., Green, S., and Nova, N. A. V. 2006. Penman–Monteith reference evapotranspiration adapted to estimate irrigated tree transpiration. *Agric. Water Manag.* 83:153-161.
- Ploetz, R. C., Schaffer, B., Vargas, A. I., Konkol, J. L., Salvatierra, J., and Wideman, R. 2015. Impact of laurel wilt, caused by *Raffaelea lauricola*, on leaf gas exchange and xylem sap flow in avocado, *Persea americana*. *Phytopathology* 105:433-440.
- Rexrode, C. O., and Lincoln, A. C. 1965. Distribution of oak wilt. *Plant Dis. Rep.* 49:1007-1010.
- Rioux, D., and Blais, M. 2023. Review and new insights into wood anatomy that help understand and control oak wilt. *Phytoprotection* 103:1-25.
- Snover-Clift, K., and Rosenthal, E. 2016. Is oak wilt really a threat to New York State landscapes and forests? https://ecommons.cornell.edu/bitstream/handle/1813/60592/BranchingOut_OakWilt5-16.pdf?sequence=1. Last cessed December 2023.
- Tainter, F. H., and Baker, F. A. 1996. Oak wilt. Pages 673-682 in: *Principles of Forest Pathology*. John Wiley and Sons, Inc., New York, NY.
- Tchernoff, V. 1966. Methods for screening and for the rapid selection of elms for resistance to Dutch elm disease. *Acta Bot. Neerl.* 14:409-452.
- USDA-FAS. 2022. U.S. Dept. of Agriculture, Foreign Agricultural Service, Global Agricultural Trade System. <https://apps.fas.usda.gov/gats/default.aspx>. Last accessed December 2023.
- Yang, A., and Juzwik, J. 2017. Use of nested and real-time PCR for the detection of *Ceratocystis fagacearum* in the sapwood of diseased oak species in Minnesota. *Plant Dis.* 101:480-486.
- Wilson, A. D. 2005. Recent advances in the control of oak wilt in the United States. *Plant Pathol. J.* 4:177-191.

CHAPTER 3: NOVEL NON-DESTRUCTIVE DETECTION METHODS FOR *BRETZIELLA FAGACEARUM* IN NORTHERN RED OAK AND CHESTNUT

Abstract

Oak wilt, caused by the fungal pathogen *Bretziella fagacearum*, spreads via root grafts and insect vectors, posing a significant threat to oaks (*Quercus* spp.) in the United States and Canada. Detection and management are crucial, as oak wilt can devastate forested and urban ecosystems. However, oak wilt disease diagnosis presents challenges and requires laboratory confirmation due to symptom similarities with other stressors. Commonly used detection methods also have limitations. In this study, we optimized and validated a TaqMan real-time PCR assay. Results were compared with a culture-based method, and a nested PCR assay served as the standard. The real-time PCR assay demonstrated a consistent 100% detection rate and accuracy across all branch sapwood conditions. In contrast, the culture-based method varied significantly, only achieving 100% detection rate and accuracy for fresh samples with discoloration. In the absence of sapwood discoloration, the detection rate and accuracy were 80% and 90%, respectively. For dry sapwood samples, the rates decreased significantly to 22% and 52%, respectively. Additionally, we evaluated a non-destructive sampling method using leaf petioles of fallen leaves to detect *B. fagacearum* from northern red oak and chestnut trees, using both real-time PCR and culture-based methods. The real-time PCR outperformed the culture-based method consistently, regardless of the severity of symptoms in leaf samples. This technique offers superior efficiency, specificity, sensitivity, and turnaround time compared to nested PCR and culture-based methods. Our findings highlight the potential of detecting vascular-inhabiting pathogens from leaf petiole samples, particularly in scenarios requiring non-destructive sampling or more efficient and high-throughput screening.

Introduction

Oak wilt is caused by the fungal pathogen, *Bretziella fagacearum* (Bretz) Z.W. de Beer, Marinc., T.A. Duong & M.J. Wingf., previously known as *Ceratocystis fagacearum* (Bretz) J. Hunt (de Beer et al. 2017). Oak wilt is an economically and ecologically important disease of oaks (*Quercus* spp.) in the United States (Juzwik et al. 2011) and Canada (Gauthier et al. 2023). The fungal pathogen spreads below-ground from infected trees to neighboring oaks through networks of grafted roots, thus forming centers or pockets of diseased oaks (Juzwik et al. 2011). *B. fagacearum* is also transmitted above-ground by sap or nitidulid beetles (Coleoptera: Nitidulidae) and oak bark beetles (*Pityophthorus* spp.) (Gibbs and French 1980). Oak wilt has the potential to change urban and natural forested ecosystems significantly if disease epicenters remain undetected and unmanaged (Appel 1995, Gauthier et al. 2023). Currently there are disease epidemics in portions of the midwestern states and Texas (Chahal et al. 2019b, 2021; Juzwik et al. 2011). Oak wilt infestations can be managed when disease centers are detected and treated in a timely manner (Juzwik et al. 2011; Koch et al. 2010).

Oak species have different levels of susceptibility to *B. fagacearum*. Red oak species in the section *Lobatae* (i.e., *Q. rubra*, *Q. nigra*) are highly susceptible and can die within months of infection (Appel 1995; Chahal et al. 2022b). White oak species in the section *Quercus* (i.e., *Q. macrocarpa*, *Q. alba*) are moderate to low in susceptibility based on disease severity. In white oaks, *B. fagacearum* infection typically leads to branch dieback, and tree mortality is rare, sometimes taking decades to occur (Juzwik et al. 2011). While there is variation in the rate of disease progression among oak species, none of the *Quercus* species are immune to the disease. Symptoms of oak wilt in red oak species include wilting of green leaves, often starting at the top crown and progressing downward (Appel 1995; Chahal et al. 2022b; Juzwik et al. 2011). The

leaves turn dull green or bronze, appearing water-soaked, with leaf abscission throughout the crown. Infected trees exhibit noticeable crown flagging, with well-defined tanning of leaf tips and outer edges, progressing towards the midrib and leaf base. Water sprouts or epicormic shoots often emerge on infected tree boles and limbs but quickly become symptomatic (Chahal et al. 2022b).

Oak wilt symptoms can be confused with other biotic and abiotic stressors commonly observed in oaks. These symptoms can be confused with bacterial leaf scorch (*Xylella fastidiosa*), Armillaria root rot (*Armillaria* spp.), Anthracnose (*Apiognomonina quercinia*), bur oak blight (*Tubakia iowensis*), Tubakia leaf spot (*Tubakia* spp.), and oak decline (Abrams 2003; Gould and Lashomb 2007; Harrington et al. 2012; Lee et al. 2016; Pearce and Williams-Woodward 2009). Abiotic stress and insect infestations such as environmental scorch, two-lined chestnut borer (*Agrilus bilineatus*), cynipid gall wasp (*Cynipis* spp.) can result in crown flagging resembling oak wilt symptoms (Haack and Acciavatti 1992; Rauschendorfer et al. 2022; Stone et al. 2002). Variability in symptoms development in white oaks poses an additional challenge for diagnosing based on crown symptoms (Juzwik et al. 2011). Due to these oak wilt look-alike issues a precise and timely laboratory diagnosis is crucial when implementing management options.

Diagnostic laboratories use both culture-based and molecular methods to detect *B. fagacearum* in diseased tree samples (Yang and Juzwik 2017). For culture-based isolation, fresh sapwood samples are required for successful pathogen isolation. Culture plates undergo incubation for 10-14 days and the process is labor-intensive. Significant limitations are associated with sample quality, which can result in false negatives (Yang and Juzwik 2017; Wu et al. 2011). For instance, desiccated or overheated branch samples typically constitute poor-

quality material, reducing the likelihood of isolating the pathogen (Bretz and Morrison 1953). Moreover, *B. fagacearum* is a weak saprophyte, which presents challenges in culturing from dead or moribund material colonized by secondary microorganisms.

Molecular assays for detecting of *B. fagacearum* include three real-time PCR assays (Bourgault et al. 2022; Kurdyla and Appel 2011; Lamarche et al. 2015), a nested PCR (Wu et al. 2011), and a nanoaggregation-enhanced chemiluminescence assay (Singh et al. 2017). And two in-field detection assays include DNA endonuclease-targeted CRISPR trans reporter (DETECTR) (Bourgault et al. 2022) and the commercially available LAMP assay (AgroLAMP, PureBioX, Saint Paul, MN), lack in detection accuracy. Similarly, real-time PCR assay developed by Kurdyla and Appel (2011) yield unreliable results attributed to a lack of detection consistency and sensitivity, and currently not preferred (Yang 2015). Yang and Juzwik (2017) reported that the nested PCR (Wu et al. 2011) had a higher pathogen detection rate compared to the real-time PCR (Kurdyla and Appel 2011) protocol. The low success rate of the real-time PCR (Kurdyla and Appel 2011) may be attributed to a high concentration of PCR-inhibiting compounds (e.g., tannic acid and polyphenolic compounds) and a low target concentration (Yang and Juzwik 2017, Johnson et al. 2009; Opel et al. 2010). The limited sensitivity of the real-time PCR developed by Lamarche et al. (2015) often arises from the low copy number of target gene regions, as the amplification target, transcription elongation factor 1-a (TEF), is a single-copy gene. The TaqMan real-time PCR developed by Bourgault et al. (2022) requires validation with disease wood samples before clinical adoption. Further optimization and validation are necessary before the real-time PCR protocols are ready for operational deployment. The nested PCR has inherent issues such as carryover contamination and the extra time required (Cardwell et al.

2023). Therefore, a different real-time PCR assay with comparable results to the nested assay would be highly beneficial for diagnostic clinics (Yang and Juzwik 2017).

For the diagnosis of oak wilt, samples from symptomatic branches are considered ideal. In cases where branches are out of reach, taking window sections from tree boles is suggested (Pokorny 1999). However, this method is destructive and can facilitate the entry of insect pests and decay pathogens (Haavik et al. 2008; Tsen et al. 2016). Furthermore, if wounds are not painted after taking branch or bole samples, the tree is at risk of above-ground infection by nitidulid beetles. The risk is particularly high during peak insect-vector activity, which coincides with the timing of oak wilt symptom development in the summer in the midwestern US (Chahal et al. 2019b, 2022b; Morris 2020). Therefore, the validation of a non-destructive sampling method is crucial for *B. fagacearum* detection without negatively impacting tree health.

This study aimed to 1) standardize and validate of a real-time PCR assay, 2) compare the real-time PCR with the standard nested PCR assay and the widely adopted culture-based detection method, 3) develop a non-destructive sampling method for *B. fagacearum* detection, and 4) couple the non-destructive sampling method with both molecular and culture-based detection methods.

Materials and methods

Sample collection:

For branch samples, during the 2020 growing season, homeowners and arborists in Michigan collected branch samples approximately 2.5-5 cm in diameter and 15 cm in length from diseased oak trees suspected of oak wilt infection. Samples for *B. fagacearum* detection were submitted to Plant & Pest Diagnostics clinic at Michigan State University. Typically, 3 to 6 branch sections were received per tree (Fig. 3.1). Samples were mailed or dropped off in sealed

plastic bags without any additional moisture, wet paper towels, or ice bags. Samples were stored in a cold room (4°C) until being assayed with both culture-based and molecular detection methods.

Petiole samples were collected in August 2023, fallen leaves displaying symptoms of oak wilt were randomly collected under the crowns and within 6 m radius of northern red oak (*Q. rubra*) trees in natural infection centers. Petioles were split (see, method of petiole processing) analyzed with culture-based and molecular detection were collected under four different trees at site 1 (44.6053130, -85.8144990). Additionally, leaves were sampled under two trees at each of three distinct sites: site 2 (44.6004655, -85.7980916), site 3 (44.5745210, -85.3631764), and site 4 (44.5596650, -85.8068220). The whole petioles (see, method of petiole processing) exclusively analyzed using real-time PCR were collected from two different trees at site 5 (44.51058333, -84.83761111) and site 6 (44.7366944, -85.44555556). Leaves collected under a non-symptomatic tree at site 1 and site 5 were processed as controls. The collected leaf samples were placed into 2-gallon Ziploc bags (SC Johnson, Racine, WI) and transported to the laboratory. Subsequently, the Ziploc bags were stored at 4°C until sample processing. The leaf samples designated as oak wilt ‘herbarium specimens’ were collected in August 2019 at site 5 (44.51058333, -84.83761111) and site 2 (44.6004655, -85.7980916). Senescing leaves collected from healthy (non-symptomatic) trees in August 2019 were used as controls for processing herbarium specimens. These samples underwent dry mounting and were stored in an herbarium file at room temperature until processed in November 2023. Chestnut leaves were collected from artificially inoculated seedlings, with a conidial suspension containing 10⁶ spores (Chahal et al. 2024). Leaves collected from mock-inoculated seedlings were processed as controls.

Disease severity ratings for leaves:

Chestnut and northern red oak leaf samples were visually assessed into three severities of symptoms: asymptomatic, moderate, and severe (Fig. 3.2). An 'asymptomatic' rating indicated the absence of observable foliar symptoms, while 'moderate' denoted approximately half of the leaf area turned bronze or necrotic. A 'severe' rating indicated the entire leaf displaying bronze or necrotic symptoms. Necrotic leaves typically exhibit curling around the mid-rib, commonly observed on oaks and chestnuts infected by *B. fagacearum* (Fig. 3.2). Five leaves were randomly selected from each of ten northern red oaks and categorized into one of three symptom severity ratings. Likewise, chestnut leaves were collected from the inoculated seedlings at different time intervals. 'asymptomatic' leaves were collected fourteen days after inoculation, before any foliar symptoms were observed, except for the bending of petioles (Fig. 3.2). Leaves with 'moderate' and 'severe' symptoms were collected 24 to 34 days after inoculation, respectively (Chahal et al. 2024).

Sample processing:

Branch samples were sprayed with 70% ethanol and wiped using paper towels to remove potential contaminants, including lichens and moss. The outer bark was removed, exposing the cambium layer. Samples were then categorized as 'fresh' if the cambium was green and 'dry' if it had turned brown (Fig. 3.1). To expose the sapwood, both outer bark and cambium layers were removed using a knife (Stanley, 6 in. Classic Retractable Utility Knife, Model # 10-099). Sapwood discoloration was variable among the samples (Fig. 3.1). However, samples were categorized only based on the presence or absence of discoloration. In a biosafety hood, samples were flame sterilized after being sprayed with 95% ethanol. Pieces measuring 2.5 to 5cm from the outer 1-2 layers of sapwood were excised for further processing. Excised wood pieces were

cut into $\sim 1.5 \times 0.5 \text{ cm}^2$ chips for plating, and smaller $\sim 0.3 \times 0.2 \text{ cm}^2$ pieces for DNA extraction (Fig. 3.1). The resulting smaller pieces, weighing $100 \pm 2 \text{ mg}$, were stored in 1.7 ml centrifuge tubes (Fisher Scientific, Pittsburgh, PA) at -20°C until DNA extraction.

Detection of *B. fagacearum* from petioles involved using leaf petioles (4 cm) through both culture-based and molecular methods. If petioles were less than 4 cm long, the midrib of leaves was included. For sessile chestnut leaves, the leaf blades were removed to expose a 4 cm segment of the midrib (Fig. 3.3). The cut petioles were surface sterilized by dipping in 75% ethanol (30 s), followed by 10% (v/v) bleach (1 min), and two rinses with sterile deionized water ($>1 \text{ min}$). Surface-sterilized petioles were vertically split into two from the middle using sterilized scissors (JAPONESQUE Beauty Scissors, UPC: 639428592295). One half was allocated for culture-based detection, divided into five pieces ($\sim 0.8 \text{ cm}$). The remaining half was cut into smaller pieces ($\sim 0.2 \text{ cm}$) for sample maceration and DNA extraction. ‘Whole petiole’ samples consisted of unsplit 4-cm long petioles. From each sampled tree, three sub-samples were collected for each of the three disease severity ratings. The first sub-sample consisted of a single petiole, the second included two, and the third comprised three petioles. This resulted in a total of 12 samples per severity rating, each with varying numbers of petioles. Herbarium samples were processed without considering severity ratings. In total, 21 samples were processed, with each set of seven samples containing either one, two, or three petioles.

Culture-based detection of B. Fagacearum:

Acidified full-strength potato dextrose agar (PDA; Difco, Sparks, MD) medium was used to isolate *B. fagacearum* from sapwood and petiole pieces. To make acidified PDA, 1 ml of 80% lactic acid (JT Baker, Phillipsburg, NJ) was added into autoclaved 1 L of full-strength PDA. From each sample, five sapwood chips ($\sim 1.5 \times .5 \text{ cm}$) were cultured per plate, totaling 4 plates

used per single tree. Five petiole pieces (~0.8 cm) from each split-petiole were cultured on a single Petri dish. Half of each of the five petiole, and sapwood pieces were submerged into the media, while the rest remained on the surface. The plates were incubated at room temperature (~24°C) under ambient lighting and checked regularly for fungal growth. *B. fagacearum* growth was observed 5-7 days after culturing (Fig. 3.3). Plates were held for a maximum of 21 days. Cultured plates that yielded mixed fungal species were sub-cultured until pure cultures were obtained. Pure cultures of *B. fagacearum* were confirmed by the presence of gray to olive-green colonies, a characteristic fruity odor, and the presence of endoconidia (de Beer et al. 2017). The identity of two representative pure cultures was also confirmed by sequencing of the internal transcribed spacer (ITS1F and ITS4R), as described in Chahal et al. 2019a. The obtained sequences showed 100% identity to an ex-type (KU042044) of *B. fagacearum* and were deposited in GenBank (PP563673, PP563674).

Nucleic acid extraction:

The DNA extractions from branch and petiole samples were performed using QIAamp Fast DNA Stool Mini Kit (Qiagen, Germantown, MD) following the manufacturer's suggested protocol. The tissue lysis step of incubation at 95°C for 5 min was opted. Sapwood and petiole pieces were transferred into Lysing Matrix A (MP Biomedicals, SKU:116910050-CF) 2-ml tubes with two ceramic beads. After adding 1000 µl of InhibitEX buffer, samples were macerated using a Bead Mill 24 homogenizer (Fisher Scientific) or FastPrep-FP120 (Thermo Fisher Scientific, Waltham, MA), with two 45-second cycles at 6.5 m/s speed and a 5-minute rest in between. Samples were visually inspected to confirm complete maceration (Fig. 3.1). If necessary, a third maceration cycle was performed.

Nested PCR:

Amplifications of extracted DNA samples were performed using the nested PCR protocol developed by Wu et al. (2011). Negative controls without template DNA were used in each experiment to test the potential for contamination. The products from the second round of PCR, with expected amplicon size of 280 bp, were observed on a 2% agarose gel and subsequently sequenced for confirmation. Representative sequences were deposited in GenBank (accession nos. PP563665-PP563672).

Real-time PCR:

The real-time PCR was performed using a CFX96 Real-time PCR system (BioRad, Hercules, CA). Reactions were carried out as described by Bourgault et al. (2022) with modifications. The reaction volume was doubled, and QuantiTect Multiplex PCR NoROX Master Mix (Qiagen) was substituted with PerfeCTa qPCR ToughMix (Quanta Biosciences, Gaithersburg, MD). Each 20- μ l reaction contained 10 μ l of PerfeCTa qPCR ToughMix, 1.2 μ l of each primer (10 μ M), 0.2 μ l of probe (10 μ M), 2 μ l of extracted DNA, and 5.4 μ l of molecular-grade water. Reactions were performed as described to calculate the cycle threshold (Ct) values for each sample. All reactions were performed in duplicate, including those containing the *B. fagacearum* pure DNA standard, non-template control, and DNA from non-symptomatic, mock-inoculated trees. The Ct values were compared among different sample types. A standard curve was generated using genomic DNA from a pure culture of *B. fagacearum and am.* A 10-fold serial dilution of DNA concentrations from 1 ng/ μ l to 1 fg/ μ l was used in generating the standard curve and amplified in triplicate. To obtain the slope of the real-time PCR standard curve, the log transformation of the DNA concentration (x-axis) was plotted against the average Ct value (y-axis) for each sample (Fig. 3.4). Efficiency of the assay was calculated by using the formula $E =$

$10^{(1/\text{slope})}$. The specificity of the assay was assessed using diseased samples from oak wilt-like issues and other fungi isolated on host species in Michigan (Table 3.1).

Statistical analyses

A Generalized Linear Mixed Model (GLMM) was fitted in R to identify detection differences of *B. fagacearum* from infected northern red oak branches, using culture-based, real-time PCR, and nested PCR. Methods, sapwood, and their interactions were treated as fixed effects, while branch samples were treated as random effects. The logistic-normal mixed model was:

$$\text{Logit } [P(Y_{ijk}=1)] = \mu + D_i + S_j + D:S_{ij} + \alpha_k + e$$

Here, P is the probability of detecting *B. fagacearum*, μ is the overall mean, D_i represents levels of the detection method variable, S_j represents levels of the sapwood variable, α denotes the random error associated with branch sample k , and e represents the overall error.

A logistic-normal mixed model analysis was used to estimate differences in detecting *B. fagacearum* in the petioles of both northern red oak, and chestnut across various detection methods, severity levels. Fixed effects included methods, species, severity, and their interactions. Trees within species and petiole subsamples within trees were treated as random effects. The model was formulated as:

$$\text{Logit } [P(Y_{ijklm}=1)] = \mu + M_i + S_j + Se_k + M:S_{ij} + M:Se_{ik} + S:Se_{jk} + M:S:Se_{ijk} + ul(m) + vn(m) + e$$

Here, P denotes the probability of detecting *B. fagacearum*, μ is the overall mean, M_i , S_j , Se_k represent the levels of the detection method, species, and severity factors, respectively. The $ul(m)$, and $vn(m)$ denote the random error for trees l within species and subsample n within trees l , respectively. Mixed models were fitted using the ‘glmmTMB’ package in R.

Analysis of variance (ANOVA) was conducted using the ‘car’ package in R. Post hoc tests were performed using the ‘emmeans’ package in R when significant differences between the sources of variation in the ANOVA were detected. Standard errors (SEs) were backtransformed from the logit scale and reported. Letters of significance at $\alpha = 0.05$ with a Bonferroni adjustment were obtained from the ‘multcomp’ package in R. In this study, accuracy is defined as the ability of a detection method to distinguish between true positive and true negative using the formula $([\text{true positives} + \text{true negatives}]/[\text{total number of samples}])$ (Baratloo et al. 2015). The detection rate is defined as the ability of a detection method to correctly identify the presence of *B. fagacearum* in a given population of samples and was calculated using the formula: $[\text{true positives}]/[\text{true positives} + \text{false negatives}]$.

Results

Sensitivity of the real-time PCR assay:

The real-time PCR assay was sensitive even at low DNA concentrations, and successfully detected *B. fagacearum* (Fig. 3.4). The detection limit for *B. fagacearum* in the real-time PCR assays was 1 fg/ μl , detected in all replications with the lowest DNA concentration having a Ct value of 37.83. The Ct value of 37.83 was determined as a cutoff limit for detection of the pathogen in branch and petiole samples. A linear correlation was observed between the log DNA concentration of detected *B. fagacearum* DNA and the Ct value of the assay ($R^2 = 0.9967$). The amplification efficiency of the real-time PCR reactions was determined to be 92% based on the slope of the standard curve.

Specificity of the real-time PCR assay:

No amplifications were observed in the extracted DNA from oak leaf petiole samples showing symptoms of various biotic and abiotic issues that resemble oak wilt (Table 3.1).

Similarly, extracted DNA from axenic cultures of *Armillaria* spp., *Gnomoniopsis paraclavulata*, *Ophiostoma quercus*, *Cladosporium* spp., also did not amplify. Additionally, extracted DNA from petioles and sapwood of mock-inoculated northern red oak (Chahal et al. 2022b) and chestnut (Chahal et al. 2024) did not yield amplifications.

Real-time PCR CT values and weight of different samples:

In branch samples, *B. fagacearum* was detected at an average (avg) Ct value of 27.53 ± 2.81 . Split petiole samples from northern red oak and chestnut trees showed avg Ct values of 33 ± 3.29 and 34.60 ± 2.63 , respectively. Among the northern oak whole petiole samples, those with one, two, and three petioles showed avg Ct values of 29.09 ± 2.10 , 27.62 ± 0.69 , and 29.05 ± 1.08 , respectively. In northern red oak herbarium samples, processing single, two, and three petioles resulted in avg Ct values of 31.58 ± 1.77 , 30.27 ± 1.74 , and 29.42 ± 1.80 , respectively.

The average weight of northern red oak branch sapwood samples processed with molecular assays was 100 ± 2 mg. Split petioles of northern red oak and chestnut, used for *B. fagacearum* detection via real-time PCR, yielded avg sample weights of 35.91 ± 15.23 mg and 69.57 ± 26.34 mg, respectively. Among whole petiole samples, those with one, two, and three petioles had avg weights of 105.66 ± 27.74 , 169.75 ± 28.45 , and 250.67 ± 28.94 , respectively. Herbarium samples with one, two, and three petioles had avg weights of 44.62 ± 12.50 , 86.26 ± 7.73 , and 128.27 ± 11.37 , respectively.

B. fagacearum detection from branch samples:

The detection of *B. fagacearum* in northern red oak branch samples is influenced by the method and condition (fresh or dry) of the sapwood. Real-time PCR consistently detected *B. fagacearum* with 100% accuracy and detection rate, regardless of the sapwood condition (Table 3.2, 3.3). However, the culture-based method's performance varied depending on sapwood

conditions (Table S3). While it achieved 100% accuracy and detection rate in fresh samples with sapwood discoloration, these rates decreased for fresh samples without discoloration (90% accuracy, 80% detection rate) and further declined for dry samples (51.72% accuracy, 22.22% detection rate) (Table 3.2). Overall, the culture-based method had an accuracy rate of 82.60% and a detection rate of 77.46 %. The nested PCR and the real-time PCR detection results were not influenced by sample condition. Detection differences among nested PCR, real-time PCR, and the culture-based method for fresh samples were not statistically significant (Table S3). However, the culture-based method's detection probability for dry samples was notably lower than that of the other methods, resulting in a higher rate of false negative results (Table 3.2, 3.3). Negative control samples yielded no amplification in real-time PCR, and *B. fagacearum* was not isolated in culture.

B. fagacearum detection from split petiole samples:

The detection of *B. fagacearum* in split petioles is influenced by the method, severity of symptoms, and host species (Table S4). In the overall analysis, real-time PCR detected *B. fagacearum* in 75% of the total petiole samples, while the culture-based method detected it in 57% of the samples (Table 3.3). Among symptom categories, *B. fagacearum* was detected in 79.16%, 67.85%, and 50.59%, of the analyzed asymptomatic, moderate, and severely affected samples from both species, respectively. Real-time PCR detected the pathogen in 81%, 76%, and 68% of asymptomatic, moderate, and severely affected samples, respectively, while the culture-based method detected it in 77%, 60%, and 30% of these samples, respectively. The pathogen was detected in 83% and 42% of the analyzed samples northern red oak and chestnut, respectively.

In northern red oak petiole samples, both culture-based and real-time PCR detected *B. fagacearum* in 98% of asymptomatic samples (Table 3.3). However, differences in detections between the culture-based method and real-time PCR were significant for processing severely affected samples (Table 3.4). For samples with moderate severity, the culture-based and real-time PCR detected the pathogen in 80% and 94% of the samples, respectively. The culture-based method detected the pathogen in 51% of the samples, while real-time PCR detected it in 78% of the analyzed samples. Significant differences in detections using the culture-based method observed between samples with moderate and severe symptoms.

In chestnut samples, *B. fagacearum* detection highly differed between culture-based and real-time PCR methods (Table 3.3). Culture-based method detected *B. fagacearum* in 49% of asymptomatic samples and 31% of samples with moderate severity. In contrast, real-time PCR detected the pathogen in 57% of asymptomatic samples and 51% of samples with moderate severity (Table 3.5). Significant differences in detections were observed for samples with severe symptoms, with the culture-based method detecting the pathogen in only 9% of the samples compared to 54% by real-time PCR. The negative control samples for both host species yielded no amplification in real-time PCR, and the pathogen was not isolated in culture.

B. fagacearum detection from whole petiole samples:

The pathogen was detected in 100% of the analyzed whole petiole samples, regardless of the number of petioles included in the sample and the severity of symptoms. (Table 3.3).

Similarly, *B. fagacearum* was detected in all of the analyzed herbarium samples. Negative control samples in both categories did not amplify in real-time PCR.

Discussion

We compared the efficacy of real-time PCR and culture-based methods in detecting *B. fagacearum* in northern red oak branch sapwood that were confirmed to be infected with the pathogen using nested PCR. Regardless of sapwood condition, real-time PCR was most successful in detecting the pathogen in branch samples, with actual and estimated probabilities of detection similar to those of nested PCR. The culture-based method exhibited detection rate of 96.22% in isolations of the pathogen from fresh sapwood samples. However, its reliability decreased significantly when applied to dry samples. Similar findings have been reported previously, with no significant differences observed between culture-based method and molecular detection assays in actively wilting branch samples (Yang and Juzwik 2017). Given that *B. fagacearum* is a weak saprophyte, isolating the pathogen from dry or heat-stressed samples is challenging (Bretz and Morrison 1953). Therefore, molecular detection emerges as the preferred option for confirming the presence of the pathogen, especially before implementing management strategies, which are usually cost-prohibitive. Nonetheless, the culture-based method remains reliable when applied to actively wilting or fresh branch samples, as defined in this study. Furthermore, we observed a 100% isolation detection rate when sapwood discoloration was present, compared to an 80% detection rate in samples lacking sapwood discoloration. Based on these results, confirming sapwood discoloration is important before sending samples to diagnostic clinics that rely on culture-based isolation for pathogen confirmation.

We evaluated a non-destructive sampling method for detecting *B. fagacearum* in infected northern red oak and chestnut trees. We compared real-time PCR and culture-based method for *B. fagacearum* detection in split petioles of diseased northern red oak and chestnut. In northern

red oak, real-time PCR coupled with asymptomatic or moderately symptomatic samples, along with culture-based detection from asymptomatic samples, demonstrated the highest success rates, with estimated detection probabilities of 99%. In chestnut, real-time PCR exhibited the highest actual and estimated probabilities of *B. fagacearum* detection in all symptom categories compared to the culture-based method. In both species, detections from petioles of moderately and severely symptomatic leaves decreased using the culture-based method. This decrease in detection frequency may be attributed to the vulnerability of the weak-saprophyte pathogen to heat and desiccation, as petiole xylem vessels may not provide the same buffer and protection as the sapwood of branches or lower stems. Detection of *B. fagacearum* was lower in chestnut petioles using both methods compared to northern red oak, with the pathogen detected in 92.34% of asymptomatic and moderately affected northern red oak petioles, versus only 47.14% of the same category of petioles in chestnut. Despite the lower number of detections, both detection methods successfully identified the presence of the pathogen in chestnut leaves. Possible reasons for this disparity may include: 1) potential non-uniform pathogen distribution due to artificial inoculation in chestnut, 2) varied sampling of leaves between chestnut (randomly plucked from crowns) and northern red oak (fallen leaves), possibly indicating the pathogen's role in crown defoliation, 3) inherent differences between the two host species. Future studies should investigate the frequency of *B. fagacearum* detection in fallen leaves of naturally infected chestnuts.

Using the real-time PCR, *B. fagacearum* was detected in 100% of the analyzed whole petiole samples, irrespective of the numbers of processed petioles in a sample or the severity of the symptoms. Similarly, in whole petiole herbarium samples, *B. fagacearum* was detected in all of the analyzed samples. Notably, real-time PCR Ct values of samples comprising two whole

petioles (fresh, not herbarium samples) (27.62 ± 0.69) were approximately the same as Ct values of branch sapwood samples (27.53 ± 2.81), representing the standardized sampling method for detecting *B. fagacearum*. Similar to the sample weight of two fresh whole petioles and branch samples in our study, previous research has also suggested that 150 mg of fresh wood sample weight is optimal for the QIAamp Fast DNA Stool Mini Kit (Chahal et al., 2022a; Nicolotti et al. 2009). The lower detections observed in split petioles of both host species, compared to whole northern red oak petioles, might have resulted from insufficient sample biomass for DNA extractions. Additionally, excessive sample biomass beyond the optimum volume required for a DNA extraction kit can impede pathogen detection using real-time PCR, potentially leading to increased PCR inhibitors, poor DNA quality, reduced PCR efficiency, and inadequate sample homogenization. This could explain the unexpected increase in Ct values observed when processing three fresh whole petiole samples weighing 250.67 ± 28.94 mg.

The real-time PCR assay in this study offers several advantages over nested PCR and culture-based methods for detecting *B. fagacearum* in infected samples. The culture-based method is unreliable for dry samples lacking sapwood discoloration, requiring about two weeks for detection. Nested PCR, requiring two reactions, is time-, labor-, and cost-intensive, using nearly double the reagents of real-time PCR assays, and is prone to false positives due to increased risk of carryover contamination. Additionally, the nested PCR cross-reacts with *Cladosporium* spp. and an undescribed species of *Cucurbitariaceae*, necessitating sequencing for confirmation, which adds to the overall cost. In contrast, the real-time PCR assay evaluated in this study did not amplify any non-target fungal species, sapwood samples of mock-inoculated trees. Our real-time PCR protocol employs PerfeCTa qPCR ToughMix polymerase, known for high resistance to various PCR inhibitors including tannic acid, commonly found in oaks

(Johnson et al. 2009; Luedtke et al. 2014; Opel et al. 2010). The real-time PCR provides detection within 2-3 hours, whereas nested PCR and culture-based methods require 6-7 hours and 10-14 days, respectively. Timely detection results facilitate prompt implementation of management strategies and decision-making. The real-time PCR assay in this study is sensitive enough to detect the pathogen even in minute sample quantities, such as 4 cm long split petioles. This optimized assay could serve as a valuable tool for early detection of *B. fagacearum*, including from trapped insect vectors, previously detected using nested PCR (McLaughlin et al. 2022).

The non-destructive sampling method for detecting *B. fagacearum* in infected oak and chestnut host species offers advantages over destructive sampling methods for disease diagnosis. Fallen leaves present an excellent opportunity for *B. fagacearum* detection, as crown defoliation is a characteristic feature of *B. fagacearum* infection (Gibbs and French 1980). Similarly, defoliation of oaks during the growing season due to other biotic and abiotic stresses (Abrams 2003; Gould and Lashomb 2007; Harrington et al. 2012; Pearce and Williams-Woodward 2009; Rauschendorfer et al. 2022; Samtani et al. 2010), makes detection from fallen leaves useful for ruling out potential infections. The 100% detections in over three-year-old herbarium samples suggests potential detections can be made from fallen leaves later in the season or next spring when fallen leaves turn completely tan, resembling senescing leaves. Destructive sampling often adversely impacts tree health by attracting wood boring insects and decay fungi (Haavik et al. 2008, Tsen et al. 2016). Branch or stem wounds if left untreated can attract *B. fagacearum* insect vectors, leading to potential infection of previously healthy trees. In taller trees, where leaf collection is challenging due to crown height, a big shot sling shot, or arborist throw-line launcher can be employed to remove leaves from upper crowns or twigs (Youngentob et al.

2016). *B. fagacearum* detection in petioles can also serve as a crucial screening tool in seedling experiments, where detection from non-lignified stems without harming the plants is impractical. These experiments include assessing root-graft transmission, pathogen movement within fungicide-treated seedlings, and pathogenicity trials as reported by Chahal et al. (2024). Utilizing petioles for detection could enhance real-time protocols (Kurdyla and Appel 2011), as sapwood may contain PCR inhibitors (Yang and Juzwik 2017). PCR inhibitors, like oak tannins, are more prevalent in bark and wood than in leaf petioles (Opel et al. 2010). Petiole sampling can expedite field work compared to sapwood sampling, which is time-consuming, labor-intensive, requires skill to obtain appropriate samples, and raises safety concerns associated with the use of sharp tools. Future studies should evaluate petiole sampling coupled with oak wilt in-field detection methods, such as LAMP, RPA, and CRISPR-CAS based assays (Bourgault et al. 2022; Novi et al. 2024).

The real-time PCR assay, along with the branch sapwood and petiole non-destructive sampling method, can be easily adapted by diagnostic clinics, offering enhanced speed, sensitivity, specificity, quantification, cost-effectiveness, and labor efficiency, while reducing contamination risks compared to nested PCR and culture-based methods. Diagnosticians may find it easier to obtain chips from sapwood, as described in this study compared to drilling for sapwood shavings detailed in Yang and Juzwik (2017). Drilling may inadvertently collect shavings from non-target sapwood layers, protruding beyond the two outer sapwood rings. The depth of sapwood outer layers varies depending on branch sample diameter and other tree growth factors. Drilling through these layers requires time, skill, and special sample collection tubes. In contrast, removing 1-2 outer layers of discolored sapwood with a razor blade or knife is simpler and more precise, in our experience. Furthermore, using detections from petioles instead of

sapwood can decrease sample preparation time from 10-12 minutes to 1-2 minutes for each sample.

For non-destructive sampling coupled with culture-based or molecular detection, we recommend processing at least three whole petioles, each 4 cm long, per sample (see suppl. protocol). For molecular detection, more than 10 petioles can be processed per sample, but adjustments to the sample fresh weight and InhibitEX buffer ratio should be made to 150 mg:1000 μ l (data not shown). Maceration of such large volumes is feasible using 12 x 15 cm extraction bags (Bioreba AG, Reinach, Switzerland) instead of the standard 2 ml matrix tubes used in this study. This protocol is recommended for red oak species due to their similar response to oak wilt progression and xylem anatomical features with northern red oak (Rioux and Blais 2023). Testing is needed for white oak species and Texas live oak, as their xylem anatomy and disease progression differ from northern red oak.

This study introduces a method for detecting vascular-wilt pathogens using leaf petiole samples, could be applicable to other disease systems requiring non-destructive sampling and high-throughput screening of plant stock. Traditional destructive sampling can increase the risk of infection by insect vectors such as elm bark beetles and ambrosia beetles, which vector Dutch elm disease (*Ophiostoma novo-ulmi*) and laurel wilt (*Raffaelea lauricola*) pathogens, respectively (Copeland et al. 2023; Navia-Urrutia et al. 2022). Similar to oak wilt, where current sampling is destructive, petiole sampling may offer a clean and efficient alternative, especially for non-lignified seedlings. This technique may detect other xylem-inhabiting fungi such as *Ceratocystis* (vascular wilts of cocoa, eucalyptus, Ohia), *Verticillium* (broad host range), *Fusarium* (broad host range), and Ophiostomatoid fungi (such as *Ophiostoma* spp., *Leptographium* spp., *Graphilbum* spp. and *Sporothrix* spp.) that move through xylem vessels and

cause foliar chlorosis, necrosis, and wilting (Berlanger and Powelson 2000; Platt and Mahuku, 2000; Yadeta and Thomma 2013.). Furthermore, petiole sampling can be used to monitor and screen germplasm in field and nursery settings before shipment, adhering to quarantine restrictions for these vascular pathogens (Back et al. 2024; Roberts et al. 2024). The xylem-limited bacterial and viral pathogens are mainly vectored by xylem-feeding hemipterans into many economically important hosts, including grape, citrus, olive, almond, blueberry, and forest trees (Krugner et al. 2019; Sun et al. 2022). In-field and early detection, facilitated by petiole sampling, may aid in identifying such bacterial pathogens and prompt removal of diseased plant material (Osman et al. 2008).

Acknowledgments

The authors thank Mario Mandujano (Michigan State University) for his assistance in growing chestnut seedlings. We appreciate statistical consulting support by KC Rabin at College of Agriculture and Natural Resources, Michigan State University. This research was funded in part by the Michigan Invasive Species Grant Program and Project GREEN

Figures

Figure 3.1. Processing of diseased *Quercus rubra* branch samples for culture-based, and molecular detection of *Bretziella fagacearum*. Samples were sprayed with 70% ethanol and wiped to remove potential contaminants (A). Removal of outer bark reveals the cambium layer, distinguishing between fresh (green cambium) and dry samples (brown cambium) (B). Sapwood was exposed to assess the presence and absence of discoloration: discoloration was variable among samples such as light (C), moderate (D), severe (E), or absent (F). Samples were flame sterilized after spraying with 95% ethanol (G). Only the outer 1-2 layers of sapwood were excised for further processing (H). Excised wood pieces (I) were cut into ~1.5 X 0.5 cm chips for plating (J), and smaller ~0.3 X 0.2 cm pieces for DNA extraction (K). These samples were macerated into a coarse powder using Lysing Matrix A (MP Biomedicals) tubes with 2 ceramic beads (L). Culture-based detection involved plating wood chips onto acidified potato dextrose agar: brownish to olive-green mycelium growing from infected tissue can be observed 10 days after incubation on upper and underside of the plate, respectively (M, N).



Figure 3.2. Oak wilt severity ratings on red oak and chestnut leaves. “asymptomatic” rating indicates no observable foliar symptoms, “moderate” denotes about half of the leaf area turned bronze or necrotic, and “severe” signifies the entire leaf displaying bronze or necrotic symptoms. Necrotic leaves typically exhibit curling around the mid-rib, commonly observed on *Bretziella fagacearum* infected oaks and chestnuts. Red oak leaves are illustrated with asymptomatic (A), moderate (B), and severe (C) disease severity ratings. Chestnut leaves are depicted with asymptomatic (D), moderate (E), and severe (F) disease severity ratings.

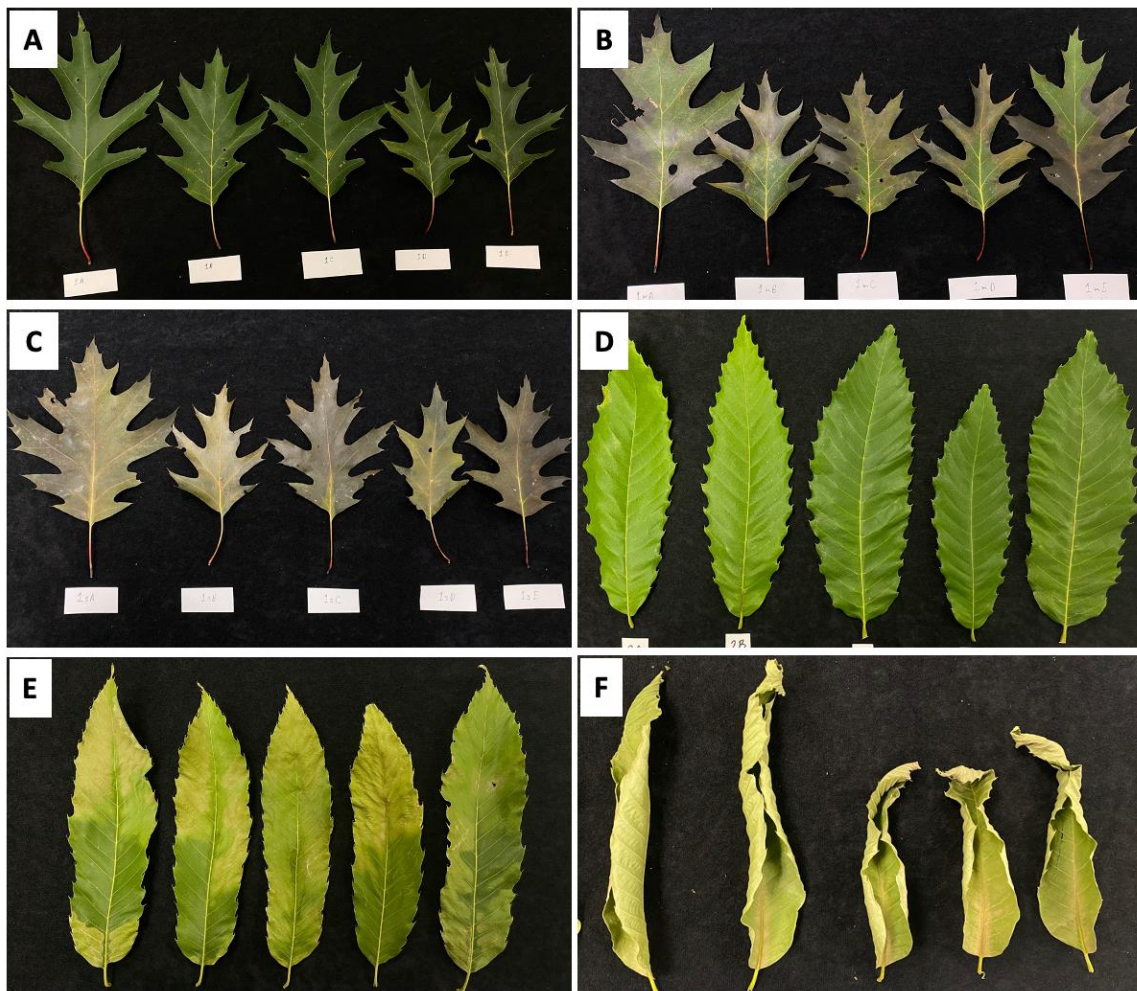


Figure 3.3. Processing petioles from diseased red oak and chestnut leaves for culture-based, and molecular detection of *Bretziella fagacearum*. Fallen leaves were collected under the crown of oak wilt symptomatic red oaks (A). Chestnut leaves were collected from artificially inoculated seedlings (B). Midrib of leaves was considered as a sample when petioles were less than 4 cm long (C). Discoloration of xylem conduits (indicated with red arrow) can be observed in petioles of infected and no discoloration (indicated with yellow arrow) was observed in non-infected chestnut petioles (D). Similar discoloration (indicated with red arrow) can be observed in split petioles from infected red oaks and petioles from non-infected trees lack discoloration (indicated with yellow arrow) (E). One half of split petioles was cut into 5 pieces and were placed onto acidified potato dextrose agar for culture-based detection (F). Mycelium growth from infected petiole pieces can be observed after 7 days of incubation (G). The other half of each petiole was cut into smaller (~0.2 cm) pieces (H) and further macerated into a fine powder using Lysing Matrix A (MP Biomedicals) tubes with 2 ceramic beads for DNA extractions (I).

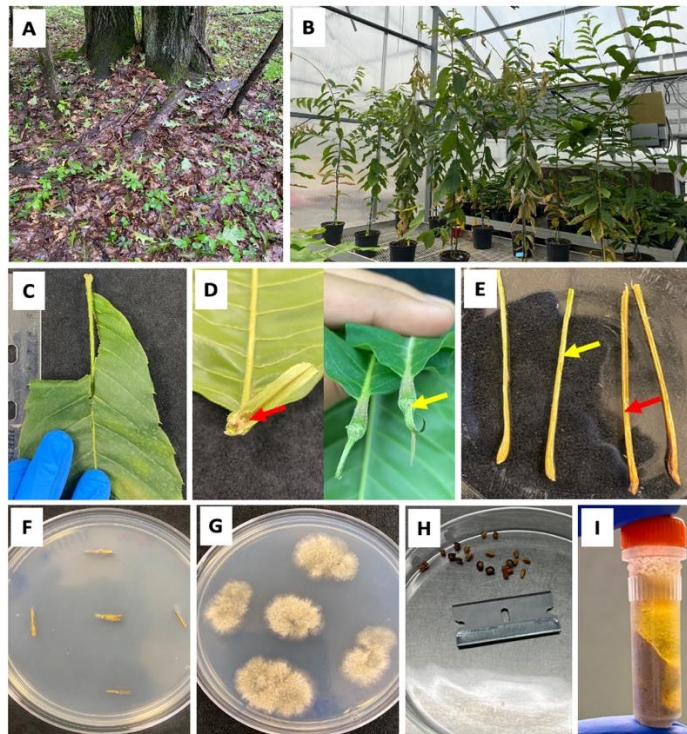
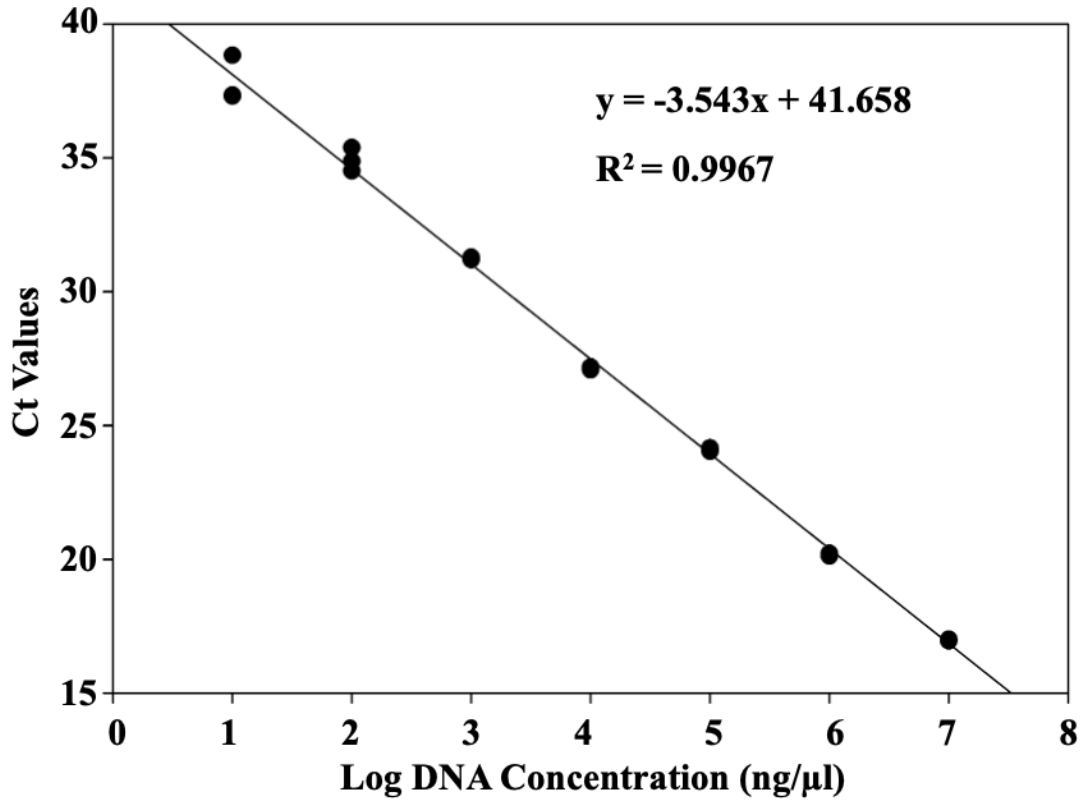


Figure 3.4. Standard curve generated using genomic DNA from pure culture of *Bretziella fagacearum*. A 10-fold serial dilution of DNA concentrations from 1 ng/μl to 1 fg/μl was used in generating the standard curve.



Tables

Table 3.1. Specificity test panel used to evaluate the real-time PCR assay developed by Bourgault et al. 2022 and modified at Michigan State University was assessed for cross-amplification with microorganisms associated with the oak wilt pathosystem, as well as with samples from biotic and abiotic stresses commonly mistaken for oak wilt or other common oak diseases.

Symptoms ^a	Abiotic or Biotic cause ^b	Host ^c	Result ^d
Bacterial leaf scorch	<i>Xylella fastidiosa</i> subsp. <i>multiplex</i>	<i>Quercus rubra</i>	-
Powdery mildew	<i>Erysiphe alphitoides</i>	<i>Quercus rubra</i>	-
Tubakia leaf spot	<i>Tubakia</i> spp.	<i>Quercus rubra</i>	-
Environmental scorch	Heat, drought	<i>Quercus rubra</i>	-
Cynipid wasp gall	<i>Cynips</i> spp.	<i>Quercus rubra</i>	-
Armillaria root rot	<i>Armillaria</i> spp.	<i>Quercus rubra</i>	-
Wood staining fungus	<i>Ophiostoma quercus</i>	Mycelial mat*	-
Oak anthracnose	<i>Apiognomonina quercinia</i>	<i>Quercus alba</i>	-
Bur oak blight	<i>Tubakia iowensis</i>	<i>Quercus macrocarpa</i>	-
Oak decline	<i>Gnomoniopsis paraclavulata</i> [†]	<i>Quercus alba</i>	-
Unspecified	<i>Cladosporium</i> spp. ^{††}	Nitidulid beetles ^{**}	-

^aDisease name or common name of the organism.

^bName of the agent which is known to cause that disease or disorder.

^cHost or agent from where the samples were collected.

^dAmplification results for the real-time PCR assay, (-) indicates no amplifications in the assay, (+) amplification in the assay.

* *Bretziella fagacearum* mycelial mat collected from *Q. rubra*.

** Nitidulid beetles (Coleoptera: Nitidulidae) collected from *B. fagacearum* mycelial mats

[†] Isolated from a white oak branch, but *G. paraclavulata* is not known as causal or contributing agent.

^{††} Various oak wilt molecular detection assays reported cross-amplifying with the species.

Table 3.2. Detection of *Bretziella fackearum* in branch samples of *Quercus rubra* submitted to Plant & Pest Diagnostics at Michigan State University using culture-based, nested PCR, and real-time PCR detection methods. Nested PCR served as the standard for comparing the accuracies and detection rates of culture-based and real-time PCR methods.

<i>Quercus rubra</i>	<u>Nested-PCR</u>		<u>Culture-based method</u>				<u>Real-time PCR</u>			
	Pos ^b	Neg ^c	Pos ^b	Neg ^c	Acc ^d	Dr ^e	Pos ^b	Neg ^c	Acc ^d	Dr ^e
Branch samples ^a										
Dry samples	18	11	4	25	51.72%	22.22%	18	11	100%	100%
Fresh samples										
Discoloration -present	43	0	43	0	100%	100%	43	0	100%	100%
Discoloration -absent	10	10	8	12	90%	80%	10	10	100%	100%
Grand total	71	21	55	37	82.60%	77.46%	71	10	100%	100%

^aData shown are numbers of ^bpositive and ^cnegative samples out of the total processed *Q. rubra* branch samples in each sapwood category.

^dAccuracy of the assay was calculated using the formula: $([\text{true positives} + \text{true negatives}]/[\text{total number of samples}])$. Accuracy for each type of branch samples was calculated using the total number of samples tested within that category.

^eDetection rate of the assay was calculated using the formula: $([\text{true positives}]/[\text{true positives} + \text{false negatives}])$.

Table 3.3. Detection of *B. fagacearum* in petioles samples collected from fallen leaves, herbarium samples of naturally infected *Quercus rubra*, and artificially infected ‘Colossal’ (*Castanea sativa* × *C. crenata* hybrid) chestnut seedlings. The real-time PCR and culture-based detection method are compared for their ability to detect *B. fagacearum* from petioles of leaves exhibiting different disease severity ratings.

Samples^a	<u>Real-time PCR</u>		<u>Culture-based method</u>		Total samples^g
	Pos^e	Neg^f	Pos^e	Neg^f	
<u>Split petiole <i>Q. rubra</i> samples</u>					
Asymptomatic ^b	48	1	48	1	49
Moderate ^c	46	3	39	10	49
Severe ^d	38	11	25	24	49
<u>Whole petiole <i>Q. rubra</i> samples</u>					
Asymptomatic ^b	12	0			12
Moderate ^c	12	0			12
Severe ^d	12	0			12
Herbarium samples	21	0			21
<u>Split petiole chestnut samples</u>					
Asymptomatic ^b	20	15	17	18	35
Moderate ^c	18	17	11	24	35
Severe ^d	19	16	3	32	35

^aPetiole from leaves showing different disease severity ratings, ^b asymptomatic: indicates no observable foliar symptoms, ^cmoderate: denotes about half of the leaf area turned bronze or necrotic, ^dsevere: signifies the entire leaf displaying bronze or necrotic symptoms.

Data shown are numbers of ^epositive and ^fnegative samples out of the total processed samples.

^gTotal number of processed petiole samples from each host, *Q. rubra*, and ‘Colossal’ (*Castanea sativa* × *C. crenata* hybrid) chestnut.

Table 3.4. The post-hoc tests examining the interactions between detection methods (culture-based, real-time PCR) used for detecting *Bretziella fagacearum* and disease severity (asymptomatic, moderate, severe) of infected *Quercus rubra* leaves.

Detection Method ^a	Severity ^b	Estimated Probability ^c	SE ^d	Actual Probability ^e	Group ^f
Culture-based	asymptomatic	0.99	0.003	0.98	a
Culture-based	Moderate	0.93	0.057	0.80	ab
Culture-based	Severe	0.55	0.218	0.51	c
Real-time PCR	asymptomatic	0.99	0.003	0.98	a
Real-time PCR	Moderate	0.99	0.010	0.94	ab
Real-time PCR	Severe	0.92	0.068	0.78	b

^aMethod used to detect *B. fagacearum* from petioles of infected *Q. rubra* leaves.

^bSeverity ratings, asymptomatic: indicates no observable foliar symptoms, moderate: denotes about half of the leaf area turned bronze or necrotic, severe: signifies the entire leaf displaying bronze or necrotic symptoms.

^cEstimated probability based on logit transformation from model estimates.

^dStandard error of the mean.

^eActual probability based on calculated proportions from samples used in this study.

^fGroups labeled with different letters indicate significant differences ($P < 0.05$), while groups sharing the same letter are not significantly different ($P > 0.05$).

Table 3.5. The post-hoc tests examining the interactions between detection methods (culture-based, real-time PCR) used for detecting *Bretziella fagacearum* and disease severity (asymptomatic, moderate, severe) of infected ‘Colossal’ (*Castanea sativa* × *C. crenata* hybrid) chestnut leaves.

Detection Method ^a	Sapwood ^b	Estimated Probability ^c	SE ^d	Actual Probability ^e	Group ^f
Culture-based	asymptomatic	0.56	0.258	0.49	ab
Culture-based	Moderate	0.19	0.170	0.31	bc
Culture-based	Severe	0.01	0.008	0.09	c
Real-time PCR	asymptomatic	0.72	0.209	0.57	a
Real-time PCR	Moderate	0.61	0.247	0.51	ab
Real-time PCR	Severe	0.67	0.230	0.54	ab

^aMethod used to detect *B. fagacearum* from petioles of infected ‘Colossal’ (*Castanea sativa* × *C. crenata* hybrid) chestnut leaves.

^bSeverity ratings, asymptomatic: indicates no observable foliar symptoms, moderate: denotes about half of the leaf area turned bronze or necrotic, severe: signifies the entire leaf displaying bronze or necrotic symptoms.

^cEstimated probability based on logit transformation from model estimates.

^dStandard error of the mean.

^eActual probability based on calculated proportions from samples used in this study.

^fGroups labeled with different letters indicate significant differences ($P < 0.05$), while groups sharing the same letter are not significantly different ($P > 0.05$).

LITERATURE CITED

- Abrams, M. D. 2003. Where has all the white oak gone? *BioScience*. 53:927-939.
- Appel, D. N. 1995. The oak wilt enigma: perspectives from the Texas epidemic. *Annu. Rev. Phytopathol.* 33:103-118.
- Back, M. A., Bonifácio, L., Inácio, M. L., Mota, M., and Boa, E. 2024. Pine wilt disease: A global threat to forestry. *Plant Pathol.* 73:1026-1041.
- Baratloo, A., Hosseini, M., Negida, A., and El Ashal, G. 2015. Part 1: Simple definition and calculation of accuracy, sensitivity, and specificity. *Emerg (Tehran)* 3:48-49.
- Berlanger, I., and Powelson, M. L. 2000. Verticillium wilt. *Plant Health Instr.* <https://doi.org/10.1094/PHI-I-2000-0801-01>
- Bourgault, E., Gauthier, M. K., Potvin, A., Stewart, D., Chahal, K., Sakalidis, M. L., and Tanguay, P. 2022. Benchmarking a fast and simple on-site detection assay for the oak wilt pathogen *Bretziella fagacearum*. *For. Glob. Change.* 5:1068135. <https://doi.org/10.3389/ffgc.2022.1068135>
- Bretz, T. W., and Morrison, D. W. 1953. Effect of time and temperature on isolation of the oak wilt fungus from infected twig samples. *Plant Dis. Rep.* 37:162-163.
- Cardwell, K. F., Harmon, C. L., Luster, D. G., Stack, J. P., Hyten, A. M., Sharma, P., and Nakhla, M. K. 2023. The need and a vision for a diagnostic assay validation network. *PhytoFrontiers.* 3:9-17.
- Chahal, K., Gazis, R., Klingeman, W., Hadziabdic, D., Lambdin, P., Grant, J., and Windham, M. 2019a. Assessment of alternative candidate subcortical insect vectors from walnut crowns in habitats quarantined for thousand cankers disease. *Environ. Entomol.* 48:882-893.
- Chahal, K., Gazis, R., Klingeman, W., Lambdin, P., Grant, J., Windham, M., and Hadziabdic, D. 2022a. Differential virulence among *Geosmithia morbida* isolates collected across the United States occurrence range of thousand cankers disease. *For. Glob. Change.* 5:726388. <https://doi.org/10.3389/ffgc.2022.726388>
- Chahal, K., Morris, O., McCullough, D. G., and Sakalidis, M. L. 2019b. Biology, epidemiology and detection of oak wilt in Michigan. (Abstr). *Phytopathology.* 109.S2.33. <https://doi.org/10.1094/PHYTO-109-10-S2.1>
- Chahal, K., Morris, O., McCullough, D. G., Cregg, B., and Sakalidis, M. L. 2021. Sporulation timing of the invasive oak wilt fungus, *Bretziella fagacearum* in Michigan. (Abstr.). *Phytopathology.* 111.S2.51. <https://doi.org/10.1094/PHYTO-111-10-S2.1>

Chahal, K., Morris, O. R., McCullough, D. G., Cregg, B., and Sakalidis, M. L. 2022b. Seasonal variation of northern red oak, *Quercus rubra* infection by *Bretziella fagacearum* (oak wilt) in Michigan. (Abstr.). *Phytopathology*. 112.S3.37. <https://doi.org/10.1094/PHYTO-112-11-S3.1>

Chahal, K. S., Wachendorf, E. J., Miles, L. A., Stallmann, A., Lizotte, E. L., Mandujano, M., Byrne, J., Miles, T. D., and Sakalidis, M. L. 2024. First report of *Bretziella fagacearum* infecting chestnut in Michigan. *Plant Dis*. <https://doi.org/10.1094/PDIS-10-23-2267-PDN>

Copeland, C. A., Harper, R. W., Brazee, N. J., and Bowlick, F. J. 2023. A review of Dutch elm disease and new prospects for *Ulmus americana* in the urban environment. *Arboric. J.* 45:3-29.

De Beer, Z. W., Marincowitz, S., Duong, T. A., and Wingfield, M. J. 2017. *Bretziella*, a new genus to accommodate the oak wilt fungus, *Ceratocystis fagacearum* (Microascales, Ascomycota). *MycoKeys*. 27:1–19.

Gauthier, M. K., Bourgault, É., Potvin, A., Bilodeau, G. J., Gustavsson, S., Reed, S., Therrien, P., Barrette, É., and Tanguay, P. 2023. Biosurveillance of oak wilt disease in Canadian areas at risk. *Can. J. Plant Pathol.* 46:27-38. <https://doi.org/10.1080/07060661.2023.2261890>

Gibbs, J. N., and French, D. W. 1980. The transmission of oak wilt. USDA Forest Service Research Paper NC-185. Central Forest Experiment Station, St. Paul, MN.

Gould, A. B., and Lashomb, J.H. 2007. Bacterial leaf scorch (BLS) of shade trees. *Plant Health Instr.* <https://doi.org/10.1094/PHI-I-2007-0403-07>

Haack, R. A., and Acciavatti, R. E. 1992. Twolined chestnut borer. USDA forest service forest insect and disease leaflet 168. USDA Forest Service, North Central Forest Experiment Station, East Lansing, MI.

Haavik, L. J., Stephen, F. M., Fierke, M. K., Salisbury, V. B., Leavitt, S. W., and Billings, S. A. 2008. Dendrochronological parameters of northern red oak (*Quercus rubra* L. (Fagaceae)) infested with red oak borer (*Enaphalodes rufulus* (Haldeman) (Coleoptera: *Cerambycidae*)). *For. Ecol. Manag.* 255:1501-1509.

Harrington, T. C., McNew, D., and Yun, H. Y. 2012. Bur oak blight, a new disease on *Quercus macrocarpa* caused by *Tubakia iowensis* sp. nov. *Mycologia*. 104:79-92.

Johnson, P. S., Shifley, S. R., and Rogers, R., eds. 2009. The ecology and silviculture of Oaks, 2nd ed. CAB International, Wallingford, Oxfordshire, UK.

Juzwik, J., Appel, D. N., MacDonald, W. L., and Burks, S. 2011. Challenges and successes in managing oak wilt in the United States. *Plant Dis*. 95:888-900.

Koch, K. A., Quiram, G. L., and Venette, R. C. 2010. A review of oak wilt management: a summary of treatment options and their efficacy. *Urban For. Urban Green*. 9:1-8.

- Krugner, R., Sisterson, M. S., Backus, E. A., Burbank, L. P., and Redak, R. A. 2019. Sharpshooters: a review of what moves *Xylella fastidiosa*. *Austral Entomology*. 58:248-267.
- Kurdyla, T., and Appel, D. 2011. The detection of *Ceratocystis fagacearum* in Texas live oak using real-time polymerase chain reaction. (Abstr.). *Phytopathology*. 101.S95.
- Lamarche, J., Potvin, A., Pelletier, G., Stewart, D., Feau, N., Alayon, D. I. O., Dale, A. L., Coelho, A., Uzunovic, A., Bilodeau, G. J., Briere, S. C., Hamelin, R. C., and Tanguay, P. 2015. Molecular detection of 10 of the most unwanted alien forest pathogens in Canada using real-time PCR. *PLoS One* 10.e0134265. <https://doi.org/10.1371/journal.pone.0134265>
- Lee, C. A., Dey, D. C., and Muzika, R. M. 2016. Oak stump-sprout vigor and *Armillaria* infection after clearcutting in southeastern Missouri, USA. *For. Ecol. Manag.* 374:211-219.
- Luedtke, B. E., Bono, J. L., and Bosilevac, J. M. 2014. Evaluation of real time PCR assays for the detection and enumeration of enterohemorrhagic *Escherichia coli* directly from cattle feces. *J. Microbiol. Methods*. 105:72-79.
- McLaughlin, K., Snover-Clift, K., Somers, L., Cancelliere, J., and Cole, R. 2022. Early detection of the oak wilt fungus (*Bretziella fagacearum*) using trapped nitidulid beetle vectors. *For. Pathol.* 52.e12767. <https://doi.org/10.1111/efp.12767>
- Morris, O. R. 2020. Seasonal Activity and Phorsey Rates of Sap Beetles (Coleoptera: Nitidulidae) in Oak Wilt Infection Centers, Volatile Organic Compounds Related to the Oak Wilt Cycle, and Long-Term Evaluation of Red Oak Provenances. Master's thesis, Michigan State University.
- Navia-Urrutia, M., Sánchez-Pinzón, L., Parra, P. P., and Gazis, R. 2022. A diagnostic guide for laurel wilt disease in avocado. *Plant Health Prog.* 23:345-354.
- Nicolotti, G., Gonthier, P., Guglielmo, F., and Garbelotto, M. M. 2009. A biomolecular method for the detection of wood decay fungi: a focus on tree stability assessment. *Arboric. Urban For.* 35:14-19.
- Novi, V. T., Aboubakr, H. A., Moore, M. J., Juzwik, J., and Abbas, A. A rapid LAMP assay for the diagnosis of oak wilt the naked eye. Preprint at <https://doi.org/10.21203/rs.3.rs-3960787/v1> (2024).
- Opel, K., Chung, D., and McCord, B. 2010. A study of PCR inhibition mechanisms using real-time PCR. *J. Forensic Sci.* 55:25-33.
- Osman, F., Leutenegger, C., Golino, D., and Rowhani, A. 2008. Comparison of low-density arrays, RT-PCR and real-time TaqMan® RT-PCR in detection of grapevine viruses. *J. Virol. Methods*. 149:292-299.

Pearce M., and Williams-Woodward, J. 2009. Key to diseases of oaks in the landscape. The University of Georgia Co-operative Extension Bulletin 1287, 16 pp. Available online at: https://secure.caes.uga.edu/extension/publications/files/pdf/B%201286_3.PDF (last accessed 25 March 2024).

Platt, H. W., and Mahuku, G. 2000. Detection methods for *Verticillium* species in naturally infested and inoculated soils. *Am. J. Potato Res.* 77:271-274.

Pokorny, J. 1999. How to collect field samples and identify the oak wilt fungus in the laboratory. NA-FR-01-99. USDA Forest Service, Northeastern Area State and Private Forestry, St. Paul, MN.

Rauschendorfer, J., Rooney, R., and Külheim, C. 2022. Strategies to mitigate shifts in red oak (*Quercus* sect. *Lobatae*) distribution under a changing climate. *Tree Physiol.* 42:2383-2400.

Rioux, D., and Blais, M. 2023. Review and new insights into wood anatomy that help understand and control oak wilt. *Phytoprotection.* 103:1-25.

Roberts, J. M., Carvahais, L. C., O'Dwyer, C., Rincón-Flórez, V. A., and Drenth, A. 2024. Diagnostics of *Fusarium* wilt in banana: Current status and challenges. *Plant Pathol.* 73:760-776.

Samtani, J. B., Masiunas, J. B., and Appleby, J. E. 2010. White oak and northern red oak leaf injury from exposure to chloroacetanilide herbicides. *HortSci.* 45:696-700.

Singh, R., Feltmeyer, A., Saiapina, O., Juzwik, J., Arenz, B., and Abbas, A. 2017. Rapid and PCR-free DNA detection by nanoaggregation-enhanced chemiluminescence. *Sci. Rep.* 7:14011. <https://doi.org/10.1038/s41598-017-14580-w>

Stone, G. N., Schönrogge, K., Atkinson, R. J., Bellido, D., and Pujade-Villar, J. 2002. The population biology of oak gall wasps (Hymenoptera: Cynipidae). *Ann. Rev. Entomol.* 47: 633-668.

Sun, Y. D., Spellman-Kruse, A., and Folimonova, S. Y. 2022. Blaze a new trail: plant virus xylem exploitation. *Int. J. Mol.* 23:8375. <https://doi.org/10.3390/ijms23158375>

Tsen, E. W., Sitzia, T., and Webber, B. L. 2016. To core, or not to core: The impact of coring on tree health and a best-practice framework for collecting dendrochronological information from living trees. *Biol. Rev.* 91:899-924.

Wu, C. P., Chen, G. Y., Li, B., Su, H., An, Y. L., Zhen, S. Z., and Ye, J. R. 2011. Rapid and accurate detection of *Ceratocystis fagacearum* from stained wood and soil by nested and real-time PCR. *For. Pathol.* 41:15-21.

Yang, A., and Juzwik, J. 2017. Use of nested and real-time PCR for the detection of *Ceratocystis fagacearum* in the sapwood of diseased oak species in Minnesota. *Plant Dis.* 101:480-486.

Youngentob, K. N., Zdenek, C., and van Gorsel, E. 2016. A simple and effective method to collect leaves and seeds from tall trees. *Methods Ecol. Evol.* 7:1119-1123.

Yadeta, K. A., and Thomma, B. P. 2013. The xylem as battleground for plant hosts and vascular wilt pathogens. *Front. Plant Sci.* 4:97. <https://doi.org/10.3389/fpls.2013.00097>

CHAPTER 4: COMPLETE GENOME RESOURCE OF *BRETZIELLA FAGACEARUM*, THE CAUSAL FUNGUS OF OAK WILT

Abstract

Bretziella fagacearum is a destructive vascular wilt fungal pathogen affecting oaks in the United States and Canada. The epidemiology of oak wilt varies across different geographical locations, indicating the need to investigate the population dynamics of *B. fagacearum* to discern potential differences in its genotypes using genomic tools. A complete genome of *B. fagacearum* is crucial as a reference for population studies. Here, we report the complete genome of *B. fagacearum* isolate C519. The genome assembly consists of nine chromosomes totaling 27,072,536 bp, with a GC content of 47.29% and is predicted to encode 7,554 proteins, which were annotated using RNA sequencing data obtained from the same isolate. The circular mitochondrial genome consists of a chromosome of 174,403 bp with a GC content of 28.59% and contains 54 open reading frames, including 14 core genes, 28 tRNAs, 4rRNAs, and 8 hypothetical proteins. The reference genome can enhance understanding of molecular epidemiology and biology of *B. fagacearum*, aiding in identifying genetic variations, pathogen-host interactions, developing diagnostic tools and disease management strategies.

Genome announcement

Oak wilt, caused by the fungal pathogen *Bretziella fagacearum* (Bretz) Z.W. de Beer, Marinc., T.A. Duong & M.J. Wingf., (formerly *Ceratocystis fagacearum* (Bretz)), is a significant disease affecting oaks (*Quercus* spp.) in the United States (U.S.) (De Beer et al. 2017; Henry 1944). *B. fagacearum* spreads through below-ground networks of grafted roots among neighboring trees, thereby forming centers or pockets of diseased host species (Blaedow and Juzwik 2010; Chahal et al. 2024). *B. fagacearum* is also transmitted above-ground by sap or

nitidulid beetles (Coleoptera: Nitidulidae) and oak bark beetles (*Pityophthorus* spp.) (Gibbs and French 1980; Rexrode and Jones 1970). *B. fagacearum* infections can disrupt both urban and natural forest ecosystems if not timely detected and managed. Currently, oak wilt has been confirmed in 24 states in the U.S., and widespread epidemics are reported in the Great Lakes region and Texas (Appel 1986; Chahal et al. 2019, 2021; Juzwik et al. 2011; Rexrode and Lincoln 1965). Oak wilt continues to spread, expanding into new geographical locations where it has not been previously reported (Gauthier et al. 2023; McLaughlin et al. 2022). Detection of oak wilt in Ontario, Canada, in June 2023 marked the first identification of *B. fagacearum* outside the U.S. (Canadian Food Inspection Agency 2023).

The epidemiology of oak wilt varies between the Great Lakes region and Texas disease epidemics. In the Great Lakes region, red oaks (section *Lobatae*) are prevalent and highly susceptible compared to white oaks (section *Quercus*) that exhibit moderate to high levels of resistance (Appel 1995; Juzwik et al. 2011). In the Great Lakes region, *B. fagacearum* infections have also been reported on orchard-grown chestnuts (Bretz and Long 1950; Chahal et al. 2024). In Texas, the widespread and key host, Texas live oak (*Quercus fusiformis*, section *Virentes*) shows intermediate susceptibility compared to red and white oaks (Appel 1986, 1995). However, clonal propagation of Texas live oak through sprouts originating from a shared root system facilitates spread of *B. fagacearum*, leading to expanding pockets of mortality (Appel 1995). The outcomes of oak wilt occurrences observed in Texas live oak populations have not been observed in any other host or state within its distribution range.

The sporulation structures of *B. fagacearum*, known mycelial mats, predominantly occur on red oaks, rarely on white oaks and have never reported on Texas live oak (Appel 1995; Juzwik et al. 2011). In the Great Lakes region, oak wilt incidence is high due to the homogenous

stands of highly susceptible red oaks, prevalent fungal sporulation, sandy soils that favor root grafting, and presence of active insect vectors (Juzwik et al. 2011). In the Great Lakes region, insect-vector activity, and mycelial mat formation peak during the growing season, particularly from April to June (Chahal et al. 2021; Curl 1955; Juzwik et al. 2011; Morris 2020). No mycelial mat formation has been reported in Michigan from mid-November through mid-April (Chahal et al. 2021). Whereas in Texas, insect vectors remain active year-round, coinciding with the continuous formation of fungal mycelial mats (Appel 1995). In Texas, *B. fagacearum* infection centers typically span several hectares and expands at rates up to 50 meters per year, resulting in annual tree mortality (Appel 2009). This contrasts with the slower growth and smaller sizes of foci in deciduous red oaks in the Great Lakes region, expanding at rates of 12 meters per year in Michigan and 1.9 to 7.6 meters per year in Minnesota (Bruhn et al. 1991; Gearman and Blinnikov 2019). Anthropogenic activities, such as poorly timed pruning of oaks, contribute to vector-mediated infections across the widespread oak wilt distribution range in Texas and Great Lakes region (Gearman and Blinnikov 2019). Factors contributing to differences in oak wilt epidemiology include the land cover and distribution of different host species, climatic, soil type, human population density (Gearman and Blinnikov 2019), and potentially the genotypes of *B. fagacearum*.

Population genetics studies of *B. fagacearum* are crucial to understand the population structure, and diversity within pathogen populations, with implications for disease epidemiology. Given the impact of oak wilt in the Great Lakes region and Texas, identifying introduction events of *B. fagacearum* and potential pathways of spread within the U. S. is imperative. The aim of this study was to generate a high-quality genome sequence of *B. fagacearum* and annotate it using the RNA sequencing data from the same isolate.

B. fagacearum isolate C519 was isolated from infected *Q. rubra* in Sherburne County, MN in 1992. The isolate was confirmed as *B. fagacearum* using real-time PCR (Bourgault et al. 2022) and amplifying, sequencing the 60S, LSU, and MCM7 gene regions previously employed in phylogenetic classification of the fungus, as detailed in de Beer et al. (2017). The consensus sequences of the gene regions were submitted to GenBank. Mycelium was grown on potato dextrose broth and harvested following established protocol (Chahal et al. 2022). Genomic DNA was extracted from harvested mycelium using a phenol-chloroform protocol described in Parada-Rojas and Quesada-Ocampo (2018). Five µg of genomic DNA was sheared to >10 kb using Covaris g-Tubes. The sheared DNA was treated with exonuclease to remove single-stranded ends and a DNA damage repair mix, followed by end repair and ligation of blunt adapters using the SMRTbell Template Prep Kit 1.0 (Pacific Biosciences). The library was purified with AMPure PB beads. PacBio sequencing primer was annealed to the SMRTbell template library, and sequencing polymerase was bound using the Sequel II Binding Kit 1.0. The prepared SMRTbell template libraries were sequenced on a Pacific Biosciences Sequel II sequencer using 8M v1 SMRT cells and Version 1.0 sequencing chemistry with 1x900 minute sequencing movie run times. Sequence data were processed with the JGI QC pipeline to remove artifacts. The genome was assembled with Falcon (Chin et al. 2016), improved with finisherSC version 2.1 (Lam et al. 2015), and polished with Arrow version SMRTLlink v7.0.1.66975. Contigs shorter than 1000 bp were excluded, and those identified as contaminants were removed. Contaminants were detected by performing BLAST searches of the contigs separately against bacterial/viral and fungal UniProt accessions. Contigs with a higher number of bacterial/viral hits in length compared to fungal hits were discarded. To better assemble *B. fagacearum*, which had substantially higher coverage than the contaminant, preads were subsampled using BBtools

v38.79 (reformat.sh samplerate=0.3). The subsampled reads were assembled with Flye v2.6 (flye --pacbio-corr -g 40m --asm-coverage 50) and polished with GCpp (--algorithm arrow, SMRTLINK v8.0.0.80529). The genome features are presented in circo plots (Krzywinski et al. 2009) that were created using SAMtools (Danecek et al. 2021), bedtools (Quinlan and Hall 2010) for data extraction and bedtops (Neph et al. 2021) was used for converting between formats (Fig. 4.1). Mitochondrial genome was assembled separately from the Falcon pre-assembled reads (preads) using an in-house tool (assemblemito.py). The preads were filtered and polished with Arrow (SMRTLlink v7.0.1.66975) (Fig. 4.2).

For transcriptome analysis, total RNA from harvested mycelium of *B. fagacearum* C519 was extracted using EZNA Fungal RNA Mini Kit (Omega Bio-tek Inc., Norcross, Georgia). Plate-based RNA sample preparation was performed on the PerkinElmer Sciclone NGS robotic liquid handling system using Illumina's TruSeq Stranded mRNA HT sample prep kit, following the protocol outlined by Illumina for poly-A selection of mRNA. Total RNA starting material was 1 µg per sample, and 8 cycles of PCR were used for library amplification. The prepared library was quantified using KAPA Biosystem's next-generation sequencing library qPCR kit (Roche) and run on a Roche LightCycler 480 real-time PCR instrument. The quantified library was multiplexed with other libraries, and the pooled libraries were prepared for sequencing on the Illumina NovaSeq 6000 platform using NovaSeq XP v1.5 reagent kits and an S4 flow cell, following a 2x150 bp indexed run recipe. After sequencing, read artifacts (kmer = 25 bp, 1 mismatch) were detected with BBDuk (<https://sourceforge.net/projects/bbmap/>). Detected artifacts were trimmed from the 3' end of reads. General quality trimming was performed with the Phred trimming method set at Q6. Reads shorter than 25 bp or one-third of the original read length were removed, as well as RNA spike-in reads, PhiX reads, and reads containing any

ambiguous characters (Ns). Filtered transcriptome sequencing (RNA-Seq) reads were assembled using Trinity v. 2.8.5 (Grabherr et al. 2011). RNA-Seq capture was performed by aligning a 1% subsample of RNA reads to the final DNA assembly using BBTools v. 38.67. Gene clusters of interest were searched in the clustering table available at the JGI MycoCosm portal (Grigoriev et al. 2014). Clusters were computed following the TRIBE-Markov cluster (MCL) clustering method (Enright et al. 2002), from all-versus-all BLAST analysis of the proteins in the set of organisms included in a clustering run (Table 4.1).

The BUSCO (Manni et al. 2021) analysis of the whole genome with Ascomycota fungal group reveals a completeness of 96.7%, with 1650 complete BUSCOs found out of 1706 total BUSCO group searched. Of this, 1649 was found to be complete and single copy, one was complete and duplicated BUSCO, while 52 were missing and 4 fragmented BUSCO were reported.

While a draft genome of *Bretziella fagacearum* is available from Wingfield et al. (2016), our study presents a complete and high-quality genome (Table 4.2). Our genome assembly demonstrates significant improvements with a larger assembly size (27.07 Mbp vs. 26.8 Mbp) and greater sequencing read coverage depth (1464.36X vs. 123.2X). Additionally, our assembly achieved a chromosome-level resolution with only 9 contigs and scaffolds, compared to the scaffold-level resolution with 2949 contigs and 1257 scaffolds in the previous study, eliminating gaps and improving scaffold L50 and N50 values.

This publicly available genome resource can serve as a reference for future studies, including population and comparative genomics, to explore molecular mechanisms underlying epidemiology and biology of *B. fagacearum*. Insights gained from this genome will enhance

understanding of genetic diversity, evolutionary history, and pathogenicity, aiding in the development of effective disease management strategies.

Data availability

The genome and transcriptome sequence of C519 was deposited in NCBI GenBank under the BioProject accession numbers PRJNA677221, PRJNA677222 and BioSample accession numbers SAMN16773066, SAMN16774004. The data can be accessed at <https://mycocosm.jgi.doe.gov/Brefa1/Brefa1.home.html>.

Acknowledgments

The work (proposal: 10.46936/10.25585/60001019) conducted by the U.S. Department of Energy Joint Genome Institute (<https://ror.org/04xm1d337>), a DOE Office of Science User Facility, is supported by the Office of Science of the U.S. Department of Energy operated under Contract No. DE-AC02-05CH11231. This research was funded in part by the Michigan Invasive Species Grant Program and Project GREEN.

Figures

Figure 4.1. Nuclear genome of *B. fagacearum*, the circo plots display from outer tracks to inner: (a) Chromosome length (X10kb), labeled 1 through 9. (b) GC-content distribution, with high GC (blue) and low GC (yellow) regions. (c) Gene density, represented as the number of genes per 10kb of genomic region (0 - 0.006). (d) Gene positions across the entire genome.

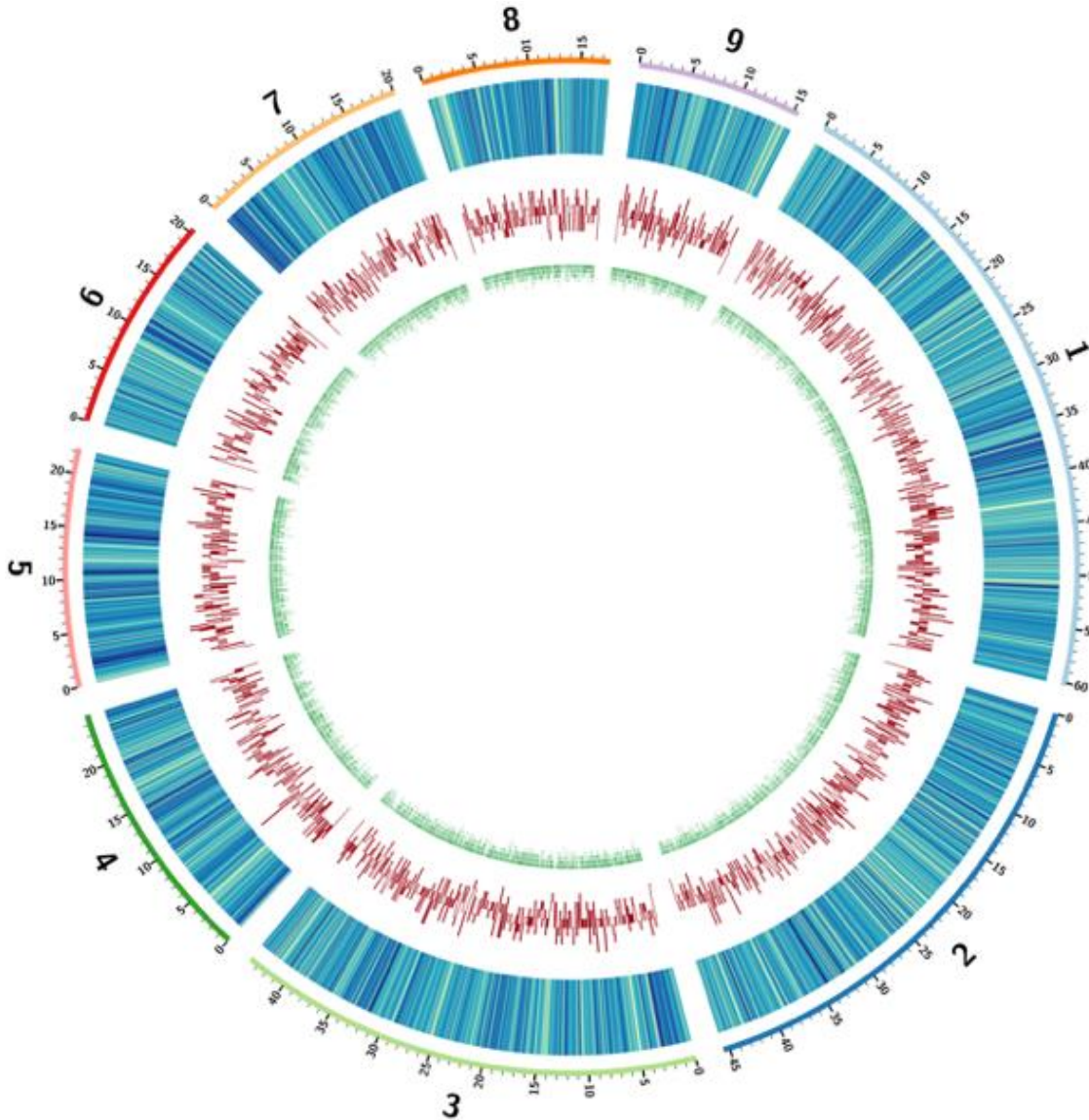
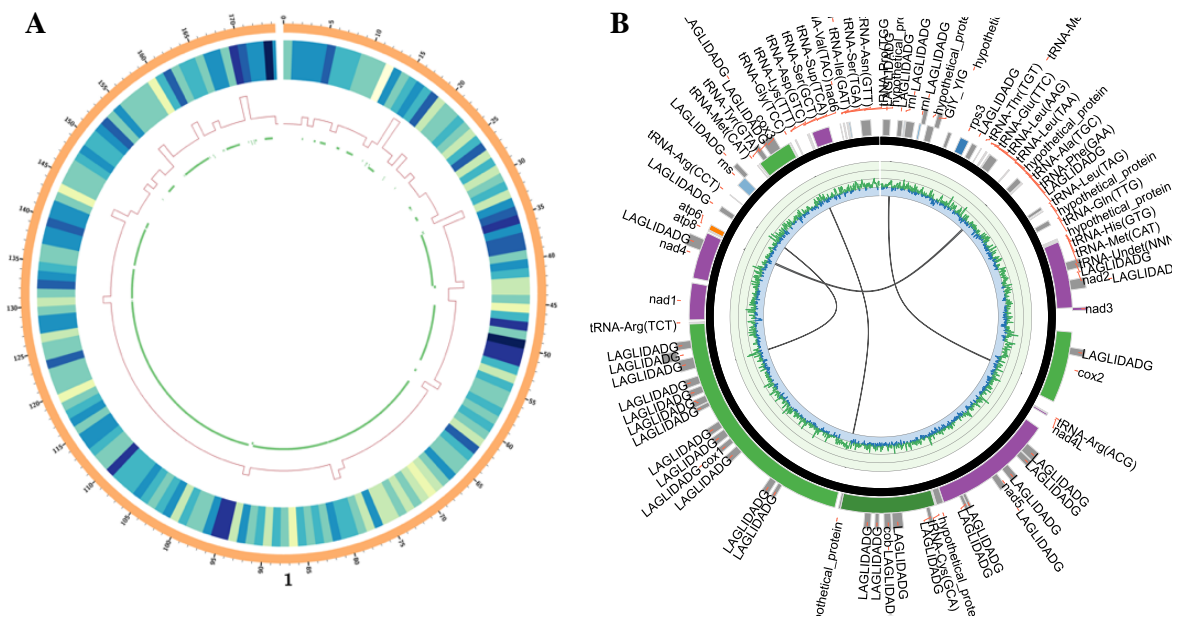


Figure 4.2. Mitochondrial genome of *B. fagacearum*. **A.** Circo plot represent from outer to inner track: (a) Chromosome length (KB), labeled as 1. (b) GC-content distribution, with high GC (blue) and low GC (yellow) regions. (c) Gene density, represented as the number of genes per 1kb of genomic region (0 - 0.005). (d) Gene positions across the genome. **B.** Genome images are produced using Circos from annotated genomes. The black line represents scaffold(s), with gene models displayed clockwise along the outside. The inner graph shows average GC% across the length of the assembly, ranging from 0-100% inside to outside: values below 25% are in blue, while values above 25% are in green. Interior links between scaffold sections denote regions of 100% identity. "LG" denotes LAGLIDADG.



Tables

Table 4.1. Functional annotation analysis of KEGG pathways.

Metabolic pathways	Gene models identified
Amino acid metabolism	282
Biosynthesis of polyketides and non-ribosomal peptides	20
Biosynthesis of secondary metabolites	146
Carbohydrate metabolism	288
Energy metabolism	75
Glycan biosynthesis and metabolism	91
Lipid metabolism	203
Metabolism of cofactors and vitamins	187
Metabolism of other amino acids	91
Nucleotide metabolism	113
Xenobiotics biodegradation and metabolism	139

Table 4.2. Parameters of available genomes of *Bretziella fagacearum*.

Assembly parameters	Wingfield et al. 2016	This study
Genome assembly size (Mbp)	26.8	27.07
Sequencing read coverage depth	123.2X	1464.36X
Number of contigs	2949	9
Number of Scaffolds	1257	9
Scaffold L50 (Mbp)	0.0422	4.39
Scaffold N50	190	3
Number of gaps (Mbp)	0.2	0
Assembly level	Scaffold	Chromosome
Sequencing technology	Illumina	PacBio

LITERATURE CITED

- Appel, D. N. 1986. Recognition of oak wilt in live oak. *J. Arboric.* 12:213-218.
- Appel, D. N. 1995. The oak wilt enigma: perspectives from the Texas epidemic. *Annu. Rev. Phytopathol.* 33:103-118.
- Appel, D. N. 2009. Oak wilt biology, impact, and host pathogen relationships: A Texas perspective. Paper presented at the 2nd National Oak Wilt Symposium, Austin, TX.
- Blaedow, R. A., and Juzwik, J. 2010. Spatial and temporal distribution of *Ceratocystis fagacearum* in roots and root grafts of oak wilt affected red oaks. *J. Arboric.* 36:28-34.
- Bourgault, E., Gauthier, M. K., Potvin, A., Stewart, D., Chahal, K., Sakalidis, M. L., and Tanguay, P. 2022. Benchmarking a fast and simple on-site detection assay for the oak wilt pathogen *Bretziella fagacearum*. *For. Glob. Change.* 5:1068135.
<https://doi.org/10.3389/ffgc.2022.1068135>
- Bretz, T., and Long, W. 1950. Oak wilt fungus isolated from Chinese chestnut. *Plant Dis. Rep.* 34:291.
- Bruhn, J. N., Pickens, J. B., and Stanfield, D. B. 1991. Probit analysis of oak wilt transmission through root grafts in red oak stands. *For. Sci.* 37:28-44.
- Canadian Food Inspection Agency. 2023. Oak wilt. <https://inspection.canada.ca/plant-health/invasive-species/plant-diseases/oak-wilt/eng/1325624048625/1325624535106>. Last accessed May 2024.
- Chahal, K., Gazis, R., Klingeman, W., Lambdin, P., Grant, J., Windham, M., and Hadziabdic, D. 2022. Differential virulence among *Geosmithia morbida* isolates collected across the United States occurrence range of thousand cankers disease. *For. Glob. Change.* 5:726388.
<https://doi.org/10.3389/ffgc.2022.726388>
- Chahal, K., Morris, O., McCullough, D. G., and Sakalidis, M. L. 2019. Biology, epidemiology and detection of oak wilt in Michigan. (Abstr). *Phytopathology.* 109:33.
<https://doi.org/10.1094/PHYTO-109-10-S2.1>
- Chahal, K., Morris, O., McCullough, D. G., Cregg, B., and Sakalidis, M. L. 2021. Sporulation timing of the invasive oak wilt fungus, *Bretziella fagacearum* in Michigan. (Abstr.). *Phytopathology.* 111:51. <https://doi.org/10.1094/PHYTO-111-10-S2.1>
- Chahal, K. S., Wachendorf, E. J., Miles, L. A., Stallmann, A., Lizotte, E. L., Mandujano, M., Byrne, J., Miles, T. D., and Sakalidis, M. L. 2024. First report of *Bretziella fagacearum* infecting chestnut in Michigan. *Plant Dis.* <https://doi.org/10.1094/PDIS-10-23-2267-PDN>

- Chin, C. S., Peluso, P., Sedlazeck, F. J., Nattestad, M., Concepcion, G. T., Clum, A., Dunn, C., O'Malley, R., Figueroa-Balderas, R., Morales-Cruz, A., and Cramer, G. R. 2016. Phased diploid genome assembly with single-molecule real-time sequencing. *Nat. Methods* 13:1050-1054.
- Curl, E. A. 1955. Natural availability of oak wilt inocula. *Ill. Nat. Hist. Surv. Bull.* 26:277-323.
- Danecek, P., Bonfield, J. K., Liddle, J., Marshall, J., Ohan, V., Pollard, M. O., Whitwham, A., Keane, T., McCarthy, S. A., Davies, R. M., and Li, H. 2021. Twelve years of SAMtools and BCFtools. *Gigascience* 10. <https://doi.org/10.1093/gigascience/giab008>
- De Beer, Z. W., Marincowitz, S., Duong, T. A., and Wingfield, M. J. 2017. *Bretziella*, a new genus to accommodate the oak wilt fungus, *Ceratocystis fagacearum* (Microascales, Ascomycota). *MycoKeys* 27:1-19.
- Enright, A. J., Van Dongen, S., and Ouzounis, C. A. 2002. An efficient algorithm for large-scale detection of protein families. *Nucleic Acids Res.* 30:1575-1584.
- Gearman, M., and Blinnikov, M. S. 2019. Mapping the potential distribution of oak wilt (*Bretziella fagacearum*) in East Central and Southeast Minnesota using Maxent. *J. For.* 117:579-591.
- Gauthier, M. K., Bourgault, É., Potvin, A., Bilodeau, G. J., Gustavsson, S., Reed, S., Therrien, P., Barrette, É., and Tanguay, P. 2023. Biosurveillance of oak wilt disease in Canadian areas at risk. *Can. J. Plant Pathol.* 46:27-38. <https://doi.org/10.1080/07060661.2023.2261890>
- Gibbs, J. N., and French, D. W. 1980. The transmission of oak wilt. USDA Forest Service Research Paper NC-185. Central Forest Experiment Station, St. Paul, MN.
- Grabherr, M. G., Haas, B. J., Yassour, M., Levin, J. Z., Thompson, D. A., Amit, I., Adiconis, X., Fan, L., Raychowdhury, R., Zeng, Q., Chen, Z., Mauceli, E., Hacohen, N., Gnirke, A., Rhind, N., di Palma, F., Birren, B. W., Nusbaum, C., Lindblad-Toh, K., Friedman, N., and Regev, A. 2011. Full-length transcriptome assembly from RNA-seq data without a reference genome. *Nat. Biotechnol.* 29:644-652.
- Grigoriev, I. V., Nikitin, R., Haridas, S., Kuo, A., Ohm, R., Otilar, R., Riley, R., Salamov, A., Zhao, X., Korzeniewski, F., and Smirnova, T. 2014. MycoCosm portal: gearing up for 1000 fungal genomes. *Nucleic Acids Res.* 42: D699-D704.
- Henry, B. W. 1944. *Chalara quercina* n. sp., the cause of oak wilt. *Phytopathology* 34:631-635.
- Juzwik, J., Appel, D. N., MacDonald, W. L., and Burks, S. 2011. Challenges and successes in managing oak wilt in the United States. *Plant Dis.* 95:888-900.
- Krzywinski, M., Schein, J., Birol, I., Connors, J., Gascoyne, R., Horsman, D., Jones, S. J., and Marra, M. A. 2009. Circos: an information aesthetic for comparative genomics. *Genome Res.* 19:1639-1645.

- Lam, K. K., LaButti, K., Khalak, A., and Tse, D. 2015. FinisherSC: a repeat-aware tool for upgrading de novo assembly using long reads. *Bioinformatics* 31:3207-3209.
- Manni, M., Berkeley, M. R., Seppey, M., Simão, F. A., and Zdobnov, E. M. 2021. BUSCO update: novel and streamlined workflows along with broader and deeper phylogenetic coverage for scoring of eukaryotic, prokaryotic, and viral genomes. *Mol. Biol. Evol.* 38:4647-4654.
- McLaughlin, K., Snover-Clift, K., Somers, L., Cancelliere, J., and Cole, R. 2022. Early detection of the oak wilt fungus (*Bretziella fagacearum*) using trapped nitidulid beetle vectors. *For. Pathol.* 52. <https://doi.org/10.1111/efp.12767>
- Morris, O. R. 2020. Seasonal Activity and Phorsey Rates of Sap Beetles (Coleoptera: Nitidulidae) in Oak Wilt Infection Centers, Volatile Organic Compounds Related to the Oak Wilt Cycle, and Long-Term Evaluation of Red Oak Provenances. Master's thesis, Michigan State University.
- Neph, S., Kuehn, M. S., Reynolds, A. P., Haugen, E., Thurman, R. E., Johnson, A. K., Rynes, E., Maurano, M. T., Vierstra, J., Thomas, S., and Sandstrom, R. 2012. BEDOPS: high-performance genomic feature operations. *Bioinformatics* 28:1919-1920.
- Parada-Rojas, C. H., and Quesada-Ocampo, L. M. 2018. Analysis of microsatellites from transcriptome sequences of *Phytophthora capsici* and applications for population studies. *Sci. Rep.* 8:5194. <https://doi.org/10.1038/s41598-018-23438-8>.
- Quinlan, A. R., and Hall, I. M. 2010. BEDTools: a flexible suite of utilities for comparing genomic features. *Bioinformatics* 26:841-842.
- Rexrode, C. O., and Lincoln, A. C. 1965. Distribution of oak wilt. *Plant Dis. Rep.* 49:1007-1010.
- Wingfield, B. D., Duong, T. A., Hammerbacher, A., van der Nest, M. A., Wilson, A., Chang, R., Wilhelm de Beer, Z., Steenkamp, E. T., Wilken, P. M., Naidoo, K., and Wingfield, M. J. 2016. Draft genome sequences for *Ceratocystis fagacearum*, *C. harringtonii*, *Grosmannia penicillata*, and *Huntia bhutanensis*. *IMA Fungus* 7:317-323.

CHAPTER 5: POPULATION STRUCTURE OF OAK WILT FUNGUS, *BRETZIELLA FAGACEARUM* IN THE UNITED STATES

Abstract

Bretziella fagacearum, the causal agent of oak wilt, has significantly impacted oak species (*Quercus* spp.) across the United States since its first description in Wisconsin in 1942. The pathogen's origin remains uncertain, though it is suspected to have been introduced from regions such as Mexico or Central and South America. Despite its widespread presence in the U.S., the dispersal patterns and genetic diversity of *B. fagacearum* remain poorly understood, posing challenges for predicting its spread and managing outbreaks. This study investigated the population genetic structure of *B. fagacearum* across its distribution in the United States. A total of 96 isolates were collected from 15 states and whole genome sequenced to generate a comprehensive dataset of 30,616 variants, including single nucleotide polymorphisms (SNPs) and insertions and deletions (indels). Our analyses using Principal Component Analysis (PCA), Minimum Spanning Network (MSN), STRUCTURE, and Discriminant Analysis of Principal Components (DAPC) consistently revealed significant population stratification. Four distinct genetic clusters were identified, corresponding to specific geographical regions: Upper Midwest (Cluster 1), Mid-Atlantic and Southeast (Cluster 2), Michigan (Cluster 3), and Texas (Cluster 4). The Upper Midwest served as a center of genetic diversity, with substantial gene flow among populations. In contrast, the Texas isolates formed a highly distinct cluster, suggesting limited gene flow and potential adaptation. Conversely, populations in the Mid-Atlantic and Southeast regions formed a separate cluster with low genetic diversity, suggesting isolation. Cluster 4, notably found in Texas, shows genetic ties to isolates from Arkansas, Missouri, Illinois, and Iowa, indicating a southward spread likely facilitated by both natural vectors and human-

mediated dispersal. In contrast, Cluster 2, encompassing the Appalachian states via Ohio and Pennsylvania, exhibits lower genetic diversity, suggestive of fewer introduction events and a more localized spread. These findings underscore the complex dynamics of pathogen dispersal in relation to oak wilt disease management and control strategies.

Introduction

Bretziella fagacearum (Bretz) Z.W. de Beer, Marinc., T.A. Duong & M.J. Wingf., previously known as *Ceratocystis fagacearum* (Bretz) Hunt, is the causal fungus of oak wilt in oaks (*Quercus* spp.) in the United States (de Beer et al. 2017; Juzwik et al. 2011). Although the origin of *B. fagacearum* is unknown, it is hypothesized that the fungus was introduced into the U.S. from regions such as Mexico, Central or South America (Hipp et al. 2018; Juzwik et al. 2008). Oak wilt was first formally described in Wisconsin in 1942 (Henry et al. 1944). However, historical evidence suggests oak wilt may affecting oaks in the upper Mississippi River valley since the 1890s (Gibbs and French 1980).

In the two decades following its initial discovery, oak wilt was reported in the midwestern, north-central, mid-Atlantic states and Texas, where it particularly affects live oaks (Rexrode and Lincoln 1965). Although officially documented in Texas in 1961, descriptions of widespread live oak mortality dating back to the 1930s imply that the disease may have been present much earlier (Appel 1995). Currently, oak wilt has been confirmed in 24 states across the U.S., with a significant prevalence in the midwestern states and Texas (Juzwik et al. 2011). The geographic range of oak wilt is limited, considering the availability of suitable hosts and climatic conditions in parts of the western U.S., like California, and nonaffected areas in the northeast and southeast (Appel 1994). However, oak wilt continues to spread and is expanding into new geographical locations where it was not previously reported (Gauthier et al. 2023; McLaughlin et

al. 2022). The recent detection of oak wilt in Ontario, Canada, in June 2023 marks the first report of *B. fagacearum* outside of the U.S. (Canadian Food Inspection Agency 2023).

It is challenging to predict the pathway of *B. fagacearum* spread from its initial detection in Wisconsin to different states and regions of U.S. Considering the inefficient long-distance dispersal by sap beetles (Coleoptera: Nitidulidae) and the erratic nature of mycelial mats production, it is very unlikely that the pathogen could have spread throughout its distribution range within two decades of its initial discovery (Appel 1995; Juzwik 2011). Thus, it has been argued that the current disease range reflects a distribution pattern that has existed for over a century (MacDonald 1995). The current understanding of the pathogen's limited long-distance spread makes it difficult to envision that the initial discoveries in Wisconsin or Texas were single-point introductions leading to widespread epidemics within a few decades. Consequently, it has not been possible to confidently place the emergence of *B. fagacearum* in the United States. The genetic diversity within and among *B. fagacearum* populations across the distribution range needed to be explored to determine the point(s) of introduction and further spread pathway of the pathogen in the United States.

The population diversity of *B. fagacearum* has been previously studied to a limited extent (Harrington 2008; Kurdyla et al. 1995; Peacock 2008). These studies have consistently demonstrated limited to no genetic variation among isolates. Kurdyla et al. (1995) used restriction fragment length polymorphisms (RFLPs) to analyze mitochondrial (mt) and nuclear (nu) DNA and found minimal variation among the 27 isolates, primarily from Texas (22), but also from West Virginia (3) and Wisconsin (2). These isolates showed no variation in mtDNA markers and only minor RFLP variation in nuDNA using anonymous probes. Similarly, Harrington (2008) examined a population of *B. fagacearum* from the Upper Midwest, utilizing

nuclear and mitochondrial markers previously applied to other *Ceratocystis* species (Wingfield et al. 1996). The study included 37 isolates from Iowa, 6 from Minnesota, and 1 from Illinois, revealing a nearly uniform mitochondrial genome and very limited nuclear genome variation, consistent with the findings of Kurdyla et al. (1995). Peacock (2008) conducted an amplified fragment length polymorphism (AFLP) study on 13 isolates from Michigan, 5 from Wisconsin, 4 from Minnesota, and 1 each from Texas and West Virginia. The study identified only one polymorphic locus out of 82 scored bands, with the Texas isolate showing a different fragment length at this locus.

These previous investigations underscore the limited genetic diversity within *B. fagacearum* populations. However, the findings seem constrained by limited sample sizes across *B. fagacearum* distribution range and the methodologies employed, which lack the resolution and robustness. Techniques such as RFLPs and AFLPs, while useful at the time, analyze only specific sections of the genome and potentially overlooking significant genetic variation. In contrast, modern methodologies like whole genome sequencing (WGS) and single nucleotide polymorphism (SNP) analysis provide comprehensive, high-resolution approaches to population genomics. WGS enables examination of the entire genome, identifying diverse genetic variations, including rare mutations that can be overlooked by older methods. SNP analysis, specifically, identifies numerous polymorphic sites across the genome, facilitating a detailed understanding of genetic diversity and population structure. Thus, a comprehensive population genetic study using these modern tools was warranted to better understand the population structure of *B. fagacearum*.

This study was conducted to investigate the population genetic structure of *B. fagacearum* affecting different host species across its distribution range in the U.S. The

objectives were to determine: (1) whether the population is structured based on host species or geographical locations, and (2) to assess gene flow and genetic differentiation within and among populations to identify potential pathways of pathogen movement within the U.S.

Materials and methods

Isolates:

A total of 93 *B. fagacearum* isolates were collected from various locations across the United States, spanning 15 states: Arkansas (AR), Iowa (IA), Illinois (IL), Maryland (MD), Michigan (MI), Minnesota (MN), Missouri (MO), New York (NY), Ohio (OH), Pennsylvania (PA), South Carolina (SC), Texas (TX), Wisconsin (WI), and West Virginia (WV). The isolates were obtained from infected oak trees (*Quercus* spp.) and chestnut hybrids (*Castanea* spp.), representing different oak subsections: red oaks (section *Lobatae*), white oaks (section *Quercus*), and intermediate forms. Representative host species of the isolates include *Q. rubra*, *Q. macrocarpa*, *Q. palustris*, *Q. alba*, *Q. ellipsoidalis*, *Q. velutina*, *Q. nigra*, *Q. buckleyi*, *Quercus fusiformis*, *Q. havardii*, *Q. laceyi*, and chestnut hybrids (*C. sativa* × *C. crenata*, *C. mollissima*) (Table 1).

DNA extraction and sequencing:

High-quality genomic DNA was extracted from Petri plate cultures for library preparation and Illumina sequencing. Isolates were cultured on acidified potato dextrose agar (aPDA; 36 g/L of PDA [Difco™, Sparks, MD], amended with 1ml/L of 80% lactic acid [JT Baker, Phillipsburg, NJ, USA] for 12 to 14 days. Fungal tissue was scraped from the surface with a sterile scalpel and placed into a screw-cap collection tube containing a stainless-steel bead. Samples were lyophilized using a Genesis Pilot Lyophilizer (SP Scientific, Warminster, PA) and homogenized with a TissueLyser II (Qiagen, Hilden, Germany) at 30 Hz for 3 minutes (Lukasko

and Hausbeck 2024). DNA extraction was performed using the Applied Biosystems MagMAX Plant DNA Isolation Kit (Thermo Fisher Scientific, Waltham, MA) manually following the user's guide. DNA quantification was done using a Qubit dsDNA High Sensitivity (HS) assay kit (Invitrogen, Carlsbad, CA) before submission to the Michigan State University Genomics Core for library preparation and sequencing. Libraries were prepared with the Illumina TruSeq Nano DNA Library Preparation kit. Quantification and quality assessments were carried out using Qubit dsDNA HS and Aligent 4200 TapeStation HS DNA1000 assays. Sequencing was performed on an Illumina NovaSeq 6000 SP or S4 flow cell in a 150-bp paired-end format. Initial read quality analysis of sequence data was conducted with MultiQC (Ewels et al. 2016), followed by filtering and trimming of reads using fastp (Chen et al. 2018) with a minimum phred score of 30.

Variant calling and filtration:

The sequence alignment and variant calling were conducted using the Genome Analysis Toolkit (GATK) germline short variant discovery pipeline (Poplin et al. 2018). The 150 bp paired-end reads from 93 samples were aligned to the reference genome of *B. fagacearum* (Chahal et al. unpublished) using BWA-MEM v0.7.17-r1188 (Li 2013). Duplicate reads were marked using the Picard tools MarkDuplicates function (Broad Institute 2019), which filtered duplicates for downstream analysis. The SAM files were converted to BAM format, sorted, and indexed using SAMtools v1.16.1 (Li et al. 2009). Variant calling was performed with the HaplotypeCaller tool of GATK v4.2.0.0, with -ploidy set to 1. The resulting VCFs were combined into a single gVCF file using CombineGCVFs (McKenna et al. 2010). Single-nucleotide variants (SNVs) and indels were hard filtered using GATK VariantFiltration, following the recommended cutoffs on GATK (Broad Institute 2019). The filters applied were:

“ $QD < 2.0$ ”, “ $MQ < 59.9$ ”, “ $FS > 60.0$ ”, “ $MQRankSum < -2.5$ ”, “ $ReadPosRankSum < -4.0$ ”, and “ $BaseQRankSum < -2.0$ ”. Further filtration of non-redundant variants was conducted using bcftools v1.9-64-g28bcc56 "prune" function, initially removing variants with a minor allele frequency (MAF) less than 0.05. Additional filtering retained variants with r^2 values less than 0.8. After all filtering steps, a total of 30,616 variants were selected for downstream analysis. All subsequent analyses were performed in R v4.4.0.

Population structure:

The gVCF files were imported and converted into genlight and genid formats in R v4.4.0 using the vcfR v1.15.0 package (Knaus and Grünwald 2017). Principal Component Analysis (PCA) of the VCF file was performed using the glPcaf function of adegenet v2.1.10 (Jombart 2008), with PC1 and PC2 components plotted using the ggplot function of ggplot2 v3.5.1 (Wickham 2016). Principal Component Analysis (PCA) was utilized due to its effectiveness in dimensionality reduction, enabling the extraction and emphasis of principal axes of variation within the dataset.

A minimum spanning network (MSN) plot was constructed using the poppr() function of poppr v2.9.6, with set.seed set to 9 for reproducibility, and a genetic tree was constructed using the about() function with the UPGMA algorithm and a bootstrap value of 100 (Kamvar et al. 2014). The UPGMA algorithm was used for its simplicity and effectiveness in constructing genetic trees for organisms with limited genetic diversity. Population structure analysis was performed using STRUCTURE v2.3.4 with the Admixture model, testing k-values from 3 to 10, and determining the optimal k-value to be 4 based on the Bayesian Information Criterion (BIC) (Pritchard et al. 2000). Violations of assumptions in STRUCTURE (such as panmixia, Hardy-Weinberg equilibrium, and linkage equilibrium in clonal subgroups) can produce incorrect

assignments. Therefore, the results from STRUCTURE were compared to a second genetic cluster assignment using Discriminant Analysis of Principal Components (DAPC). DAPC optimizes variation among clusters to the detriment of variation within clusters and, unlike STRUCTURE, is neutral to any a priori genetic hypothesis. The `dapc()` function of the `adegenet` v2.1.10 package was applied to populations stratified by the state of collection (Jombart et al. 2010). Fixation index (F_{st}) values, measuring population differentiation, were calculated using the `betas()` function of `hierfstat` v0.5-11 (Goudet 2005), and pairwise F_{st} values were calculated using the `genet.dist()` function with the Nei84 method (Nei 1984). F_{st} values are essential for quantifying the degree of genetic differentiation between populations. Analysis of Molecular Variance (AMOVA) was performed using the `poppr.amova()` function of `poppr` v2.9.6 to assess genetic variation within and between populations (Excoffier et al. 1992). AMOVA provided insights into how genetic variation is partitioned across different hierarchical levels, further informing the understanding of population structure.

Results

Population structure:

Following the filtration steps, a total of 30,616 variants were selected for downstream analysis. Among these variants, 44.45% were single nucleotide polymorphisms (SNPs) and 49.17% were insertions and deletions (indels) (Lindenbaum 2015). Bayesian Information Criterion (BIC) guided the selection of optimal clusters, using 92 principal components (PCs) that accounted for approximately 99% of the data variance. BIC values were computed for clusters ranging from 1 to 8 (Fig. 5.1). The number of clusters ($K = 4$) was chosen where the BIC value (839.9609) was lowest or indicating a slow decrease thereafter. STRUCTURE was run with $K=4$, using an admixture model to fit the data. Structure analyses indicated the presence of

four distinct ancestral genetic clusters. Genetic clusters exhibited high differentiation of populations with a low degree of admixture. Populations exhibited a high degree of differentiation with 86% of isolates having greater than 90% membership to a single cluster (Fig. 5.2). Genetic clusters or ancestral populations were correlated with geographical regions of the isolates. Populations from the Upper Midwest (MI, WI, MN, IA and MO) comprised Cluster 1. Populations from Mid-Atlantic and Southeast region (NY, PA, OH, MD, WV, SC) grouped into Cluster 2. MI was genetically diverse some isolates are forming a separate Cluster 3. Isolates from Texas formed a separate, genetic Cluster 4. Some isolates from AR, IL, MI and WI exhibited a varying level of degree admixture with having greater less than 90% membership to a single cluster (Fig. 5.2, Table 5.1). Net nucleotide distance (genetic divergence) similar to F_{st} values indicate Cluster 1 is low to moderately divergent with Cluster 3, and 4 (Table 5.2). Cluster 2 is highly divergent from rest of the three clusters. Cluster 2 and 3 are moderately divergent from each other. A genetic tree based on Bruvo's distance with bootstrapping of 100 also inferred four major clades, which corroborate the findings from other analyses, with TX forming a separate clade (Fig. 5.3).

The Discriminant Analysis of Principal Components (DAPC), based on BIC clustering, calculated the posterior probability of different populations according to the state of origin (Fig. 5.4). Isolates from MI, MN, and WI showed similar distributions of posterior membership probability, along with a few isolates from IL and IA, forming a subpopulation (subpop1). Isolates from MD, NY, OH, PA, SC, and WV formed subpop2. All isolates from MO, along with a few isolates from IA, showed shared ancestry and formed subpop3. Isolates from TX formed a separate group as subpop4 (Fig. 5.4). Similarly, pairwise F_{st} values represented lower genetic differentiation within the populations of subpop1 and subpop2. However, there was high

differentiation between states from different subpopulations (Fig. 5.5). The TX population exhibited varying levels of differentiation between other sub-populations based on geographical distance, with very high differentiation between subpop2 and moderate to high differentiation between subpop1 and subpop3 (Fig. 5.5).

Principal Component Analysis (PCA) was performed on these 30,616 filtered variants across the *B. fagacearum* genome to elucidate the population structure of the fungus across the United States (Fig. 5.6). The first principal component (PC1) represents the West-to-East distribution, accounted for 33% of the total genetic variance. The second principal component (PC2) represents the South-to-North distribution, accounted for 8% of the variance. The resulting PCA plot was grouped by state of *B. fagacearum* isolates origin (Fig. 5.6). The PCA revealed four distinct subpopulations. The first, displaying the greatest spread along PC1, consisted of isolates predominately from MI, indicating a high level of genetic diversity within this state. Moreover, populations from AR, IL, MN, WI, IA formed overlapping group as subpop1. The subpop2 included populations from WV, SC, OH, NY and PA. The subpop3 included isolates MO some isolates from IA. The isolates from TX, formed a highly distinct subpop4 with no shared variation with other populations (Fig. 5.6). Additionally, PCA was performed to group isolates based on the host species from which they were collected (Fig. 5.7). The analysis revealed that isolates collected from *Q. fusiformis*, *Q. buckleyi*, and *Q. laceyi* formed a distinct cluster, corresponding to the isolates from TX. In contrast, the remaining samples did not segregate according to host species, indicating that host-specific genetic differentiation is not pronounced in the other populations (Fig. 5.7).

Consistent with previous analyses Minimum Spanning Network (MSN) analysis depicted isolates from MI show significant genetic diversity (Fig. 5.8). TX isolates formed a distinct cluster with connections, suggesting moderate genetic diversity and gene flow, contrary to PCA. Majority of isolates clustered by geographic site, showing limited genetic variation within populations.

Discussion

Our results reveal significant population stratification within *B. fagacearum*. Consistent results were obtained across multiple clustering approaches, including Bayesian clustering, PCA, DAPC, and Neighbor-Joining clustering. Structure analyses with admixture model identified four distinct genetic clusters within the distribution range of *B. fagacearum*. Upon examining the geographic origin of isolates within these genetic clusters, we observed a clear correlation between genetic clusters and geographic regions. Populations from the Upper Midwest, including MI, WI, MN, IA and MO constituted Cluster 1. Populations from the Mid-Atlantic and Southeast regions, comprising NY, PA, OH, MD, WV, and SC formed Cluster 2. Notably, the MI population displayed significant genetic diversity, with some isolates forming an independent Cluster 3. Isolates from TX constituted a distinct genetic Cluster 4. Furthermore, few isolates from AR, IL, MI, and WI exhibited varying levels of admixture, with less than 90% membership to a single cluster.

These findings are consistent with the historical emergence of *B. fagacearum* infections in Wisconsin, suggesting a potential region of introduction or emergence. Although MI isolates exhibited the highest genetic diversity and significant membership to all ancestral populations, this could be attributed to the larger sample size and broader distribution of samples throughout the state. In contrast, MN samples, collected only from the southeast region, demonstrated

significant genetic diversity similar to WI and MI. Our analyses indicate substantial gene flow correlated with geographical distance. Populations geographically closer exhibited similar genetic compositions. For instance, populations from Upper Midwest states (Cluster 1) displayed high heterozygosity and low differentiation compared to populations in the other three genetic clusters. Notably, isolates from WI, MN, and MI show similar genetic compositions when posterior membership probability is analyzed according to the state of origin. These results suggest gene flow among these populations of WI, MN and MI, potentially through long distance dispersal of the pathogen. These genetic findings provide additional support for anthropogenic activities contributing to the spread of oak wilt. The introduction of *B. fagacearum* to the south-central portion of the Upper Peninsula of Michigan in the 1970s has been attributed to the movement of firewood from oak wilt counties in Wisconsin (Juzwik et al. 2011).

Populations within Cluster 1 began to differentiate as they moved away from the center of diversity (MI, WI, and MN). Populations moving southward into IL, IA, MO, and AR showed altered genetic compositions. For example, as populations moved south into IL, IA, MO, and AR, the genetic composition of isolates changed, indicating potential genetic drift from the initial populations toward the Midwestern U.S. Populations from MO and IA formed a sub-population, and AR showed significant admixture of Clusters 1 and 4. Cluster 4, comprising only TX isolates, suggests potential adaptation following random drift from the center of diversity. Some of isolates from MO, IA and AR isolate displayed a significant admixture with genetic Cluster 4, exhibiting some genetic composition of TX population. This pattern suggests the potential movement of *B. fagacearum* into Texas via IL, IA, MO, and AR, as indicated by the different levels of admixture from the genetic clusters.

It is crucial to investigate why TX isolates are genetically distinct from the rest of the populations. This distinctiveness could be influenced by climatic differences or adaptability to different host species that are not found elsewhere within the known range of *B. fagacearum*. However, the lack of genetic differentiation based on host species in the other clusters, despite the isolates being obtained from various host species, suggests that geographical factors might play a more significant role in shaping the genetic composition of TX population.

Cluster 2, encompassing populations from the Mid-Atlantic and Southeast regions, exhibits high levels of genetic differentiation and divergence from other clusters, suggesting limited gene flow. This isolation could be attributed to significant geographical distance from other cluster locations or specific selective pressures unique to this region. Despite this isolation, the genetic composition of isolates within Cluster 2 is remarkably similar, as indicated by low expected heterozygosity, which suggests substantial gene flow within the population. This intra-cluster gene flow is likely facilitated by human-mediated dispersal, such as the movement of infected firewood in the Appalachian regions. Likewise, the genetic composition of *B. fagacearum* from the first reported case in Schenectady, NY, suggests human-mediated introduction from oak wilt sites in the neighboring states as hypothesized (Snover-Clift and Rosenthal 2016). All isolates of Mid-Atlantic and Southeast regions show over 99% membership to Cluster 2, except for an isolate from Ontario County, New York, where oak wilt was discovered in 2016. This isolate shared 4% genetic ancestry with Cluster 1, which is intriguing since other isolates geographically closer to Cluster 1, such as those from OH, PA, did not show any membership to Cluster 1.

A possible explanation for this gene flow could be the proximity of Ontario County, NY, to the Ontario province, Canadian border, where oak wilt was discovered in 2023. This suggests

potential gene flow between oak wilt sites in Ontario Province, Canada, and Ontario County, NY. It might also indicate that oak wilt might have been present in NY and Canada for a longer period, with substantial genetic diversity, including substantiable admixture of Cluster 1. Comprehensive genetic diversity analyses of Canadian, and more NY isolates will be necessary to elucidate these potential scenarios and confirm the pathways of gene flow.

Interestingly, Genetic Cluster 3 consists predominantly of isolates from MI with a notable presence of admixture from Cluster 3 in isolates from IL, IA, WI, MO, and AR. Similarly, admixture from Cluster 2 is also detected in isolates from IL, WI, and MI. Notably, isolates from MI and one of the two isolates from IL exhibit admixture from all four clusters. This suggests that the Upper Midwest may serve as a center of diversity or an initial point of introduction for the pathogen. From this area, the pathogen populations appear to have migrated in two distinct directions. Interestingly, the unique genetic composition of Cluster 4 isolates from Texas, with traces of its genetic ancestry among isolates of AR, MO, IL and IA indicates a southward spread of the pathogen, likely involving both vector and human-mediated dispersal. Conversely, the less diverse lineage or likely involved fewer introductions and spread into the Appalachian states via OH and PA. Similar results have been observed in the population structure of various introduced fungal pathogens, which show low to little genetic differentiation among geographically proximate populations, indicating gene flow (Adamčíková et al. 2021; Crouch et al. 2023; Orton et al. 2018; Zerillo et al. 2014). Long-distance dispersal of certain lineages has been suggested through human-mediated dispersal, which is beyond the flight range of insect vectors (Adamčíková et al. 2021; Zerillo et al. 2014). For instance, the population structure of *Dothistroma pini*, a pathogen causing needle blight in pines, showed significant clonality and low genetic diversity across Slovakia, suggesting recent introductions and human-mediated

movement (Adamčíková et al. 2021). Similarly, *Macrophomina phaseolina*, which affects soybean and dry bean, exhibited distinct genetic clusters across the United States, Colombia, and Puerto Rico, with evidence of long-distance dispersal likely facilitated by human activities (Crouch et al. 2023).

Future research can prioritize understanding the genetic architecture of these clusters through detailed genomic studies, including identifying specific loci under selection and elucidating the roles of genetic drift and gene flow. Additionally, developing and validating a SNPchip can significantly enhance our ability to assign future detections to their source populations/clusters. Alternatively, SNPs that can differentiate different clusters can be identified in commonly used gene regions for fungal species identification, such as the internal transcribed spacer (ITS), elongation factor (EF), and beta-tubulin genes. This approach would allow amplification and identification of these SNPs through PCR and gel electrophoresis, enabling the assignment of different isolates to their respective source populations based on genetic clusters.

Acknowledgements

We are thankful to Mohit Mahey, Dr. Jagdeep Singh Sidhu, and Dr. Eric L. Patterson for their guidance and assistance in data analyses. This research was funded in part by the Michigan Invasive Species Grant Program and Project GREEN.

Figures

Figure 5.1. Plot showing Bayesian Information Criterion (BIC) versus number of clusters. The analysis was conducted using the `find.clusters()` function from the `adegenet` package, retaining 90 Principal Components (PCs). The BIC values were computed to identify the optimal number of genetic clusters for the population structure analysis.

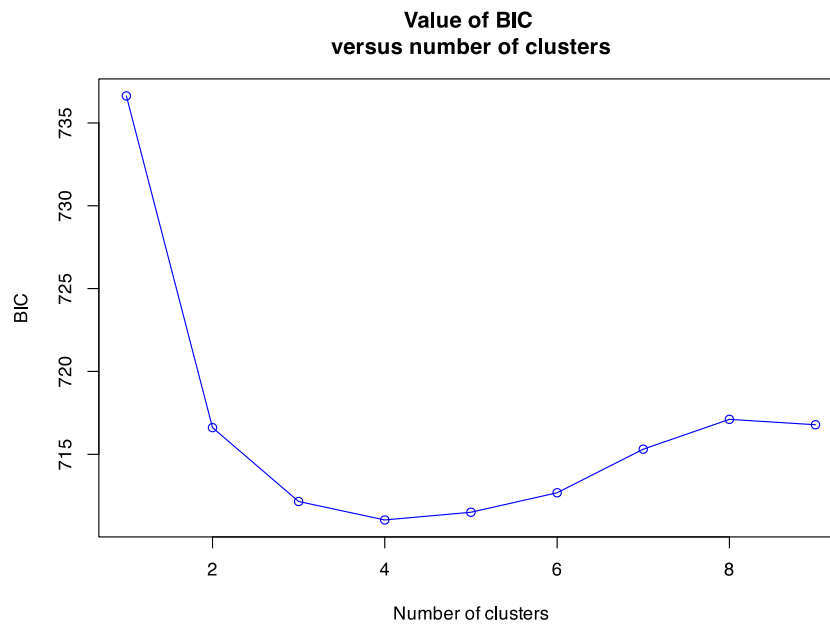


Figure 5.2. Population structure of *Bretziella fagacearum* at K=4. Each bar represents an individual isolate, and the colors correspond to the proportion of the genome assigned to each of the four clusters (K1, K2, K3, K4) as inferred by the STRUCTURE analysis using an admixture model. The x-axis represents the sample ID, and the y-axis represents the proportion of genetic membership to each cluster.

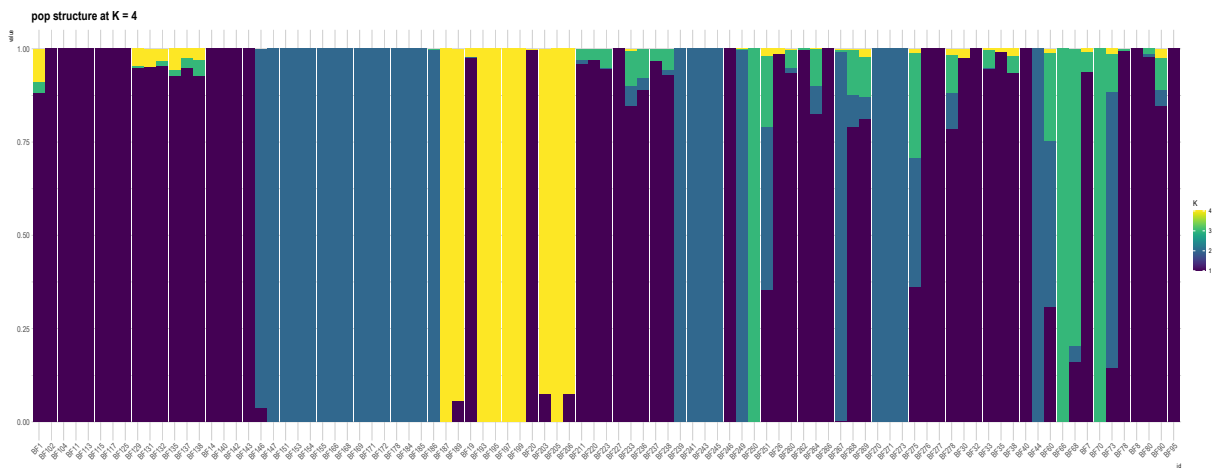


Figure 5.3. Rooted genetic tree of 93 *Bretziella fagacearum* isolates, color-coded based on the site of collection. The tree was constructed using the "UPGMA" (Unweighted Pair Group Method with Arithmetic Mean) algorithm with 100 bootstrap replicates. Bootstrap values are shown at the nodes, indicating the confidence level for each branch. The genetic distance is represented on the x-axis as the proportion of loci that are different.

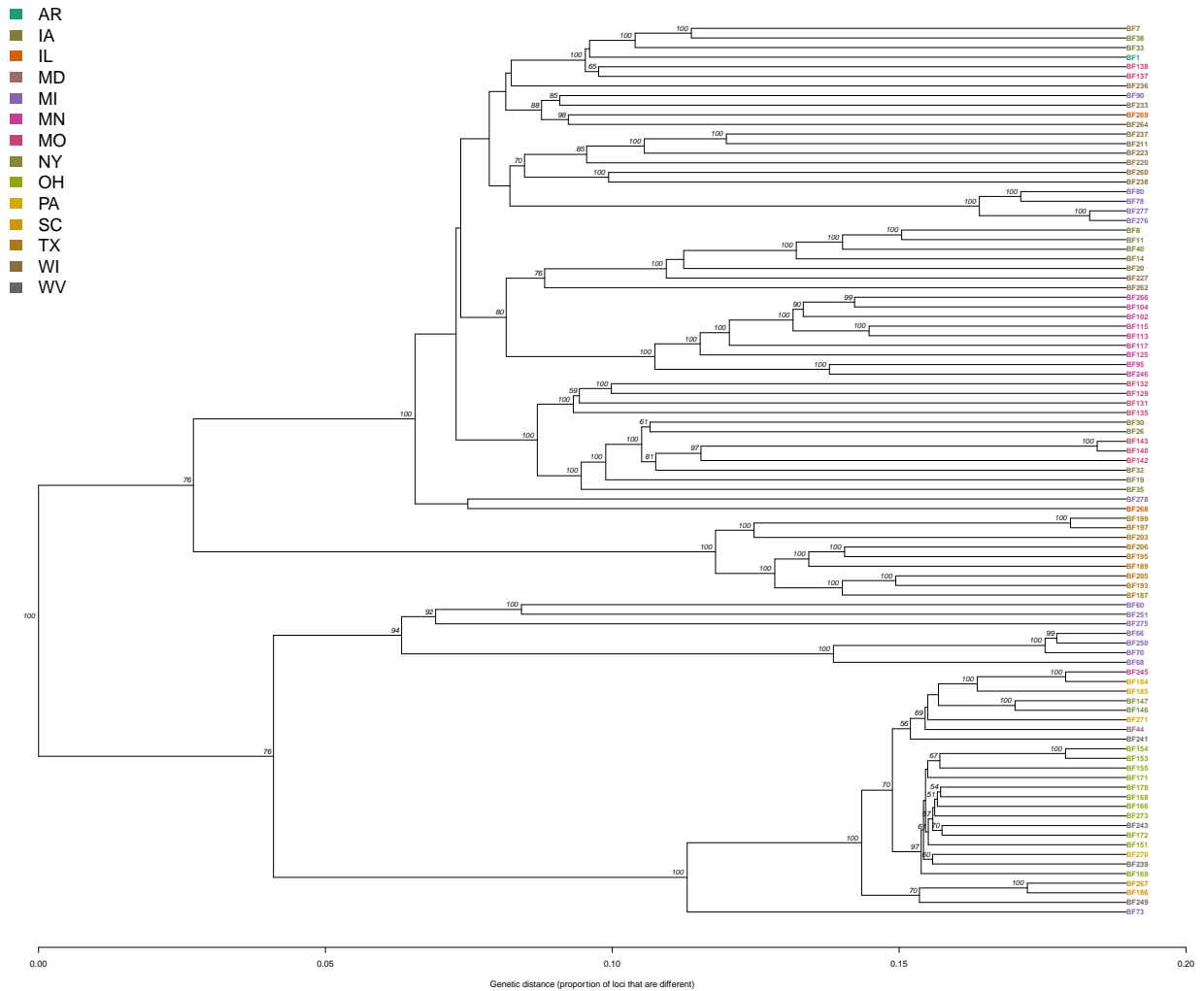


Figure 5.4. Population structure inferred through Discriminant Analysis of Principal Components (DAPC) using three principal components, capturing approximately 42% of the total variance based on 30,616 variants. The analysis identified the optimal number of populations (K=4) across 93 samples collected from various states in the USA. Each bar represents an individual isolate, with the y-axis showing the posterior membership probability from each state and the x-axis indicating the state of collection for each isolate. The colors represent the different assigned populations, and the isolates are grouped by the state from which they were collected.

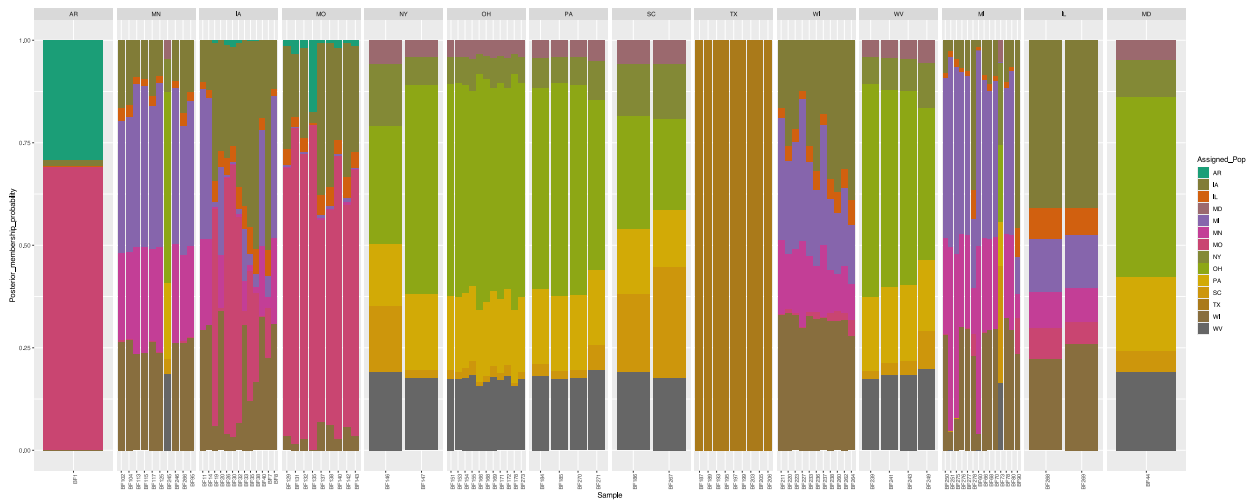


Figure 5.5. Heatmap comparing pairwise F_{st} values among different populations of *Bretziella fagacearum*. The F_{st} values represent the genetic differentiation between pairs of populations. High F_{st} values indicate high genetic differentiation, whereas low F_{st} values suggest lower differentiation and higher gene flow. The populations are listed along the axes, with each cell representing the F_{st} value between the corresponding populations.

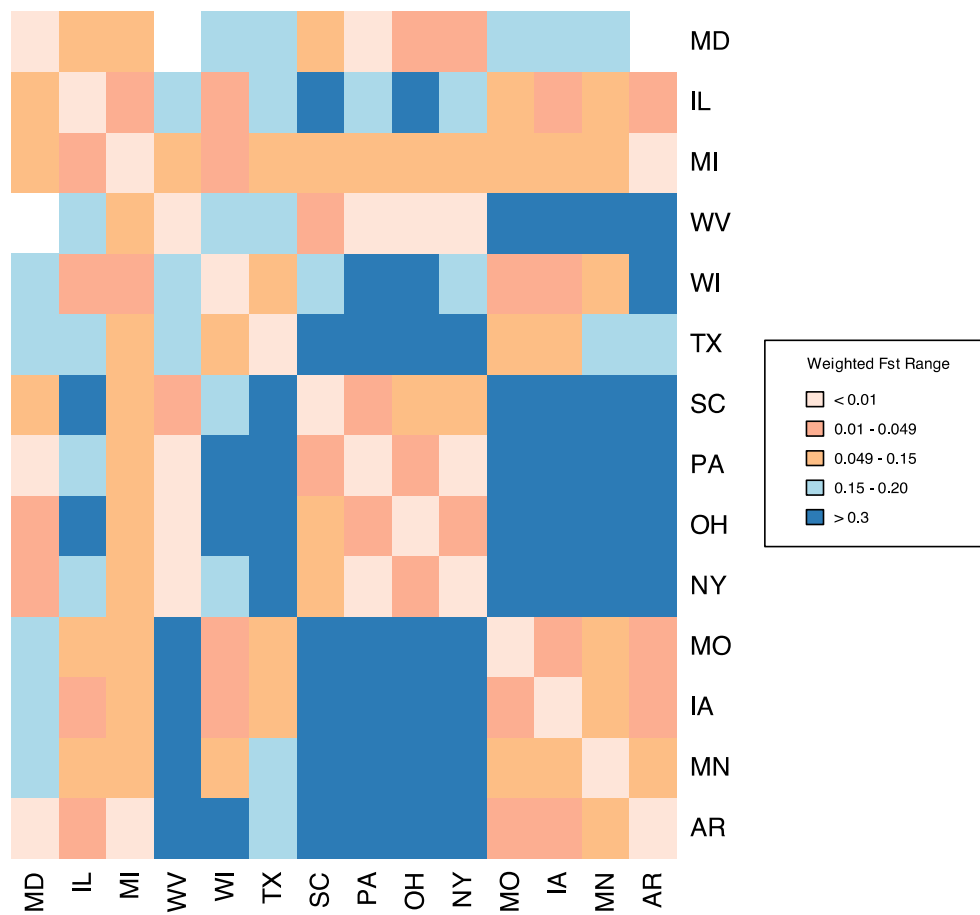


Figure 5.6. Principal Component Analysis (PCA) of 93 *Bretziella fagacearum* isolates based on 30,616 variants. The plot shows the first two principal components (PC1 and PC2), which represent approximately 40% of the variance in the data. Each point represents an individual isolate, and the ellipses, colored based on the state of collection, encompass alpha level 0.05.

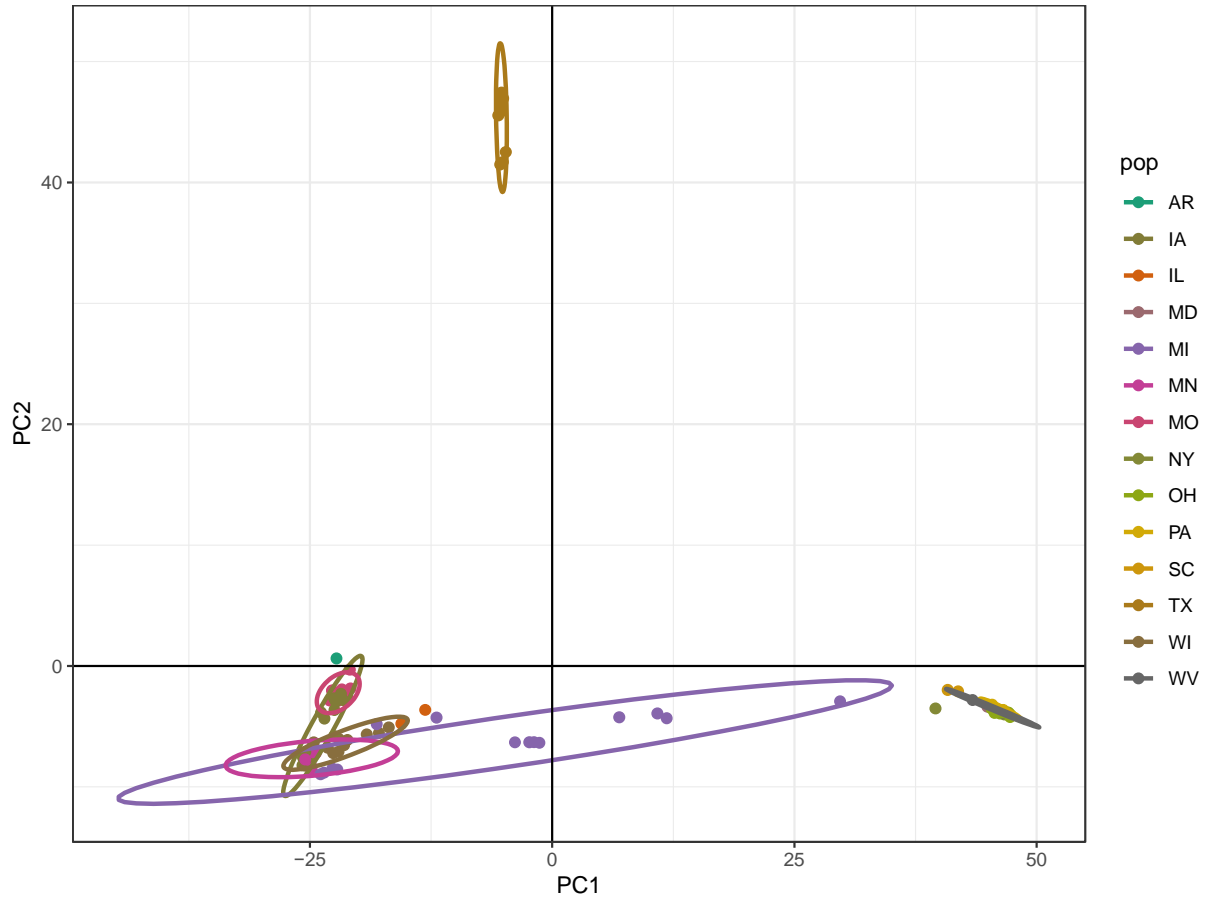


Figure 5.7. Principal Component Analysis (PCA) of 93 *Bretziella fagacearum* isolates based on 30,616 variants. The plot shows the first two principal components (PC1 and PC2), which represent approximately 40% of the variance in the data. Each point represents an individual isolate, and the ellipses, colored based on the isolate host, encompass alpha level 0.05.

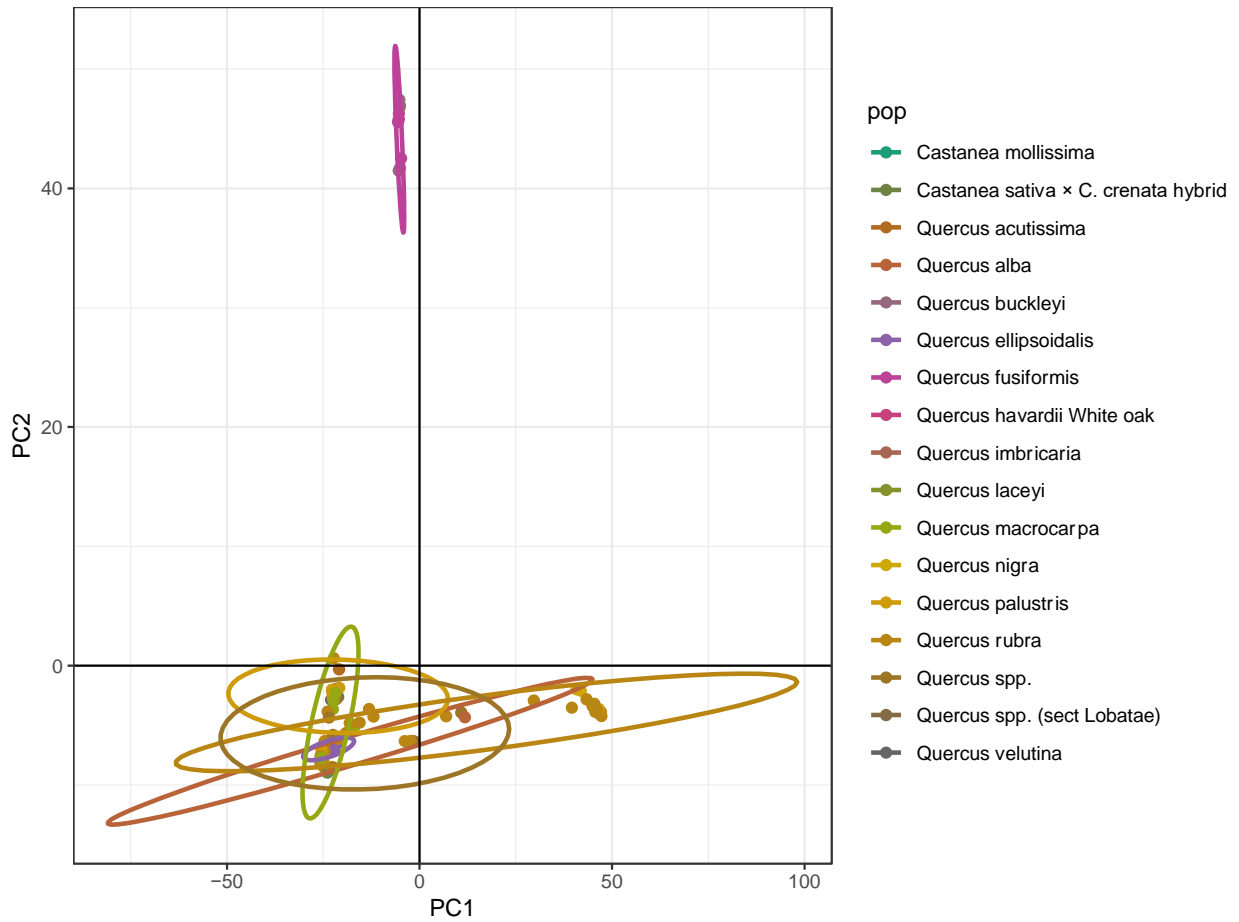
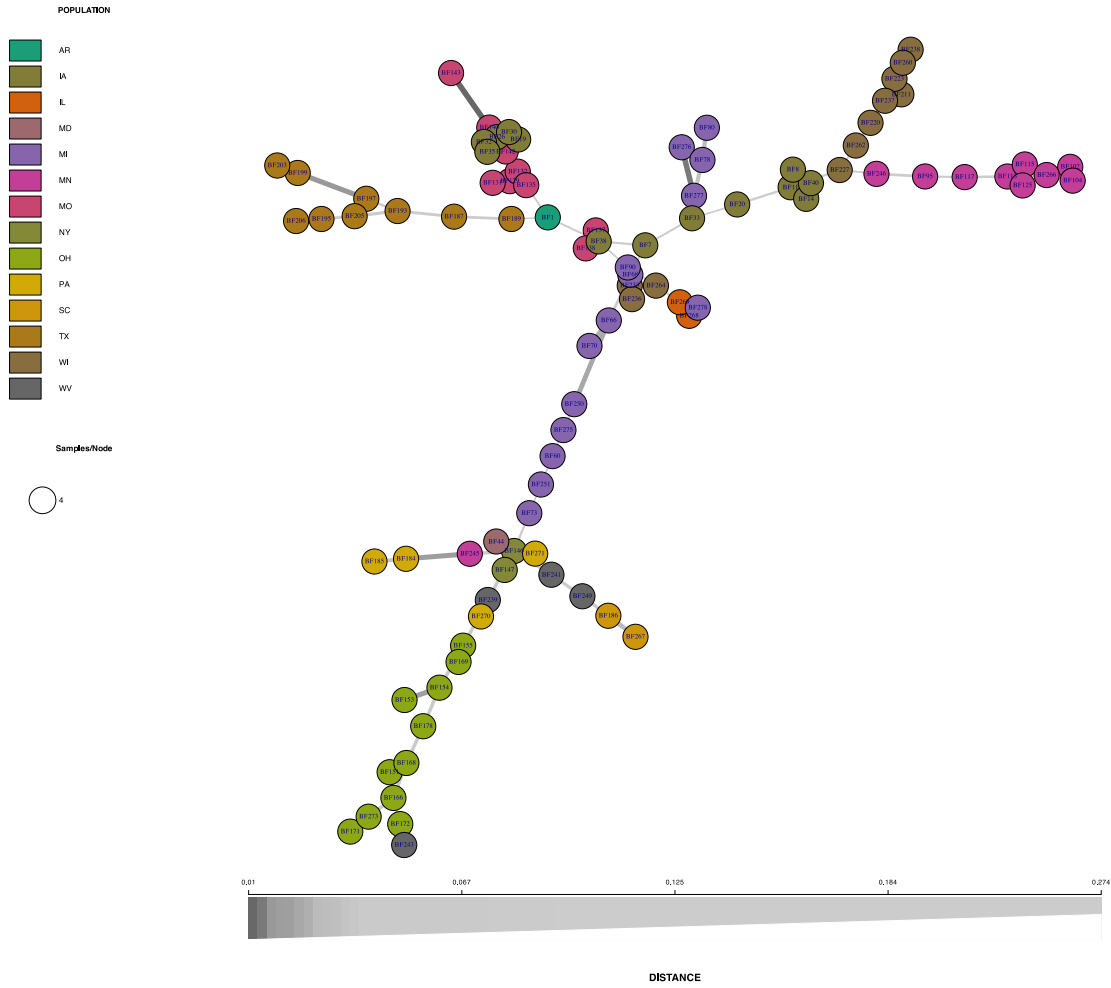


Figure 5.8. Minimum Spanning Network (MSN) of 93 *B. fagacearum* isolates. Each node represents an isolate, colored by state of collection, with sizes proportional to sample count. Edges indicate genetic distances, revealing distinct clusters and gene flow among populations.



Tables

Table 5.1. Isolates of *Bretziella fagacearum* collected from oak and chestnut hosts across the United States.

Sample ID	Previous ID	Host species	Sub-section	County	State
BF1	Baxtor 9	<i>Quercus rubra</i>	Red oak	Baxter	AR
BF11	C661	<i>Quercus macrocarpa</i>	White oak	Hardin	IA
BF30	C659	<i>Quercus macrocarpa</i>	White oak	Polk	IA
BF32	C1108	<i>Quercus macrocarpa</i>	White oak	Sac	IA
BF35	C4235	<i>Quercus macrocarpa</i>	White oak	story	IA
BF26	7378	<i>Quercus palustris</i>	Red oak	Polk	IA
BF40	C663	<i>Quercus palustris</i>	Red oak	Webster	IA
BF14	C4234	<i>Quercus rubra</i>	Red oak	Johnson	IA
BF8	C494	<i>Quercus rubra</i>	Red oak	Linn	IA
BF38	C654	<i>Quercus rubra</i>	Red oak	Wapello	IA
BF7	C516	<i>Quercus</i> spp.	UA	Des Moines	IA
BF20	C655	<i>Quercus</i> spp.	UA	Dubuque	IA
BF19	C653	<i>Quercus</i> spp.	UA	Lee	IA
BF33	C459	<i>Quercus</i> spp.	UA	Scott	IA
BF268	2021.161	<i>Quercus rubra</i>	Red oak	DuPage	IL
BF269	2021.162	<i>Quercus rubra</i>	Red oak	DuPage	IL
BF44	OW2TXP3	<i>Quercus rubra</i>	Red oak	Allegany	MD
BF277	Chestnut76	<i>Castanea sativa</i> × <i>C. crenata</i> hybrid	Chestnut	Mason	MI
BF276	Chestnut75	<i>Castanea sativa</i> × <i>C. crenata</i> hybrid	Chestnut	Mason	MI
BF60	41	<i>Quercus alba</i>	White oak	Isabella	MI
BF68	17	<i>Quercus rubra</i>	Red oak	Lake	MI
BF70	22	<i>Quercus rubra</i>	Red oak	Leelanau	MI

Table 5.1. (cont'd)

BF73	39	<i>Quercus rubra</i>	Red oak	Livingston	MI
BF78	2	<i>Quercus rubra</i>	Red oak	Mason	MI
BF275	17-3487	<i>Quercus rubra</i>	Red oak	Montmarency	MI
BF90	5	<i>Quercus rubra</i>	Red oak	Ottawa	MI
BF278	Coy11	<i>Quercus rubra</i>	Red oak	Roscommon	MI
BF250	2152	<i>Quercus</i> spp.	UA	Grand Traverse	MI
BF80	3	<i>Quercus</i> spp.	UA	Mason	MI
BF251	KF1	<i>Quercus</i> spp.	UA	Kalamazoo	MI
BF66	52	<i>Quercus</i> spp.	UA	Kalkaska	MI
BF104	C520	<i>Quercus alba</i>	White oak	Hennepin	MN
BF115	19-310	<i>Quercus alba</i>	White oak	Hennepin	MN
BF113	19-354a	<i>Quercus alba</i>	White oak	Hennepin	MN
BF102	19-542R	<i>Quercus ellipsoidalis</i>	Red oak	Hennepin	MN
BF117	19-446	<i>Quercus ellipsoidalis</i>	Red oak	Ramsey	MN
BF95	19-510	<i>Quercus macrocarpa</i>	White oak	Dakota	MN
BF246	Dakota	<i>Quercus rubra</i>	Red oak	Dakota county	MN
BF266	C519	<i>Quercus rubra</i>	Red oak	Sherburne	MN
BF125	C504	<i>Quercus rubra</i>	Red oak	Sherrune	MN
BF245	Washington	<i>Quercus rubra</i>	Red oak	Washington	MN
BF135	17-130	<i>Quercus acutissima</i>	White oak	Johnson	MO
BF131	19-006	<i>Quercus imbricaria</i>	Red oak	Boone County	MO
BF132	19-012	<i>Quercus palustris</i>	Red oak	Boone County	MO
BF138	19-015	<i>Quercus palustris</i>	Red oak	Marion	MO
BF142	18-010	<i>Quercus palustris</i>	Red oak	Putnam	MO
BF143	18-011	<i>Quercus palustris</i>	Red oak	Putnam	MO
BF129	18-006	<i>Quercus</i> spp. (sect <i>Lobatae</i>)	Red oak	Boone	MO
BF137	18-007	<i>Quercus velutina</i>	Red oak	Marion	MO

Table 5.1. (cont'd)

BF140	18-012	<i>Quercus velutina</i>	Red oak	Putnam	MO
BF146	OW1800078	<i>Quercus rubra</i>	Red oak	Ontario	NY
BF147	OW1800051	<i>Quercus velutina</i>	Red oak	Schenectady	NY
BF151	201900204	<i>Castanea mollissima</i>	Chestnut	Carroll	OH
BF155	201900206	<i>Quercus rubra</i>	Red oak	Columbiana	OH
BF153	201900200	<i>Quercus rubra</i>	Red oak	Columbiana	OH
BF154	201900201	<i>Quercus rubra</i>	Red oak	Columbiana	OH
BF273	202100036	<i>Quercus rubra</i>	Red oak	Cuyahoga	OH
BF166	201900165	<i>Quercus rubra</i>	Red oak	Cuyahoga	OH
BF168	201900175	<i>Quercus rubra</i>	Red oak	Harrison	OH
BF169	201900198	<i>Quercus rubra</i>	Red oak	Jefferson	OH
BF171	201900203	<i>Quercus rubra</i>	Red oak	Mahoning	OH
BF172	201900144	<i>Quercus rubra</i>	Red oak	Morgan	OH
BF178	201900212	<i>Quercus rubra</i>	Red oak	Tuscarawas	OH
BF270	Oakmont	<i>Quercus palustris</i>	Red oak	Allegheny	PA
BF271	Ridge Rd	<i>Quercus rubra</i>	Red oak	Huntingdon	PA
BF181	2019-99-99-0160	<i>Quercus rubra</i>	Red oak	Perry	PA
BF184	2019-99-99-0145	<i>Quercus rubra</i>	Red oak	Tioga	PA
BF185	2019-99-99-0146	<i>Quercus rubra</i>	Red oak	Tioga	PA
BF267	21.225	<i>Quercus nigra</i>	Red oak	Aiken	SC
BF186	Lexington, SC	<i>Quercus nigra</i>	Red oak	Lexington	SC
BF272	202100552	<i>Quercus nigra</i>	Red oak	Lexington	SC
BF193	2,320	<i>Quercus buckleyi</i>	Red oak	Kerr	TX
BF203	112	<i>Quercus buckleyi</i>	Red oak	Tarrant	TX
BF205	109	<i>Quercus buckleyi</i>	Red oak	Tarrant	TX
BF189	115	<i>Quercus fusiformis</i>	White oak	Brazos	TX
BF206	114	<i>Quercus fusiformis</i>	White oak	Brazos	TX

Table 5.1. (cont'd)

BF197	111	<i>Quercus fusiformis</i>	White oak	Lampasas	TX
BF199	106	<i>Quercus fusiformis</i>	White oak	Lampasas	TX
BF195	119	<i>Quercus havardii</i>	White oak	Kerr	TX
BF187	2,314	<i>Quercus laceyi</i>	White oak	Bondera	TX
BF223	S19-07-11(D)	<i>Quercus ellipsoidalis</i>	Red oak	Marathon	WI
BF264	I859	<i>Quercus macrocarpa</i>	White oak	Racine	WI
BF211	S19-08-08	<i>Quercus rubra</i>	Red oak	Bayfield	WI
BF262	S19-09-24(15)	<i>Quercus rubra</i>	Red oak	Chippewa	WI
BF220	Wisconsin 2	<i>Quercus rubra</i>	Red oak	Juneau	WI
BF260	S19-09-24(2)	<i>Quercus rubra</i>	Red oak	Marinette	WI
BF227	S19-09-08(B)	<i>Quercus rubra</i>	Red oak	Rusk	WI
BF233	S19-07-01(2)	<i>Quercus rubra</i>	Red oak	Walworth	WI
BF234	S19-07-03	<i>Quercus rubra</i>	Red oak	Washburn	WI
BF236	S19-07-31(1)	<i>Quercus rubra</i>	Red oak	Waukesha	WI
BF237	S19-07-11(C)	<i>Quercus ellipsoidalis</i>	Red oak	Marathon	WI
BF238	S19-07-29	<i>Quercus rubra</i>	Red oak	Oneida	WI
BF239	Romney1	<i>Quercus rubra</i>	Red oak	Hampshire	WV
BF241	Charleston Airport	<i>Quercus rubra</i>	Red oak	Kanawha	WV
BF249	Hillsboro, Wv	<i>Quercus rubra</i>	Red oak	Pocahontas	WV
BF243	Parkersburg	<i>Quercus rubra</i>	Red oak	Wood	WV

Table 5.2. Genetic divergence among (net nucleotide distance) and within (expected heterozygosity, genetic differentiation) *B. fagacearum* genetic clusters, determined using Structure analysis.

	Net nucleotide distance*				Eh**	Fst***
	Cluster 1	Cluster 2	Cluster 3	Cluster 4		
Cluster 1	-	0.2522	0.1600	0.1417	0.2364	0.3658
Cluster 2		-	0.2510	0.2498	0.1350	0.6987
Cluster 3			-	0.2379	0.0909	0.8259
Cluster 4				-	0.1715	0.6102

*Net nucleotide distance among genetic clusters

** Expected heterozygosity within genetic clusters

*** Genetic differentiation (Fst) within genetic clusters

LITERATURE CITED

- Adamčíková, K., Jánošíková, Z., van der Nest, A., Adamčík, S., Ondrušková, E., and Barnes, I. 2021. Population structure and genetic diversity suggest recent introductions of *Dothistroma pini* in Slovakia. *Plant Pathol.* 70:1883-1896. <https://doi.org/10.1111/ppa.13428>.
- Appel, D. N. 1995. The oak wilt enigma: perspectives from the Texas epidemic. *Annu. Rev. Phytopathol.* 33:103-118.
- Appel, D. N. 1994. The potential for a California oak wilt epidemic. *J. Arboric.* 20:79-86.
- Bruvo, R., Michiels, N. K., D'Souza, T. G., and Schulenburg, H. 2004. A simple method for the calculation of microsatellite genotype distances irrespective of ploidy level. *Mol. Ecol.* 13:2101-2106. <https://doi.org/10.1111/j.1365-294X.2004.02209.x>.
- Chen, S., Zhou, Y., Chen, Y., and Gu, J. 2018. fastp: an ultra-fast all-in-one FASTQ preprocessor. *Bioinformatics* 34. <https://doi.org/10.1093/bioinformatics/bty560>.
- Crouch, J. A., Clarke, B. B., and Hillman, B. I. 2023. Population genomic analysis reveals geographic structure and climatic diversification for *Macrophomina phaseolina* isolated from soybean and dry bean across the United States, Puerto Rico, and Colombia. *Front. Genet.* 14:1103331. <https://doi.org/10.3389/fgene.2023.1103331>.
- De Beer, Z. W., Marincowitz, S., Duong, T. A., and Wingfield, M. J. 2017. *Bretziella*, a new genus to accommodate the oak wilt fungus, *Ceratocystis fagacearum* (Microascales, Ascomycota). *Mycology* 27:1-19.
- Gauthier, M. K., Bourgault, É., Potvin, A., Bilodeau, G. J., Gustavsson, S., Reed, S., Therrien, P., Barrette, É., and Tanguay, P. 2023. Biosurveillance of oak wilt disease in Canadian areas at risk. *Can. J. Plant Pathol.* 46:27-38. <https://doi.org/10.1080/07060661.2023.2261890>.
- Gibbs, J. N., and French, D. W. 1980. The transmission of oak wilt. USDA Forest Service Research Paper NC-185. Central Forest Experiment Station, St. Paul, MN.
- Goudet, J. 2005. hierfstat, a package for R to compute and test hierarchical F-statistics. *Mol. Ecol. Notes* 5:184-186. <https://doi.org/10.1111/j.1471-8286.2004.00828.x>.
- Harrington, T. C. 2008. The genus *Ceratocystis*: Where does the oak wilt fungus fit? *Proc. Natl. Oak Wilt Symp.*, 2nd, Austin, TX. In press.
- Henry, B. W. 1944. *Chalara quercina* n. sp., the cause of oak wilt. *Phytopathology* 34:631-635.
- Hipp, A. L., Manos, P. S., González-Rodríguez, A., Hahn, M., Kaproth, M., McVay, J. D., Avalos, S. V., and Cavender-Bares, J. 2018. Sympatric parallel diversification of major oak clades in the Americas and the origins of Mexican species diversity. *New Phytol.* 217:439-452.

- Jombart, T. 2008. adegenet: a R package for the multivariate analysis of genetic markers. *Bioinformatics* 24:1403-1405. <https://doi.org/10.1093/bioinformatics/btn129>.
- Jombart, T., Devillard, S., and Balloux, F. 2010. Discriminant analysis of principal components: a new method for the analysis of genetically structured populations. *BMC Genet.* 11:94.
- Juzwik, J., Appel, D. N., MacDonald, W. L., and Burks, S. 2011. Challenges and successes in managing oak wilt in the United States. *Plant Dis.* 95:888-900.
- Juzwik, J., Harrington, T. C., MacDonald, W. L., and Appel, D. N. 2008. The origin of *Ceratocystis fagacearum*, the oak wilt fungus. *Annu. Rev. Phytopathol.* 46:13-26.
- Kamvar, Z. N., Tabima, J. F., and Grünwald, N. J. 2014. Poppr: an R package for genetic analysis of populations with clonal, partially clonal, and/or sexual reproduction. *PeerJ* 2. <https://doi.org/10.7717/peerj.281>.
- Knaus, B. J., and Grünwald, N. J. 2017. vcfr: a package to manipulate and visualize variant call format data in R. *Mol. Ecol. Resour.* 17:44-53. <https://doi.org/10.1111/1755-0998.12549>.
- Kurdyla, T. M., Guthrie, P. A. I., McDonald, B. A., and Appel, D. N. 1995. RFLPs in mitochondrial and nuclear DNA indicate low levels of genetic diversity in the oak wilt pathogen *Ceratocystis fagacearum*. *Curr. Genet.* 27:373-378.
- Li, H. 2013. Aligning sequence reads, clone sequences and assembly contigs with BWA-MEM. *arXiv:1303.3997*.
- Li, H., Handsaker, B., Wysoker, A., Fennell, T., Ruan, J., Homer, N., Marth, G., Abecasis, G., and Durbin, R. 2009. The sequence alignment/map format and SAMtools. *Bioinformatics* 25:2078-2079.
- Lindenbaum, P. 2015. JVarkit: java-based utilities for Bioinformatics. *figshare*. <https://doi.org/10.6084/m9.figshare.1425030.v1>.
- Lukasko, N. T., and Hausbeck, M. 2024. Whole-genome resource of seven *Botrytis cinerea* sensu lato isolates with resistance or sensitivity to seven site-specific fungicides. *PhytoFrontiers* (in First Look).
- McKenna, A., Hanna, M., Banks, E., Sivachenko, A., Cibulskis, K., Kernytzky, A., Garimella, K., Altshuler, D., Gabriel, S., Daly, M., and DePristo, M. A. 2010. The Genome Analysis Toolkit: a MapReduce framework for analyzing next-generation DNA sequencing data. *Genome Res.* 20:1297-1303.
- McLaughlin, K., Snover-Clift, K., Somers, L., Cancelliere, J., and Cole, R. 2022. Early detection of the oak wilt fungus (*Bretziella fagacearum*) using trapped nitidulid beetle vectors. *For. Pathol.* 52. <https://doi.org/10.1111/efp.12767>.

Milgroom, M. G., and Peever, T. L. 2003. Population biology of plant pathogens: the synthesis of plant disease epidemiology and population genetics. *Plant Dis.* 87:608-617.

Nei, M. 1984. *Molecular Evolutionary Genetics*. Columbia University Press, New York.

Poplin, R., Ruano-Rubio, V., DePristo, M. A., Fennell, T. J., Carneiro, M. O., Van der Auwera, G. A., Kling, D. E., Gauthier, L. D., Levy-Moonshine, A., Roazen, D., Shakir, K., Thibault, J., Chandran, S., Whelan, C., Lek, M., Gabriel, S., Daly, M. J., Neale, B., MacArthur, D. G., and Banks, E. 2017. Scaling accurate genetic variant discovery to tens of thousands of samples. *bioRxiv* 201178. <https://doi.org/10.1101/201178>.

Peacock, K. L. 2008. Control of oak wilt and the genetic structure of *Ceratocystis fagacearum*. Ph.D. dissertation. Michigan State University.

Poplin, R., Chang, P. C., Alexander, D., Schwartz, S., Colthurst, T., Ku, A., Newburger, D., Dijamco, J., Nguyen, N., Afshar, P. T., Gross, S. S., Dorfman, L., McLean, C. Y., and DePristo, M. A. 2018. Scaling accurate genetic variant discovery to tens of thousands of samples. *bioRxiv* 201178.

Rexrode, C. O., and Lincoln, A. C. 1965. Distribution of oak wilt. *Plant Dis. Rep.* 49:1007-1010.

Snover-Clift, K., and Rosenthal, E. 2016. Is Oak Wilt really a threat to New York State landscapes and forests? https://ecommons.cornell.edu/bitstream/handle/1813/60592/BranchingOut_OakWilt5-16.pdf?sequence=1. Accessed December 2023.

Pritchard, J. K., Stephens, M., and Donnelly, P. 2000. Inference of population structure using multilocus genotype data. *Genetics* 155:945-959. <https://doi.org/10.1093/genetics/155.2.945>.

Wickham, H. 2016. *ggplot2: Elegant Graphics for Data Analysis*. Springer-Verlag, New York.

Wingfield, B. D., Harrington, T. C., and Steimel, J. 1996. A simple method for detection of mitochondrial DNA polymorphisms. *Fungal Genet. Newsl.* 43:56-60.

Zerillo, M. M., Ibarra Caballero, J., Woeste, K., Graves, A. D., Hartel, C., Pscheidt, J. W., Tonos, J., Broders, K., Cranshaw, W., Seybold, S. J., and Tisserat, N. 2014. Population structure of *Geosmithia morbida*, the causal agent of thousand cankers disease of walnut trees in the United States. *PLoS One* 9. <https://doi.org/10.1371/journal.pone.0112847>.

CONCLUSION AND FUTURE DIRECTIONS

This dissertation provides a comprehensive investigation into the oak wilt pathosystem. Epidemiology studies revealed *Q. rubra* can be susceptible *B. fagacearum* infection March through September in Michigan. However, disease progression is fastest when sapwood is composed of earlywood vessels that corresponds to highest rate of predicted sap flow. *Q. rubra* was not susceptible to infection in October and November. The research addressed the challenges of oak wilt diagnosis from infected host material. A TaqMan real-time PCR assay was optimized and validated along with coupling with non-destructive sampling practices. Moreover, best practices for detection of *B. fagacearum* using conventional (culture-based) detection method from various type of samples were demonstrated. The complete annotated genome of *B. fagacearum* served as reference for population structure study and can be great resource for future studies to further elucidate molecular biology and epidemiology of the pathogen. The population structure analyses identified four distinct genetic clusters correlated with geographic regions. The dissertation also detailed the morphology, development, spore loads and infectious stages of mycelial mats, essential for assessing above-ground infection risks. Additionally, *B. fagacearum* first report of *fagacearum* infection on chestnut trees in Michigan was documented, and Koch's postulates were completed following pathogenicity trial on non-lignified seedlings. The insights gained from this research offer critical tools for diagnosing and decision making for management and control on further dispersal for the deadly fungal pathogen.

Future research should prioritize understanding the role of sap flow dynamics in oak wilt progression, and determining if host genotypes with reduced sap flow rate can tolerate or survive the infection. Future inoculation trials can mimic natural infection conditions, including varying conidial concentrations to better understand temporal host susceptibility. Further refinement and

validation of onsite detection tools such as LAMP, RPA, and CRISPR-CAS-based assays, may help in reliable and rapid detection of *B. fagacearum* from various sample types, including trapped insect vectors in the field. Population genomic studies can be extended to include more isolates from different regions, particularly newly affected areas like Ontario, Canada, and NY to elucidate pathways of gene flow and potential introduction events of *B. fagacearum*. Future research/data analyses can focus on understanding the genetic architecture of these clusters, identifying specific loci under selection and elucidating the roles of genetic drift and gene flow. Developing and validating a SNPchip can significantly improve our ability to assign the potential future detection events to their source populations. Additionally, identifying SNPs in gene regions commonly used for fungal species identification, such as the internal transcribed spacer (ITS), elongation factor (EF), and beta-tubulin genes, can help differentiate between clusters.

**APPENDIX A: FIRST REPORT OF *BRETZIELLA FAGACEARUM* INFECTING
CHESTNUT IN MICHIGAN**

Abstract

In the summer of 2021, ‘Colossal’ (*Castanea sativa* × *C. crenata* hybrid) chestnut trees in a commercial orchard in northwest Michigan suddenly declined. By 2023, additional adjacent trees also showed symptoms indicating a wilt disease. *Bretziella fagacearum* (Bretz) Z.W. de Beer, Marinc., T.A. Duong & M.J. Wingf. was detected in samples collected from the symptomatic chestnut trees. Koch’s postulates were confirmed, marking the first record of *B. fagacearum* infecting chestnut trees in Michigan (see, Plant Disease, 2024, 108:5.1397, <https://doi.org/10.1094/PDIS-10-23-2267-PDN>).

APPENDIX B: CLASSIFICATION AND SPORE LOADS ON OAK WILT FUNGUS, *BRETIELLA FAGACEARUM* MYCELIAL MATS

Abstract

Oak wilt, caused by fungal pathogen, *Bretziella fagacearum* can kill red oaks (section *Lobatae*) within 6 weeks of infection. Detection of oak wilt in 24 states and 61 out of 83 Michigan counties are of great concern. *Bretziella fagacearum* is vectored by sap beetles (Nitidulidae) when spore-laden insects visit fresh wounds on healthy trees. Root grafts allow transmission of *B. fagacearum* from infected to healthy trees. Production of fungal mycelial mats, spore bearing structures under the bark of diseased trees is a unique character used for oak wilt confirmation by the public, arborists, and forestry stakeholders. Detailed study and characterization of oak wilt mycelial mats by their morphology, developmental, and infectious stages was warranted. Tagged *Quercus rubra* trees at 12 oak wilt centers in the lower peninsula of MI were monitored at two-week intervals, Apr-Nov in 2018, 2019, and 2020 for mycelial mat production. Individually collected mycelial mats were categorized into different morphological, and developmental stages. Mycelial mat viability and spore loads were evaluated using serial dilution plating. Percentage infectious rate of mat stage 1, 2, 3, 4, 5, 6, 7, and 8 reported 95, 78, 100, 97, 76, 32, 17 and 0 respectively. Range of colony forming units varied (0 to 522,000) with different mycelial mat stages. This detailed characterization of oak wilt mycelial mats by their morphology, developmental, and infectious stage may help arborists, and forestry stakeholders to determine the risk of oak wilt above-ground infection.

Introduction

Oak wilt, caused by the fungal pathogen, *Bretziella fagacearum* can kill red oaks (section *Lobatae*) within 6 weeks of infection. Oak wilt has been detected in 24 U.S. states and in 61/83

counties in Michigan. Sporulating structures of *B. fagacearum*, known as mycelial mats, form on infected red oaks several weeks to months after the trees exhibit complete foliar wilting (Juzwik et al. 2011). These mats develop as mirror images on the inner bark and outer xylem. The opposing pressure from these mats causes the bark to split, resulting in a vertical crack that allows for insect visitation to the mats. The opening facilitates insect-vectors visitation of mycelial mats. Aboveground spread of *B. fagacearum* is a result of spore-laden sap beetles (Nitidulidae) visiting fresh wounds on healthy trees. The aboveground transmission is responsible for the long-distance spread of the fungus to healthy oak stands. The expansion of disease centers typically occurs through root graft transmission from initially infected trees (Juzwik et al. 2011).

To prevent or reduce the overland transmission of the fungus, it is crucial to remove potential inoculum-producing trees before the formation of mycelial mats. It is important to understand the timing of sporulation, the number of mats that may form, the infectious nature of various mat stages, and the duration of mat production to determine the best time for removing infected trees. To gain insight into the patterns of mat production and morphological stages, the sporulation of the fungus was monitored over a three-year period in numerous trees within oak wilt infection centers.

Moreover, field diagnosis of oak wilt is only possible with the observation of mycelial mats (Appel 1995). Mycelial mats may persist on host tissue for weeks; however, they remain infectious for only a short period. To refine our ability to evaluate visually if a mycelial mat is infectious, *B. fagacearum* mycelial mats were classified based on morphological and developmental stages and spore loads were evaluated by determine colony forming units from

different stages of mycelial mats. A visual rating system of mycelial mats will assist in the risk assessment of aboveground oak wilt spread.

Materials and methods

Mycelial mats were observed on recently dead *Quercus rubra* trees at 12 field sites with active oak wilt infection centers in northwest Michigan from 2018 to 2020. Trees were monitored for mycelial mat development at 15-days intervals. Tree trunks were tapped with a hatchet to find mats, while binoculars were used locating mats above 3 m, based on visible bark splits (**Fig. A.3**). Only mats causing bark ruptures were recorded on trunks above 3 m. Representative mycelial mats were sampled and categorized into different morphological and developmental stages. The morphological and developmental stages were modified/updated from Curl (1954). A total of 468 mycelial mats were screened using serial dilution plating and colony forming units were counted (**Fig. A.4**). The protocol entailed the excision of three disks per mat, followed by sonication to disrupt the structures and release fungal propagules. The sonicated suspensions were then subjected to a dilution series and plated on acidified potato dextrose agar. Colony forming units were counted, and representative colonies were sub-cultured for further examination. The morphological identification of *B. fagacearum* was conducted to identify the pathogen.

Results and conclusions

Mycelial mats can be divided into eight different stages based on visual characterization (**Fig. A.5**). *Bretziella fagacearum* colony forming units were significantly ($P < .001$) different among different stages of mycelial mats (**Fig. A.6A**). Colony forming units were not significantly different from mats collected in different months and years, $P = 0.40$, and 0.49 , respectively. Infectious and non-infectious nature of mycelial mats can be determined from

different stages (**Fig. A.6B**). A visual rating system of mycelial mats is developed that can assist in differentiating infectious and non-infectious nature of a mat and potential colony forming units. In-field categorization of mat stages will assist in the risk assessment of aboveground oak wilt spread.

The data on mycelial mat production over three years (2018-2020) reveals two distinct peaks in mat formation: one in early summer (May and June) and another in early fall (August and September) (**Fig. A.7**). In 2018, mat production was relatively low throughout the year, with a slight increase in May and June. In 2019, there was a notable peak in June, followed by a smaller peak in September. The year 2020 showed the highest levels of mat production, with significant peaks in June and September. These observations suggest a consistent seasonal pattern in mycelial mat production, with the most prolific periods occurring in early summer and early fall in Michigan. Furthermore, the peak activity of insect vectors, which can transmit the pathogen, also coincides with these periods (Morris 2020). To minimize the risk of above-ground infection, it is recommended to avoid pruning or injuring oaks during these times when both mat production and vector activity are at peak.

Acknowledgments

We are thankful to Scott Lint, and Phillip Kureja, MI DNR, who provided study sites and field work assistance. This study was supported by the Michigan Invasive Species Grant Program, Michigan State University Project GREEN, Miriam and Forrest Strong endowments and by HATCH project MICL02505 from the USDA National Institute of Food and Agriculture.

Figures

Figure A.3. Foliar symptoms of oak wilt on *Quercus rubra* (**left panel**). Vertical cracks in bark, indicating presence of mycelial mats underneath the bark (**middle panel**). Mycelial mats are formed both on the outer wood and inner bark in a mirror image arrangement (**right panel**). A mycelial mat composed of two parts; sporulating mycelium (**red arrow**) and pressure pad (**yellow arrow**) that exert pressure outward causing the bark to split.



Figure A.4. Method of screening mycelial mats.

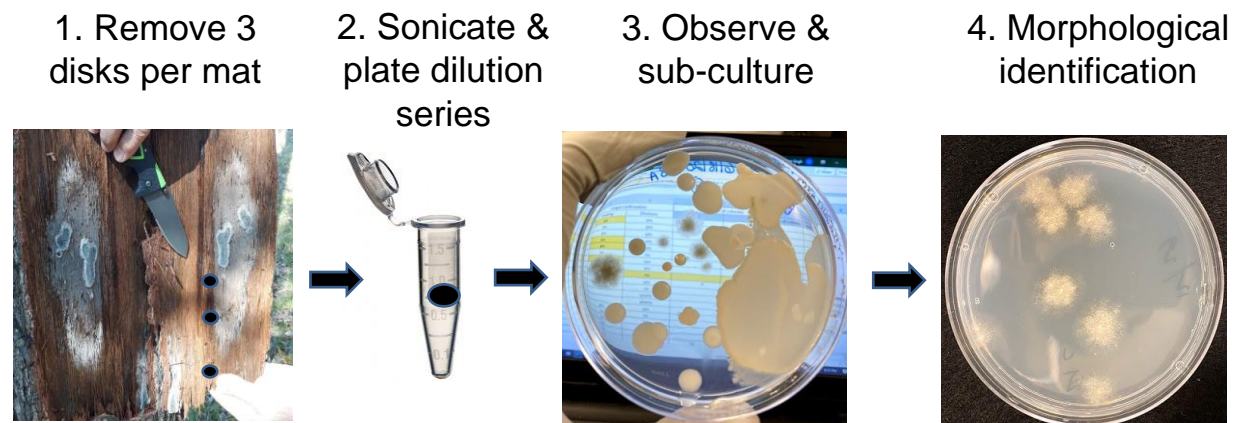


Figure A.5. Representative mycelial mats of *Bretziella fagacearum* categorized into eight stages based on different morphological and developmental stages. Other parameters studied for mat stages: Presence of vertical cracks, beetles, colony forming units of *B. fagacearum* and *Ophiostoma quercus*.



Figure A.6. (A) Different stages of mycelial mats yielded significantly different colony forming units, ($P = 0.05$). (B) Infectious and non-infectious nature of mycelial mats varied with different stages.

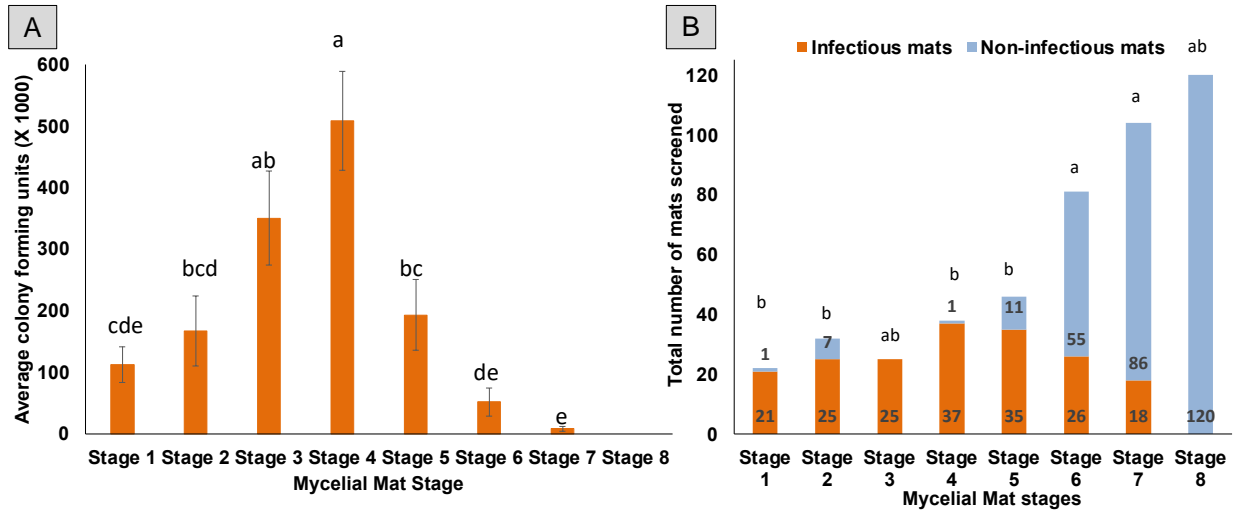
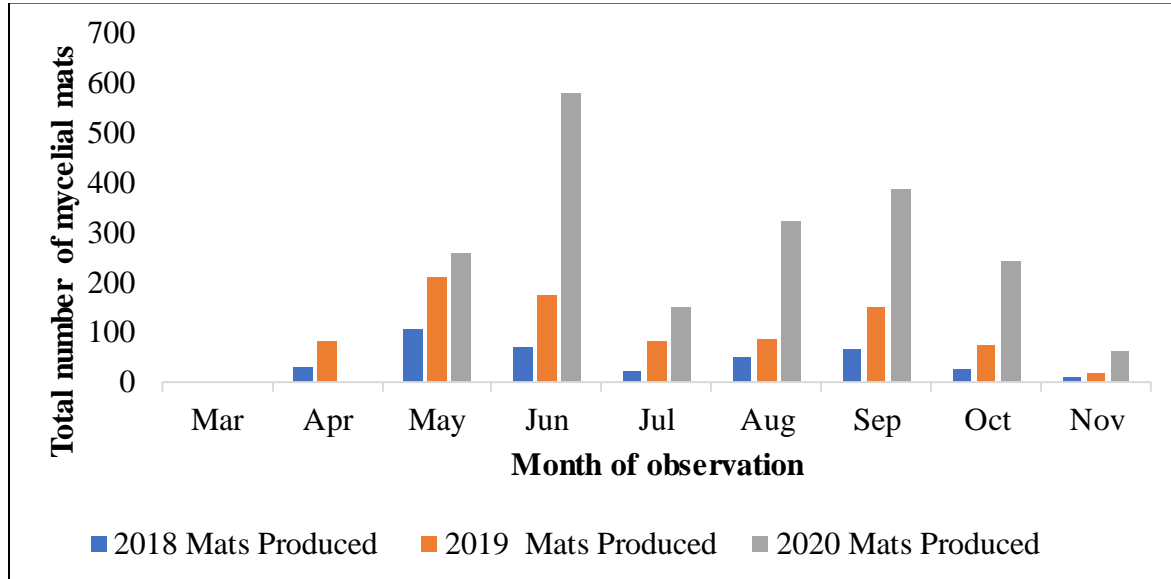


Figure A.7. Production of mycelial mats on infected *Quercus rubra* trees during 2018 - 2020.



Table

Table A.1: Description of the developmental stages of mycelial mats of *Bretziella fagacearum*.

Stage	Name	Pressure Pad	Sporulating Mycelium
Stage 1	Initial mat	Absent	Grey to tan in color, active growth phase
Stage 2	Immature mat	Present, not fully developed	Grey to tan in color, active growth phase
Stage 3	Vegetatively mature mat	Fully developed with no signs of decay	Grey, tan to buff in color, vegetative growth ceases
Stage 4	Reproductively mature mat	Starts to turn darker in color but no signs of decay	Mat edges start shrinking, crack slightly from drying
Stage 5	Early decaying mat	Becomes brownish in color with signs of decay	At least 1/3 of mat turn brown to black in color with signs of decay
Stage 6	Rapidly decaying mat	Loses shape due to decay but still distinguishable	Mycelium turns black in color with conspicuous decay
Stage 7	Advanced decaying mat	Lost its consistency, structure and not distinguishable	Decayed mycelium overgrown by other fungi and feeding insect larvae
Stage 8	Remnant mat	Turns into soil-like mass	Turns into black ashes

LITERATURE CITED

Appel, D. N. 1995. The oak wilt enigma: perspectives from the Texas epidemic. *Annu. Rev. Phytopathol.* 33:103-118.

Curl, E. A. 1954. Natural availability of oak wilt inocula. University of Illinois at Urbana-Champaign, Urbana, IL.

Juzwik, J., Appel, D. N., MacDonald, W. L., and Burks, S. 2011. Challenges and successes in managing oak wilt in the United States. *Plant Dis.* 95:888-900.

Morris, O. R. 2020. Seasonal Activity and Phoresy Rates of Sap Beetles (Coleoptera: Nitidulidae) in Oak Wilt Infection Centers, Volatile Organic Compounds Related to the Oak Wilt Cycle, and Long-Term Evaluation of Red Oak Provenances. Master's thesis, Michigan State University.

APPENDIX C: SUPPLEMENTAL TABLES

Table A.2. Analysis of variance (ANOVA) results of logistic-normal mixed-model analysis on factors that influence the likelihood of detecting *Bretziella fagacearum* in sapwood of infected *Quercus rubra* branch samples.

Effect	Chisquare	Dfa	P value
Detection method	34.47	2	<0.001
Sapwood	31.82	1	<0.001
Detection method × Sapwood	6.97	2	0.030

aDegrees of freedom

Table A.3. The post-hoc tests examining the interactions between detection methods (culture-based, nested PCR, real-time PCR) used for detecting *Bretziella fagacearum* and the sapwood condition (fresh or dry) of *Quercus rubra* branch samples.

Detection Method ^a	Sapwood ^b	Estimated Probability ^c	SE ^d	Actual Probability ^e	Group ^f
Culture-based	Fresh	0.99	5.005753e-06	0.96	a
Nested PCR	Fresh	1	1.627062e-11	1	a
Real-time PCR	Fresh	1	1.626749e-11	1	a
Culture-based	Dry	3.376794e-06	1.020481e-05	0.22	b
Nested PCR	Dry	0.99	1.367169e-05	1	a
Real-time PCR	Dry	0.99	1.357545e-05	1	a

^aMethod used to detect *B. fagacearum* from infected branch samples.

^bCondition of sapwood (fresh or dry) of infected branch samples.

^cEstimated probability based on logit transformation from model estimates.

^dStandard error of the mean.

^eActual probability based on calculated proportions from samples used in this study.

^fGroups labeled with different letters indicate significant differences ($P < 0.05$), while groups sharing the same letter are not significantly different ($P > 0.05$).

Table A.4. Analysis of variance (ANOVA) results of logistic-normal mixed-model analysis on factors influencing the likelihood of detecting *Bretziella fagacearum* in petioles of infected *Quercus rubra*, and ‘Colossal’ (*Castanea sativa* × *C. crenata* hybrid) chestnut leaves.

Effect	Chisquare	Df^a	P value
Detection method	21.22	1	<0.001
Species	7.58	1	0.005
Severity	23.04	2	<0.001
Detection method x severity	8.43	2	0.014

^aDegrees of freedom

APPENDIX D: SUPPLEMENTAL SAMPLING PROTOCOL

For oak wilt diagnosis using petiole sampling and coupling with culture-based or molecular detection protocols, here is the detailed protocol:

1. Collect at least three fallen leaves (under tree crown and within 6 m radius) for each tree showing bronzing or tanning on 1 to 50% of the leaf area as described 'moderate' symptom severity in this paper.
2. Excise 4 cm of the petiole from each leaf or expose the midrib if the petiole is short.
3. Surface sterilize cut petioles by dipping in 75% ethanol (30 s), followed by 10% (v/v) bleach (1 min), and two rinses with sterile deionized water (>1 min).
4. Chop each 4 cm petiole into eight approximately equal pieces and transfer the pieces into Lysing Matrix A (MP Biomedicals, SKU:116910050-CF) 2-ml tube with two ceramic beads.
5. Add 1000 μ l of InhibitEX buffer (QIAamp Fast DNA Stool Mini Kit) into the Lysing Matrix A tube with sample pieces.
6. Macerate the sample using a Bead Mill 24 homogenizer (Fisher Scientific) or FastPrep-FP120 (Thermo Fisher Scientific, Waltham, MA) (or other available macerator) with two 45-second cycles at 6.5 m/s speed and a 5-minute rest in between. Visually inspect the sample, it should be turned into a fine powder. If necessary, run additional maceration cycle.
7. Follow DNA extraction protocol as provided with QIAamp® Fast DNA Stool Mini kit.
8. Follow master-mix recipe and real-time PCR cycle as given below.

9. **For culture-based detection**, after the step 3, split the petioles virtually into 2 equal pieces using a scalpel or fine scissors to expose the xylem-inhabiting *B. fagacearum*.
10. Cut each split petiole into 4 equal pieces and culture the total 8 pieces from a petiole into one Petri dish containing acidified full-strength potato dextrose agar.
11. Incubate the plates at room temperature (~24°C) under ambient lighting and check regularly for fungal growth.
12. *Bretziella fagacearum* can be observed 5-7 days after culturing and hold the plates for at least 15 days before tossing.
13. Pure cultures of *B. fagacearum* can be confirmed by the presence of gray to olive-green colonies, a characteristic fruity odor, and the presence of endoconidia.

Table A.5. Primers utilized in this protocol to detect *Bretziella fagacearum*.

Bourgault et al. 2022, For. Glob. Change. 5:1068135

Primer name	Primer Sequence	Primer Length	Primer Tm	Amplicon Length
Taqman				
Cfag ITS F 75-97	TAAAACCATTTGTGAACATACCA	23	53,5	168bp
Cfag ITS R2 215- 43	TGAAAGTTTTAACTATTTTGTTAAATGCA	29	53	
Cfag ITS T RC 126-50	AACATCCCCTGAAGAAAGAAGTCC	24	62,3	FAM - ZEN probe

Table A.6. Real-time PCR reaction conditions for amplifying *Bretziella fagacearum*.

	Temperature (°C)	Time	Number of cycles
Activation	95	15 min	1
Denaturation	95	15 sec	50
Annealing	60	90 sec	

Table A.7. Reaction components in a PCR reaction for amplifying *Bretziella fagacearum*.

Modified from Bourgault et al. 2022, For. Glob. Change. 5:1068135

Master mix recipe		
Components	Volume per reaction (µl)	Final concentration
Nuclease-free water	5.4	
Quantabio PerfeCta ToughMix, 2X	10	1X
Bf_ITS_F (10 uM)	1.2	600 nM
Bf_ITS_R (10 uM)	1.2	600 nM
Bf_ITS_P (10 uM)	0.2	100 nM
<i>DNA template</i>	2	
Total	20	